FUNCTION AND DYNAMIC LOCALIZATION OF GOLGIN-160

by
Catherine Emily Gilbert

A dissertation submitted to Johns Hopkins University in conformity with the requirements for the degree of Doctor of Philosophy

Baltimore, Maryland
December, 2017

Abstract

The golgin family of proteins plays an essential role in maintaining the structure and function of the Golgi apparatus. Golgin-160 is a unique golgin that promotes the trafficking of a specific subset of cargo proteins through a currently unknown mechanism. This thesis characterizes the role of golgin-160 in the trafficking of one of its cargo proteins, the beta-1 adrenergic receptor (β1AR), and begins to connect golgin-160's dynamic localization with its function.

Previous work demonstrated that golgin-160 is required for efficient delivery of β1AR to the plasma membrane through affecting a *trans*- or post-Golgi trafficking step. Here, we demonstrate that three basic residues in the third intracellular loop of β1AR, $K_{308}RR_{310}$, are critical for β1AR binding to the golgin-160 head domain, and mutation of these residues affects β1AR trafficking similar to golgin-160 depletion. This β1AR mutant can thus be used to distinguish between golgin-160 dependent and independent trafficking pathways. Golgin-160 affects the late Golgi trafficking of β1AR, yet it localizes to the *cis*-Golgi. Interestingly, golgin-160 disperses from Golgi membranes immediately after β1AR reaches the *trans*-Golgi. Despite not being localized with β1AR on vesicles, golgin-160 depletion altered the directionality and processivity, but not speed, of β1AR-containing vesicles. This dispersal of golgin-160 from Golgi membranes prior to the alteration of vesicle dynamics suggests that additional proteins may be involved in golgin-160-facilitated trafficking of β1AR. At the *trans*-Golgi, β1AR selectively colocalizes

with golgin-97, but depletion of golgin-97 affects β1AR retrograde recycling, not anterograde trafficking to the plasma membrane.

Cargo protein synchronization is a useful tool for studying protein trafficking, however the standard technique of using cold temperature blocks (20°C and 16°C) causes golgin-160 to become cytoplasmic. This dispersal correlates with a loss of active ADP-ribosylation factor 1 (ARF1), a small monomeric GTPase, apparently due to inhibition of its specific guanine nucleotide exchange factor. ARF1 activity and golgin-160 localization slowly recovers upon return to 37°C, but these results urge caution when interpreting experiments that use temperature blocks. Thus, golgin-160 is dynamically localized at the Golgi, and this may impact its role in facilitating specific cargo trafficking.

Dr. Carolyn Machamer, Advisor

Dr. Svetlana Lutsenko, Reader

ACKNOWLEDGEMENTS

Graduate school is a challenging thing to face without support, and I am lucky enough to have had tremendous support from my colleagues, friends, and family throughout these years.

I can unequivocally say that I would not be the scientist I am today without my advisor, Dr. Carolyn Machamer. She has driven me to become more analytical and precise in my investigations. It is entirely due to her influence that I have learned to put my observations in a cellular and organism-based context, moving beyond noticing an interesting phenotype to really try to answer the question, what does this mean?

Her influence has been bolstered by that of the members of my thesis committee. The critical analysis of methodology provided by Dr. Scot Kuo, the insightful questions from Dr. Peter Espenshade, and the enthusiasm and intellectual curiosity demonstrated by Dr. Svetlana Lutsenko have all shaped my dissertation work into a more complete and more interesting story. I am also thankful to my collaborator Dr. Elizabeth Sztul for being kind enough to introduce me to the ARF and ARF GEF field when my thesis work took me in unexpected directions.

My labmates have been of great help, both academically and outside of lab. Before Jason Westerbeck became Dr. Westerbeck, we were just two students trying to figure out where all the reagents were located. His generosity of spirit and intellectual input over the years has been remarkable, and were well balanced with deliveries of his mantra: “Nobody cares, work harder.” I am also grateful for the addition of Dr. Jeanne

Sisk to our lab. Our in depth discussions of experimental design and cellular mechanisms have been just as critical to my success as our breaks to compare cat photos.

I cannot express deep enough thanks for my BCMB and BCMB-adjacent friends. The Wednesday lunch crowd (Risa Burr, Jarrett Smith, Kelsey Bettridge, Laurel Oldach, Mark Zbindin, John Bettridge, Aditya Radhakrishnan, Tom Schaffer, and Stefanie Tan) contains some of the best people I have ever met, and I would not have had half as much fun in my time here without our rambling conversations on the meaning of life, science, graduate education, and popular culture. Special thanks must be given to Risa, who organized almost all of the fun things that I did in graduate school, and Jarrett, who constantly matched or exceeded my enthusiasm for nerdy activities. I will always be thankful that Risa took an offhand comment about wanting to see Barcelona and turned it into a spectacular European adventure for the three of us. Outside of Hopkins SOM, Kate Lairmore went from being that girl I grew up next to in California, to one of my closest neighbors and friends. She has been a staggering pillar of support, and I'm so glad we had the opportunity to reconnect on the East coast.

Finally, I want to thank my family. Despite being on different coasts and different continents, I have always known that my mother, Cheryl, and sister, Lizzy, have been there for me, believing in me at all times. I don't even have the metrics to measure the emotional support they have provided. And though he wasn't here to watch me take this step in my education, I know that the source of my intellectual curiosity is my father, Lowry, who never answered with "Because" when I asked why things are the way they are, but rather, "Let's find out."

TABLE OF CONTENTS

LIST OF TABLES

LIST OF FIGURES

Chapter 1

Introduction

The Golgi Apparatus

The secretory pathway consists of three major components: the endoplasmic reticulum (ER) where proteins are synthesized, the Golgi apparatus where proteins are modified, and the endosomal system through which proteins can be trafficked or recycled. A recent proteomics study of human tissue estimated that 39% of human proteins pass through the secretory system (Uhlen *et al.*, 2015). These proteins include plasma membrane proteins, secreted proteins, lysosomal proteins, and proteins localizing to organelles within the pathway. The Golgi apparatus is an organelle found in all eukaryotic species and serves a critical role within this pathway, as it is at the hub of anterograde and retrograde trafficking. While the Golgi has been implicated in functioning as a cellular sensor for multiple other processes including mitosis, apoptosis, and cell migration (reviewed in Glick, 2000; Wilson *et al.*, 2011; Gosavi and Gleeson, 2017), this dissertation focuses on its role in facilitating the modification, processing, and packaging of newly synthesized cargo proteins as they move through the organelle.

This protein modification and packaging function is facilitated by the structure of the Golgi, though that structure itself varies among organisms (Mironov *et al.*, 2017). The mammalian Golgi consists of 3 to 8 flattened membrane-bound sacks called cisternae that are stacked together. These stacked cisternae are divided into separate regions, the *cis*-, medial, and *trans*-Golgi (Nakamura *et al.*, 2012). These regions are functionally distinct, for example the enzymes required at early stages of glycosylation concentrated on the *cis* face of the Golgi, and enzymes needed for the final steps concentrated at the *trans* face. In addition to ensuring that proteins are modified in an

accurate, sequential order, this allows for optimization of pH, ions, and substrate availability at each step (Stanley, 2011; Day *et al.*, 2013; Zhang and Wang, 2016a). In higher eukaryotes, individual Golgi cisternae stacks are laterally joined into a ribbon-like structure. Interestingly, this structure is not generally required for anterograde or retrograde trafficking, however it may be an important signaling mechanism for the Golgi's role as a cellular sensor, as mentioned above (Gosavi and Gleeson, 2017).

How proteins move through cisternae in mammalian cells is highly debated. In one model, the vesicular transport model, each cisterna is static, containing specific enzymes needed to modify cargo (for example, enzymes required for protein glycosylation), and cargo is transferred between cisternae in vesicles. The opposing model, called the cisternal maturation model, proposes that the cargo proteins remain static within one cisternae while the modifying enzymes are dynamically recruited and removed from that cisternae (Glick, 2000). Intermediate models like the cisternal progenitor model, where a static cisternae produces maturing cisternae, and the rim progression model, in which portions of the cisternae remain static while the lateral edges (rims) of the Golgi progress to the next cisternae, have also been proposed, though as of yet no consensus has been reached (Pfeffer, 2010; Lavieu *et al.*, 2013).

Trafficking Through the Secretory Pathway

The secretory pathway begins with the cotranslational insertion of proteins into the endoplasmic reticulum (ER). Within the ER, protein folding and modifications including disulfide bond formation can occur (Stanley, 2011; Spang, 2013). For proteins

acquiring N-glycosylation or glycophosphatidylinositol (GPI) anchors, the initial sugar addition also occurs in the ER. *De novo* ceramide synthesis also occurs in the ER, which then can be metabolized into other sphingolipids at the Golgi (Stanley, 2011). Newly synthesized proteins are then transported to the ER-Golgi Intermediate Compartment (ERGIC), and ERGIC-derived vesicles move on microtubules to become incorporated with the *cis*-Golgi. This fusion step, and indeed most fusion steps throughout the secretory pathway, requires tethering complexes (often golgins, discussed below) to interact with small GTPases, guanine nucleotide exchange factors (GEFs) and GTPase activating proteins (GAPs) to regulate that GTPase activity, and soluble N-ethylmaleimide-sensitive factor attachment protein receptors (SNAREs) to promote the actual fusion step (Bonifacino and Glick, 2004; Witkos and Lowe, 2017).

ER resident proteins and membrane bound transport machinery from COPII coated vesicles are captured by machinery at the *cis*-Golgi and returned back to the ER, a step which is critical for maintaining the distinct ER and Golgi structures and functions. These temporarily mislocalized ER proteins often have KDEL (named after the lysine-aspartic acid-glutamic acid-leucine) sequences or dibasic motifs which mark the ER proteins for retrograde transport. These proteins are incorporated into COPI coated vesicles through the recruitment of COPI cargo adaptors by the small GTPase ADP-ribosylation factor 1 (ARF1; discussed in depth below) (Dong *et al.*, 2010; Jackson, 2014).

The Golgi-based glycosylation of proteins begins in the *cis*-Golgi and continues in the medial-Golgi (Stanley, 2011; Day *et al.*, 2013). In these locations, different sets of glycosyltransferases and glycosidases, including but not limited to GlcNac-T I (mannosyl

(alpha-1,3-)-glycoprotein beta-1,2-N-acetylglucosaminyltransferase) and α-mannosidase II, further process glycosylated proteins by adding or removing sugar groups (Stanley, 2011). The final sialylation of glycosylated proteins occurs in the *trans*-Golgi (Opat *et al.*, 2001; Stanley, 2011; Day *et al.*, 2013). Furin, an endoprotease, also localizes to the *trans*-Golgi where it cleaves furin-dependent cargo (Molloy *et al.*, 1994).

Once all Golgi-based modifications are complete, cargo proteins must be accurately delivered to their proper localization, be it the plasma membrane (apical, basal, or nonpolarized), endosomes (late or recycling), or the extracellular space. The sorting and packaging step occurs at the *trans*-Golgi network (TGN). Recent studies have expanded our knowledge of different exit pathways and highlighted their complexity (Bonifacino and Lippincott-Schwartz, 2003; De Matteis and Luini, 2008; Anitei and Hoflack, 2011). This complexity begins with the sorting of cargo proteins. Cargo adaptor proteins recognize and bind to various cytosolic signals on membrane proteins (Rodriguez-Boulan and Müsch, 2005).

One set of proteins, the cation-dependent and cation-independent mannose 6 phosphate receptors (CD-M6PRs and CI-M6PRs), link cargo proteins and cargo adaptors. Acid hydrolases destined for lysosomes contain mannose 6-phosphate-recognition sequences that serve as signals for M6PRs binding; following that binding, the M6PRs recruit and bind the Golgi-localized γ-ear containing, ADP-ribosylation factor binding (GGA) and adaptor protein 1 (AP-1) cargo adaptor proteins at the TGN, allowing the acid hydrolases to be incorporated into clathrin coated vesicles (CCVs, discussed further below). While the GGAs bind a DXXLL motif, there are multiple AP-1 binding sites on the

M6PR cytoplasmic tails. The GGAs can bind directly to AP-1 so it is unknown why M6PRs should bind to both proteins separately. It has been hypothesized that the GGAs may bind earlier in the Golgi and help to direct M6PRs to AP-1 and CCVs (Ghosh *et al.*, 2003).

In addition to targeting sequence motifs , protein modifications such as glycosylation or the addition of glycosoaminoglycans (GAGs) can alter protein trafficking routes from the Golgi (Anitei and Hoflack, 2011; Mihov and Spiess, 2015). Lipids are sorted for delivery to distinct membranes, as well, and this sorting can impact protein cargo sorting. This can be through lipid-influenced recruitment of proteins. For example, PI4KIIIα (type III phosphatidylinositol 4-kinase alpha) and PI4P (Phosphatidylinositol 4-phosphate) modulate recruitment of GBF1 (Golgi Brefeldin A Resistant Guanine Nucleotide Exchange Factor 1) to membranes. Lipids can also affect protein sorting through phase separation of proteins due to protein interactions with their lipid environments (Choudhury *et al.*, 2005; Surma *et al.*, 2012).

Sorting allows cargo to be incorporated into the correct type of vesicles. CCVs, which can form at both the TGN and the plasma membrane, were the first coated vesicle characterized (Bonifacino and Lippincott-Schwartz, 2003). During their formation, cargo from the TGN is recruited by the AP-1 and GGA cargo adaptors, while AP-2 is utilized at the plasma membrane (Bonifacino and Lippincott-Schwartz, 2003). AP-1 and the GGAs are ARF1 effector proteins (discussed further below); in contrast AP-2 is recruited by PI(4,5)P2 (Phosphatidylinositol 4,5-bisphosphate) (Stamnes and Rothman, 1993; Dittié *et al.*, 1996; Jost *et al.*, 1998). AP-1 and the GGAs are stabilized on membranes through binding to cargo proteins (Hirst *et al.*, 2007; Lee *et al.*, 2008).

Additionally, AP-1 binding to cargo results in a conformational change in AP-1 that promotes subsequent cargo binding, leading to efficient incorporation of cargo into forming vesicles (Lee *et al.*, 2008). These adaptor proteins allow for clathrin triskelions (consisting of three light and three heavy chains) to then be recruited to Golgi membranes, where the complex forms a cage structure around the nascent vesicles (Bonifacino and Lippincott-Schwartz, 2003).

Clathrin-independent vesicles have also been observed and characterized. The adaptor proteins AP-3 and AP-4 were identified by homology with AP-1 and -2 and were found to localize on endosomes and the TGN. Like AP-1, both AP-3 and AP-4 are ARF1 effectors (Bonifacino and Lippincott-Schwartz, 2003; Robinson, 2004). AP-3 is one of the adaptors involved in cargo trafficking to lysosomes via endosomes. AP-3 can interact with clathrin, though clathrin is not required for AP-3 regulated cargo trafficking. AP-4 containing vesicles, which have never been associated with clathrin, are targeted to the basolateral plasma membrane in polarized cells, and have been reported to deliver proteins to the endosome in nonpolarized cells (Anitei and Hoflack, 2011).

In addition to small cargo transporting vesicles, large pleiomorphic structures have also been observed to carry cargo between organelles. These structures move along microtubules and some have classic coat proteins, therefore it is unclear if these large structures represent merged vesicles or if they formed directly from the TGN (Bonifacino and Lippincott-Schwartz, 2003). For the latter idea, it has been proposed that membrane or adaptor interactions with microtubule motor complexes pulls cargo-filled tubules towards their destination, and vesicle fission machinery is stimulated once

a certain membrane tension (and not a specific vesicle size) has been reached (De Matteis and Luini, 2008).

The Golgins

In higher eukaryotes, the function of the Golgi relies on the separation of protein modification processes in stacked cisternae, and the ability of cargo-containing vesicles to accurately carry cargo to the next destination. These two activities are facilitated by a unique family of proteins called the golgins. First identified using antibodies found in the sera of patients with autoimmune diseases, the golgins have been classified by two features: their Golgi localization and extended α-helical coiled-coil domains. While some golgins are found across eukaryotes, others have specialized functions only in higher eukaryotes. The golgins support Golgi structure and facilitate bulk cargo trafficking through multiple mechanisms, particularly through promoting cisternal stacking and acting as tethers (Figure 1-1 and Table 1-1).

Most golgins are cytoplasmic proteins peripherally attached to Golgi membranes, and many are recruited into Golgi membranes through interactions with small GTPases (current known interactions summarized in Table 1-1). Several golgins can bind to multiple GTPases, which may allow for more precise localization by requiring multiple GTPases to be present at the same membrane before golgins can be recruited. Alternatively, interactions with multiple GTPases may have functions outside of promoting golgin localization (Barinaga-Rementeria Ramirez and Lowe, 2009). For example, the GRIP (golgin-97, RanBP2α, Imh1p, and p230/golgin-245) domain containing golgins (golgin-97, GCC1, GCC2, p230) are localized to the *trans*-Golgi by the

Figure 1-1: Golgi structure, vesicles, and golgin tethers. Schematic of stacked Golgi cisternae and representative golgins (discussed in depth below) facilitating anterograde ER-to-Golgi (p115 and GM130), retrograde intra-Golgi (giantin), and retrograde endosome-to-Golgi (GCC2 and GMAP210) transport. Vesicles range between 50-100 nm in diameter; golgins have known or predicted lengths of 50-300 nm (Truebestein and Leonard, 2016). Image adapted from (Gillingham and Munro, 2016).

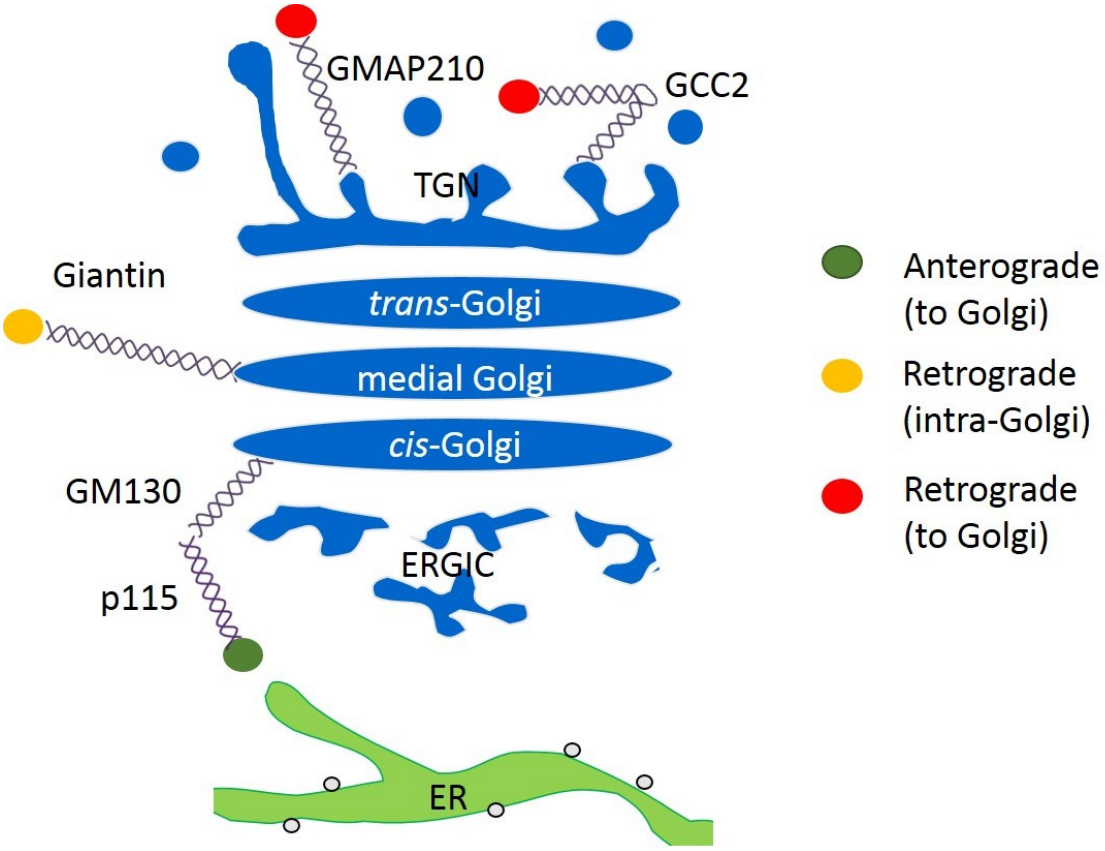

Table 1-1: Golgin localization, interactions with GTPases, and proposed functions at the Golgi. Listed below are the kingdom or subphylum in which each golgin has been reported, the Golgi subcompartment to which each golgin is localized and (in parenthesis) the protein responsible for recruiting it to that subcompartment, known GTPase interactors, and general roles at the Golgi. Data adapted from (Short *et al.*, 2005; Sinka *et al.*, 2008; Barinaga-Rementeria Ramirez and Lowe, 2009; Munro, 2011; Gillingham and Munro, 2016) and NCBI HomoloGene (Agarwala *et al.*, 2016). TMD, transmembrane domain; MT, microtubules.

Golgin	Expression	Localization	GTPase interactions	Function
GM130/ golgin-95	Vertebrates Flies Worms Yeast	*Cis* (GRASP65)	Rab1 Rab2 Rab30 Rab33b	Tether and promote fusion of COPII vesicles, cisternal tethering, nucleate MT
p115	Vertebrates Flies Worms Yeast	*Cis* (GM130, Rab1)	Rab1	Tether and promote fusion of COPII vesicles
GMAP210/ TRIP230	Vertebrates Flies Worms Yeast Plants	*Cis* (ARF1)	ARF1 Rab2	Vesicle tethering, cilia cargo sorting, bind MT
Golgin-160/ GCP170	Vertebrates	*Cis* (ARF1)	ARF1	Anterograde trafficking of specific cargos, apoptotic stress sensing, Golgi positioning
Golgin-45	Vertebrates	Medial (GRASP55)	Rab2	Cisternal tethering
Golgin-84	Vertebrates Flies Worms	*Cis*/Medial Rims (TMD)	Rab1	Promote Golgi ribbon structure, tether COPI vesicles
CASP	Vertebrates Worms Yeast	Rims (TMD)	Cytohesin-1 (ARF6 GEF)	Tether COPI vesicles
Giantin/ GCP372	Vertebrates Flies	*Cis*/Medial Rims (TMD)	Rab1 Rab6	Tether intra-Golgi COPI vesicles, Golgi ribbon tethering
Golgin-97	Vertebrates Flies Yeast Plants	TGN (ARL1)	ARL1 Rab 6 Rab19 Rab20	Promote E cadherin anterograde trafficking, tether retrograde COPI vesicles
p230/ Golgin-245	Vertebrates Flies Worms Yeast Plants	TGN (ARL1)	ARL1 Rab2 Rab30	Promote TNF anterograde trafficking, tether retrograde COPI vesicles
GCC1/ GCC88	Vertebrates Flies Worms Yeast Plants	TGN (ARL1)	ARL1 Rab6 Rab19 Rab30	Tether retrograde COPI vesicles
GCC2/ GCC185	Vertebrates Flies Worms Yeast Plants	TGN (ARL1)	ARL1 Rab2	Tether retrograde COPI vesicles, nucleate MT at the Golgi
TMF/ ARA160	Vertebrates Flies Worms Yeast Plants	TGN Rims (Rab6)	Rab6	Vesicle and/or structural tether

ARF-like (ARL) GTPase, ARL1. However, these golgins can additionally bind to multiple members of the Rab GTPase family (Sinka *et al.*, 2008). The three golgins that are concentrated on Golgi rims (giantin, golgin-85, and CASP) contain transmembrane tail anchors that dictate their localization, yet giantin and golgin-85 can bind to Rabs, as well. Vesicles are coated with Rab GTPases, and the "Rab GTPase hopping" model suggests that these Rabs sequentially bind to Rab binding sites along the length of a golgin tether, causing the vesicle to move closer to Golgi membranes (Barinaga-Rementeria Ramirez and Lowe, 2009).

Two non-golgin proteins, the *cis*-Golgi localized Golgi Reassembly Stacking Protein (GRASP) 65 and medial-Golgi localized GRASP55, were initially thought to staple mammalian Golgi cisternae together. Further research suggested that, while they may have redundant roles, the two GRASPs actually form homo-oligomers in *trans* across cisternae (Bachert and Linstedt, 2010). The conformation required for this interaction is dependent on GRASP interactions with golgins – GM130 binds to GRASP65, and GRASP55 recruits golgin-45. Recent crystal structures have helped to elucidate how these golgins interact with the GRASP proteins to facilitate cisternae stacking and, in the case of GRASP65 and GM130, vesicle tethering (Hu *et al.*, 2015; Zhao *et al.*, 2017). GRASPs may also promote the formation of the lateral connections between cisternae that create the Golgi ribbon structure (Zhang and Wang, 2016b).

Due to their extended coiled-coil domains, golgins have long been considered ideal candidates for tethering functions. The domain structure of GMAP210 has implicated it in tethering vesicles to the Golgi: its C-terminal GRIP-related ARF-binding

(GRAB) domain binds Arf1 (this binding results in GMAP210 recruitment to the *cis*-Golgi) and the N-terminus of GMAP210 has an amphipathic lipid-packing sensor (ALPS) motif that binds to curved membranes (i.e. vesicles). One hypothesis of golgin function is based on this idea of Golgi-golgin-vesicle interaction. It proposes that golgins extend out from Golgi membranes, surrounding the organelle like "tentacles," and that vesicles (or other membranes) that enter this matrix will be blocked from interacting with the Golgi until the appropriate golgin on the appropriate cisternae recognizes its vesicle-localized binding partners (Munro, 2011). This theory is supported by the finding that golgins ectopically anchored to mitochondrial membranes can redirect certain subtypes of vesicle away from the Golgi to mitochondria. Golgins localized at the *cis*-Golgi recruit ER-derived vesicles, and *trans*-Golgi golgins recruit retrograde endosome-to-Golgi vesicles (Wong and Munro, 2014). This specificity is determined by short sequence motifs within the golgin N-termini (Wong *et al.*, 2017).

How this golgin tethering function promotes vesicle fusion is not clear, and may depend on the golgin involved. Many golgins have breaks in their coiled-coil domains, leading to the hypothesis that golgins can bend at these unstructured regions, bringing tethered vesicles closer to Golgi membranes. This was demonstrated to be the case for the *trans*-Golgi localized GCC2 (also called GCC185). Atomic force microscopy demonstrated that GCC2 dimers have a loose bubble-like hinge in the middle of the coiled-coil that can bend, bringing the cargo-binding GCC2 N-terminus close to the Golgi-binding C-terminus (Cheung *et al.*, 2015). Golgins can, in some cases, promote vesicle fusion through the interaction with SNARE proteins. The best-studied example is

the interaction between GM130, p115, and SNAREs. GM130 is localized to the Golgi by GRASP65, and p115 can bind to the N-terminus of GM130. The p115 protein can also bind to COPII coated vesicles derived from the ER (see Figure 1-1). The interactions between these proteins alter vesicle fusion through modulating SNARE complex formation. GM130 binding to syntaxin 5, a member of the SNARE complex at the *cis*-Golgi, blocks fusion by preventing syntaxin 5 from interacting with other SNARE complexes. In contrast, p115 binding promotes SNARE complex formation. GM130 binding to p115 inhibits GM130 function, allowing for SNAREs to form a complex and for vesicle fusion to occur (Barinaga-Rementeria Ramirez and Lowe, 2009).

The first vesicle tethering structures to be described were oligomeric tethers that can interact with both SNAREs and small GTPases. The Golgi-localized complexes, including the Transport Protein Particle (TRAPP), Conserved Oligomeric Golgi (COG), and Golgi-associated Retrograde Protein (GARP) complexes, are smaller than golgins and recently it has been proposed that golgins are responsible for initially tethering vesicles to Golgi membranes, but then vesicles are passed to the oligomeric tethering complexes, which can promote the actual fusion step (Witkos and Lowe, 2017).

The membrane and vesicle tethering mechanisms described above promote bulk (cargo nonspecific) trafficking through the Golgi. Possibly due to these general or wide-encompassing roles, it has been thought that golgins have semi-redundant functions. Indeed, most experiments involving depletion or knock out of single golgins have only mild effects on protein trafficking (Munro, 2011; Wong and Munro, 2014). However, three golgins have been shown to promote the trafficking of specific cargo proteins. E-

cadherin was shown to colocalize with golgin-97, but not other GRIP-domain containing golgins, in TGN-derived tubules and depletion of golgin-97 caused intracellular accumulation of E-cadherin (Lock *et al.*, 2005). Depletion of another GRIP domain golgin, p230 (also known as golgin-245), had no effect on E-cadherin surface delivery, but p230 was required for tumor necrosis factor-α (TNF) delivery to the plasma membrane (Lieu *et al.*, 2008). Golgin-160, the most studied golgin, is described in depth below.

Golgin-160

Similar to other golgins, golgin-160 was discovered as an autoantigen in immune compromised patients (Fritzler *et al.*, 1993). It is the product of the GOLGA3 gene, found only in vertebrates, and the predominant splice isoform is 1498 amino acids long. It contains the typical golgin extended alpha helices in the C-terminal two thirds of the protein (residues 394-1400; Misumi *et al.*, 1997) through which it can form coiled-coil homodimers (Hicks and Machamer, 2002). Golgin-160 is a peripheral protein. The predicted globular head domain of Golgin-160 (residues 1-393) contains Golgi targeting information between residues 172-257. Interestingly, the N-terminus also contains a cryptic nuclear localization signal (P_{232}REKKTSK_{239}) that redirects truncations of the head domain to the nucleus, but is apparently inactive in the full-length protein (Hicks and Machamer, 2002). Figure 1-2 depicts the general structure of a golgin-160 monomer, as well as regions involved in golgin-160 localization and binding to interacting proteins.

Despite structural similarities to other golgins, golgin-160 has several unique functions that separate it from other members of the golgin protein family. Golgin-160 is an ARF1 effector protein; both WT and the constitutively active ARF1 Q71L mutant

Figure 1-2: Golgin-160 structure and features. Schematic of golgin-160 structure. The N-terminal head domain (residues 1-393) is predicted to form a globular structure and is expanded here to show the overlapping Golgi targeting region, cryptic nuclear localization signal (NLS), and β1AR binding regions. Arrowheads indicate caspase cleavage sites. The C-terminus consists of elongated regions of alpha-helical coiled coil domains (displayed as yellow boxes) and contains the dynein binding region.

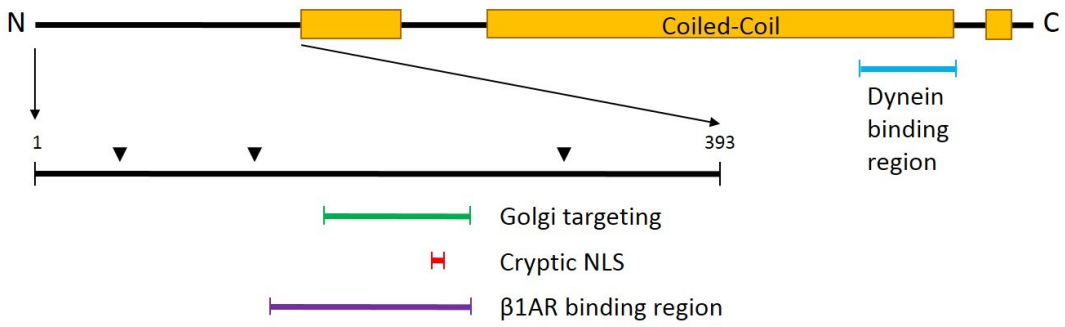

bind to the head domain of golgin-160, while the inactive ARF1 T31N does not. Golgin-160 recruitment to the Golgi is also dependent on the ARF1 GEF, GBF1 (Yadav *et al.*, 2012). While ARF1 has reported functions at both the *cis*- and *trans*-Golgi (Orci *et al.*, 1993; Stamnes and Rothman, 1993), golgin-160 is concentrated on the *cis* face of the Golgi (Hicks *et al.*, 2006). Golgin-160 has no reported role as a tether, rather it has several functions including: maintaining Golgi position and cell polarization, responding to secretory stresses, and in promoting the trafficking of specific cargo proteins (Mancini *et al.*, 2000; Maag *et al.*, 2005; Bundis *et al.*, 2006; Hicks *et al.*, 2006; Williams *et al.*, 2006; Yadav *et al.*, 2009, 2012).

When cells migrate towards cues (for example, during wound healing or towards a chemoattractant) the Golgi repositions to face the wounded edge (Kupfer *et al.*, 1982). Yadav et al. (2009) reported that golgin-160 is required for this Golgi repositioning during wound healing, and loss of golgin-160 led to impaired cell polarization. It was proposed that the role of golgin-160 in positioning the Golgi apparatus was due to its interaction with the motor protein dynein (Yadav *et al.*, 2012).

Another proposed role for golgin-160 is in responding to cell stresses at the early stages of apoptosis. Golgin-160 can be cleaved *in vitro* by caspases-2, -3, and -7. In cell culture, golgin-160 is initially cleaved by caspase-2 before undergoing further cleavage after cells are treated with staurosporine (Mancini *et al.*, 2000). Golgin-160 is cleaved at an early stage in apoptosis triggered by ER stress or ligation of death receptors. Stable expression of non-cleavable golgin-160 leads to a decrease in apoptosis induced by these apoptotic signals, indicating that golgin-160 cleavage may integrate apoptotic

signals with specific cellular stress responses. This integration is likely to be upstream of caspase activation, as expression of a caspase-resistant golgin-160 inhibited conversion of pro-caspase-2 and -8 into their cleaved, active forms (Maag *et al.*, 2005). The N-terminus of golgin-160 is also phosphorylated (Misumi *et al.*, 1997) by mixed lineage kinase 3 (MLK3), and overexpressing MLK3 led to an increase in caspase-3 cleavage of golgin-160, indicating that phosphorylation of golgin-160 may impact golgin-160 cleavage (Cha *et al.*, 2004).

This dissertation explores the role of golgin-160 in facilitating the trafficking of specific cargo proteins. It was initially reported that golgin-160 binds directly to PIST (post-synaptic density (PDZ) domain protein interacting specifically with TC10; also known as CAL, GOPC, and FIG) in an isoform-specific manner (Hicks and Machamer, 2005). PIST has been implicated in trafficking a subset of membrane proteins, and its interaction with golgin-160 indicated that golgin-160 might have a role in protein trafficking, as well. Indeed, further studies have demonstrated that golgin-160 interacts with and promotes the trafficking of three cargo proteins: the beta-1 adrenergic receptor (β1AR), glucose transporter type 4 (GLUT4), and renal outer medullary potassium channel (ROMK) (Bundis *et al.*, 2006; Hicks *et al.*, 2006; Williams *et al.*, 2006). There are likely more golgin-160 dependent cargo proteins that are currently unknown; advances in proteomics show promise in identifying novel interacting proteins and cargo (Huttlin *et al.*, 2015).

β1AR is the main adrenergic receptor in human cardiomyocyte cells. β1AR is a G protein coupled receptor (GPCR), which binds adrenaline and noradrenaline and signals

to increase heart rate through the parasympathetic response and its function in stimulating cyclic AMP (cAMP) signaling . Both increased cell surface levels and depletion of β1AR from cells are associated with heart disease, and β1AR is the main target of beta blockers for treatment of chronic heart failure (Port and Bristow, 2001; Wallukat, 2002; Christensen *et al.*, 2010; Xiang, 2011; Woo and Xiao, 2012). To ensure proper signaling, β1AR delivery to and retrieval from the plasma membrane must be tightly regulated. β1AR internalization, resensitization, and recycling back to the plasma membrane is linked to its phosphorylation state (Rapacciuolo *et al.*, 2003; Gardner *et al.*, 2004). β1AR recycling is also mediated by a dynamic palmitoylation site on its C-terminal tail (Zuckerman *et al.*, 2011).

While β1AR can bind to the PDZ domain of PIST (He *et al.*, 2004),it was found that golgin-160 can bind to β1AR directly, without PIST (Hicks *et al.*, 2006). This binding occurs between the head domain of golgin-160 (within residues 140-257) and the third intracellular loop of β1AR. Depletion of golgin-160 led to a decrease in the steady state surface levels of exogenously expressed β1AR in HeLa cells, which is due to a decrease in the rate of arrival of β1AR at the plasma membrane. Intriguingly, examination of the rate of β1AR oligosaccharide maturation demonstrated that trafficking to the *trans*-Golgi is identical with or without golgin-160, indicating that golgin-160 is affecting trafficking when β1AR is either at or past the *trans*-Golgi (Hicks *et al.*, 2006). Overexpression of golgin-160 results in increased β1AR surface levels, suggesting that golgin-160 not only promotes efficient trafficking of β1AR to the plasma membrane, it is also a limiting factor in β1AR trafficking in HeLa cells (Hicks *et al.*, 2006). This result is in

contrast to overexpression of PIST, which causes a reduction in β1AR surface levels (He *et al.*, 2004). This complex regulation is particularly interesting in light of the recent discovery that Golgi-localized β1AR is functionally active and is responsible for ~40-50% of cellular cyclic AMP signaling (Irannejad *et al.*, 2017). Golgin-160 may be important for maintaining a balanced pool of plasma membrane and Golgi localized β1AR.

Golgin-160 also mediates the trafficking of the glucose transporter GLUT4. Predominantly found in adipocytes and muscle cells, GLUT4 is a high affinity glucose transporter that translocates to the plasma membrane in the presence of insulin. In the absence of insulin, GLUT4 is stored in GLUT4 storage vesicles (GSVs) near the cell periphery (reviewed in Leto and Saltiel, 2012; Govers, 2014). Golgin-160 is upregulated during adipogenesis in 3T3-L1 adipocytes, and depletion of golgin-160 in these cells leads to a 6-fold increase in the plasma membrane levels of GLUT4 in the absence of insulin. Incomplete glycosylation of GLUT4 in golgin-160 depleted cells indicates that without golgin-160, GLUT4 bypasses both the TGN and the GSVs, instead trafficking directly to the plasma membrane (Williams *et al.*, 2006).

ROMK is an ATP-sensitive inward rectifying potassium channel that localizes to the apical membrane in human kidneys (reviewed in Hebert, 1995). Mutations that disrupt ROMK activity have been associated with Bartter's syndrome (Simon *et al.*, 1996). Binding between the C-terminus of ROMK and a region within the coiled-coil of golgin-160 was identified in a yeast two-hybrid screen, and this interaction was confirmed by immunoprecipitation of full length golgin-160 by the ROMK C-terminus from mammalian cell lysates. Co-expression of ROMK and golgin-160 in *Xenopus* oocytes

resulted in a 3.5 fold increase in plasma membrane levels of ROMK, which led to a 2-fold increase in ROMK generated currents (Bundis *et al.*, 2006).

As discussed above, many golgins promote bulk protein trafficking through the Golgi. Golgin-160 is atypical due to its selective promotion of protein trafficking. In HeLa cells depleted of golgin-160, the vesicular stomatitis virus G protein (VSV-G) has unaltered intra-Golgi transport and cell surface delivery (Hicks *et al.*, 2006). Likewise, co-expression of golgin-160 with the human cardiomyocyte potassium channel hERG (human *ether a-go-go*-related gene) did not lead to increased currents in *Xenopus* oocytes (Bundis *et al.*, 2006). This indicates that golgin-160 has evolved a specialized role distinct from most other golgins, which could be regulated by caspase cleavage in response to secretory pathway stress (Mancini *et al.*, 2000; Maag *et al.*, 2005).

While golgin-160 has not been strongly associated with diseases in humans, genetic disruptions in the mice homolog, Mea2, cause male sterility. Low expression of a truncated form of golgin-160 in a transgenic mouse was associated with loss of pachytene spermatocytes, and therefore loss of spermatozoa (Matsukuma *et al.*, 1999; Banu *et al.*, 2002). A point mutation in the GOLGA3/MEA2 gene that creates a premature stop codon decreases golgin-160 mRNA and results in undetectable golgin-160 protein in mice. While female mice with this mutation could produce offspring, male mice were sterile due to apoptosis of spermatocytes (Bentson *et al.*, 2013).

The lack of phenotypes outside of the testes in these golgin-160 disrupted mice is interesting, given the reported role of golgin-160 in facilitating the trafficking of β1AR,

GLUT4, and ROMK (Bundis *et al.*, 2006; Hicks *et al.*, 2006; Williams *et al.*, 2006) – all of which cause diseases when not expressed at the proper level (Simon *et al.*, 1996; Woo and Xiao, 2012; Govers, 2014). The defects in spermatogenesis in golgin-160 deficient mice may be due to the high requirement for protein production and trafficking in male germ cells: disruption of PIST in mice also leads to male sterility through disruption in acrosome formation, indicating the general importance of a functional secretory system in these cells (Yao *et al.*, 2002). It is also possible that stress conditions, under which the role of golgin-160 in apoptosis may become important, would unveil new phenotypes in these mouse models.

Small Monomeric GTPases

The Golgi is a dynamic organelle; membrane fusion and fission events allow for proteins to enter and exit cisternae as cargo proteins are processed through and transported from the Golgi. The Ras superfamily of small GTPases is critical for this temporal regulation of protein localization and function. They do this through their functions as molecular switches. These GTPases have different conformations when bound to GTP, GDP, and when empty. Effector proteins (proteins that bind to or are recruited by the small GTPases in a nucleotide dependent manner) have different binding affinities to each of these conformations, allowing for tight temporal regulation of the recruitment of specific proteins. Because of this, the nucleotide binding state of the GTPases must be tightly controlled. Nucleotide free Rab and ARF GTPases, which are members of the Ras superfamily, are in a closed, autoinhibited conformation and can only loosely associate with membranes. They generally require a GEF to release that

autoinhibition, allowing them to bind both to GTP and to membranes (Nawrotek *et al.*, 2016). Most small GTPases have very slow or undetectable GTPase activity, which would result in extended recruitment of effector proteins. This is prevented by the presence of GAPs, which catalyze GTPase activity (reviewed in Chavrier and Goud, 1999; Donaldson and Honda, 2005; Spang *et al.*, 2010). Three groups within the Ras superfamily - the Rab, ARF, and Arl GTPases – play essential roles in vesicle formation and fusion and are discussed further below.

Rab GTPases

The Rab GTPases constitute a large family (over 70 human Rab GTPases have been identified) with functions throughout the secretory and endocytic pathways. They have roles in sorting cargo into vesicles, trafficking vesicles along the cytoskeleton, and fusing vesicles at receptor membranes. Upon synthesis, Rabs are prenylated at their C-terminus (Chavrier and Goud, 1999; Barr, 2009; Zhen and Stenmark, 2015). An extended C-terminal tail allows for Rabs to extend 7-8 nm away from the membranes they are attached to in their GTP-bound state (Gillingham and Munro, 2007). While the nucleotide state of Rabs is not directly tied to their membrane association, GDP dissociation inhibitor (GDI) proteins, which dissociate Rabs from acceptor membranes and transport them back to donor membranes, specifically bind to GDP-bound Rabs (a simplified Rab GTPase cycle is shown in Figure 1-3A).

Rab1 is the only Rab GTPase required for anterograde trafficking through the Golgi in mammalian cells. It promotes the tethering of ER-derived vesicles to the early Golgi

through interactions with two golgins, p115 and GM130. Other Rab GTPases are thought to have semi-redundant roles in both anterograde and retrograde trafficking through the Golgi, which have been extensively reviewed (Chavrier and Goud, 1999; Monetta *et al.*, 2007; Barr, 2009; Stenmark, 2009; Hutagalung and Novick, 2011; Langemeyer and Barr, 2012; Zhen and Stenmark, 2015). One particularly interesting theory on vesicle trafficking is the "Rab GTPase hopping" hypothesis, which suggests multiple Rab binding sites on one golgin brings vesicles close to Golgi membranes, as was described previously. The interactions of various golgins with members of the Rab family can be found in Table 1-1.

ARF GTPases

The ARF family of proteins is critical for protein trafficking, particularly vesicle coating and uncoating (reviewed in D'Souza-Schorey and Chavrier, 2006; Donaldson and Jackson, 2011). There are five human members of the ARF family (ARF1, 3-6) which have semi-redundant roles in the secretory pathway (Volpicelli-Daley *et al.*, 2005). They attach to membranes through myristoyl modifications at their N-terminus, but unlike Rab GTPases this N-terminus is short, meaning that the ARF proteins sit close (1-2 nm) to membranes in their GTP-bound state (Gillingham and Munro, 2007, see Figure 1-3). While they share high sequence identity, there is enough variation to separate the ARFs into three classes based on homology: class I (ARF1 and 3), class II (ARF4 and 5), and class III (ARF6).

Figure 1-3: Small monomeric GTPase cycle. A) Cartoon depiction of the Rab GTPase cycle. The Rab (purple) in its GDP-bound form is escorted to membranes by GDI. The Rab then attaches to membranes through its prenylated tail with the assistance of GDF (GDI Dissociation Factor). A Rab GEF facilitates the transition to the GTP-bound active state, which leads to a conformation change that promotes effector recruitment. Rab GAPs promote GTP hydrolysis, and GDI can then bind to the GDP-bound Rab, remove it from the membrane, and transfer it elsewhere in the cell. B) A cartoon depiction of the ARF GTPase cycle. The ARF (green) in its GDP bound form has a myristoylated tail that is bound in an autoinhibited conformation. Upon close proximity to membranes, it can be converted into its GTP-bound form by ARF GEFs. The myristoyl modification is then inserted into the membrane and the adjacent amphipathic alpha helix interacts tightly with the membrane. Like Rab GTPases, the ARF undergoes conformational changes that allow for effector recruitment. Upon GAP-stimulated GTP hydrolysis, the ARF disassociates from the membrane, returning to the cytoplasm and regaining its autoinhibited conformation. Image adapted from (Behnia and Munro, 2005).

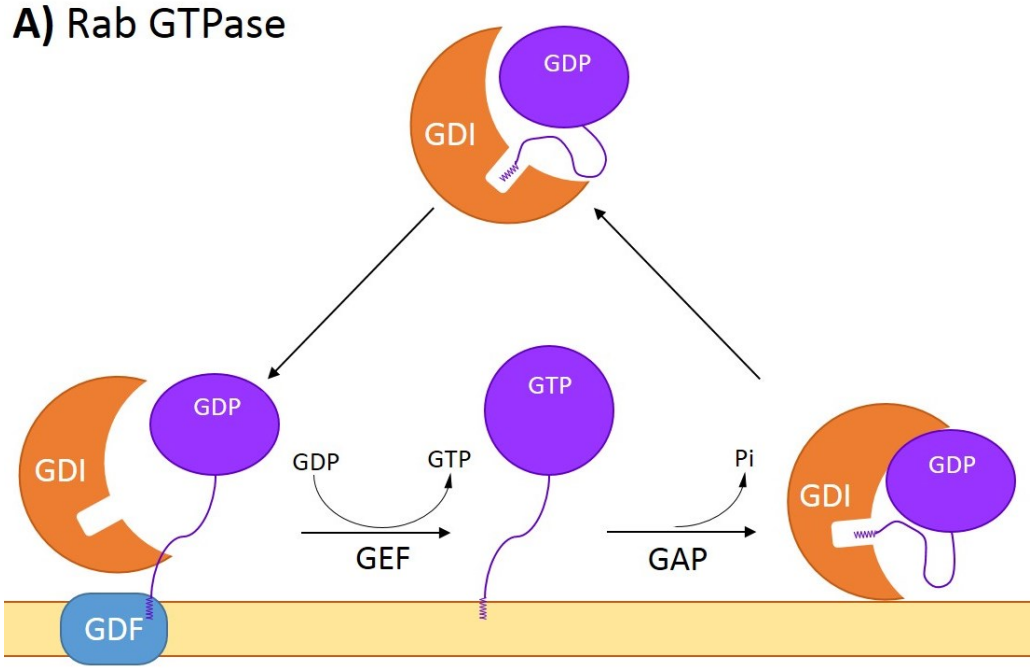
A) Rab GTPase
GDP
GDI
GDP
GDI
GTP
GDP
GTP
GEF
Pi
GAP
GDI
GDP
GDF

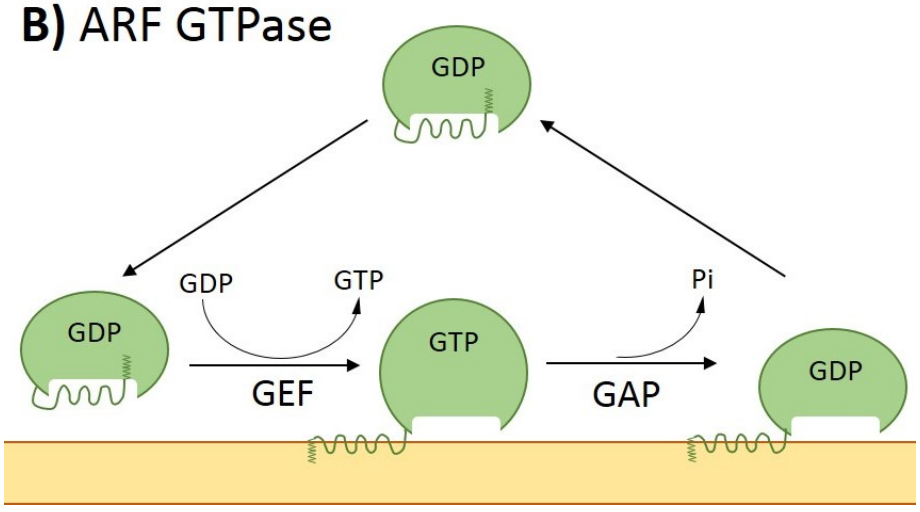
B) ARF GTPase
GDP
GDP
GDP
GTP
GEF
Pi
GAP
GTP
GDP

ARF1 is concentrated on the *cis* face of the Golgi, but has roles at the *cis*- and *trans*-Golgi, as well as at the plasma membrane (Dittié *et al.*, 1996; Pepperkok *et al.*, 2000; Kumari and Mayor, 2008). At the *cis*-Golgi, the binding of ARF1 to GTP is promoted by the ARF1 GEF, GBF1. GBF1 is a large ARF GEF, which is a GEF subtype characterized by proteins containing several additional domains outside of the catalytic sec7 domain. GBF1 is localized to Golgi membranes by the Rab1 isoform Rab1b (Monetta *et al.*, 2007). The GBF1-stimulated conversion of ARF1-GDP to -GTP creates conformational changes in ARF1 that allow for its N-terminal myristoylated amphipathic helix to insert into Golgi membranes (Antonny *et al.*, 1997; Liu *et al.*, 2009). As with other ARF GTPases, GTP binding also changes the conformation of ARF1 within the switch 1, interswitch, and switch 2 regions, allowing for specific binding of effector proteins (Donaldson and Jackson, 2011).

One major set of ARF1 effectors at the *cis*-Golgi is the COPI coat proteins needed for retrograde trafficking. The components of the heptameric COPI coat (α/β/β'/ε/γ/δ/ζ) pre-assemble into a complex in the cytoplasm, and ARF1-GTP recruits the complex onto Golgi membranes, where it can bind to cargo proteins either directly or through cargo adaptors (Donaldson *et al.*, 1992; Hara-Kuge *et al.*, 1994). ARF1-GTP hydrolysis is required for both efficient incorporation of these cargo proteins into the forming COPI vesicles and for the uncoating of vesicles prior to fusion with the ER. This hydrolysis is facilitated by three ARF GAPs (ARFGAP1, 2, and 3). It has been debated whether it is the actual ARF1 hydrolysis that is required for these steps, or if the ARFGAPs can serve as ARF1 effectors with distinct roles outside of promoting GTP hydrolysis (Lee *et al.*, 2005;

Spang *et al.*, 2010). As previously discussed, golgin-160 is another ARF1 effector at the *cis*-Golgi (Yadav *et al.*, 2012).

At the *trans*-Golgi, ARF1 promotes the formation of CCVs through the recruitment of cargo adaptor proteins. While GBF1 can localize to the *trans*-Golgi, it is another class of large ARF GEFs known as the brefeldin A-inhibited guanine nucleotide exchange proteins (BIGs) that are directly responsible for ARF1 activation in this subcompartment. GBF1 has been implicated in initiating an ARF GEF cascade at the *trans*-Golgi, interestingly through the activation of ARF4/5. These class II ARFs then recruit the BIG family of large ARF GEFs, BIG1/2, which subsequently activate ARF1/3 (Lowery *et al.*, 2013). ARF1 then, through recruitment of the clathrin adaptor proteins AP-1 and the GGAs, promotes the formation of CCVs (Dittié *et al.*, 1996; Donaldson and Honda, 2005).

ARF3 is often considered to be functionally identical to ARF1 due to high sequence homology, though there has been relatively little direct work to test this. ARF3 localizes at the *trans*-Golgi (Manolea *et al.*, 2010), indicating that it does not contribute to the ARF1 function of promoting retrograde Golgi-to-ER trafficking. It has been implicated in promoting CCV formation at the *trans*-Golgi (Volpicelli-Daley *et al.*, 2005). ARF3 has unique interactions with Golgi membranes, compared to ARF1, as demonstrated by the loss of Golgi localization of ARF3 at 20^{o}C, while ARF1 remains stably associated with Golgi membranes (Manolea *et al.*, 2010).

ARF4 and ARF5 are less abundant than the other ARFs and very little is currently known about their function *in vivo*. In ARF depletion experiments, double depletion of ARF5 with any additional ARF was associated with a defect in recycling from endosomes back to the plasma membrane (Volpicelli-Daley *et al.*, 2005), and disruptions in ARF5 binding to the golgin, Rab6-interacting (GORAB) protein have been associated with the recessive connective tissue disorder, gerodermia osteodysplastica (Egerer *et al.*, 2015). Double depletion of ARF4 and ARF5 also inhibited both dengue and hepatitis C virus infection (Kudelko *et al.*, 2012; Farhat *et al.*, 2016), though the mechanism of this inhibition is unclear.

ARF6 localizes to the plasma membrane and endosomes (Donaldson and Honda, 2005). It is important in endocytic trafficking through modulating the activity of lipid modifying enzymes. It has been implicated in the internalization of GPCRs, and interestingly it affects internalization irrespective of the pathway (clathrin-dependent, clathrin-independent, or caveolae-dependent) used by the receptor (Houndolo *et al.*, 2005; D'Souza-Schorey and Chavrier, 2006). Outside of the secretory system, ARF6 activity also impacts actin dynamics, membrane and cell movement, and cytokinesis (D'Souza-Schorey and Chavrier, 2006; Gillingham and Munro, 2007).

ARL GTPases

ARL GTPases interact closely with ARF and Rab GTPases in promoting trafficking through the secretory pathway. They have high sequence identity to ARF GTPases but have several differences, for example not all ARL proteins attach to membranes through

an N-terminal myristoyl modification. Some have no predicted modification, while others have acetylation or palmitoylation sites. ARL proteins generally are less functionally and mechanistically conserved compared to ARF family proteins (Gillingham and Munro, 2007).

ARL1 is myristoylated at its N-terminus and is recruited to the *trans*-Golgi. Its recruitment is dependent on another ARL protein, ARL3, possibly in a similar ARF GEF cascade as GBF1 and BIG1/2, as described above, though a GEF for ARL1 has yet to be identified (Munro, 2005). ARL1 has been implicated in recruiting several trafficking related proteins to the *trans*-Golgi and is the only ARL currently reported to interact with golgins. In particular, ARL1 is required for the membrane localization of the four GRIP-domain containing golgins, which have generally been associated with supporting retrograde endosome-to-Golgi trafficking (Munro, 2011; Gillingham and Munro, 2016), though golgin-97 and p230 are also implicated in promoting E cadherin and TNF anterograde trafficking, respectively (see Table 1-1). ARL1 is also required for the recruitment of the BIG1/2 ARF GEFs to the *trans*-Golgi, but not GBF1 (Christis and Munro, 2012).

Conclusions and Thesis Objectives

Protein trafficking through the Golgi requires a complex network of proteins that have tightly controlled spatial and temporal regulation. The golgin family of proteins and small monomeric GTPases work together to allow for this dynamic regulation. Three golgins have been reported to affect the trafficking of specific subsets of cargo through

unknown mechanisms. The objective of this dissertation is to examine the role of one of these atypical golgins, golgin-160, in the trafficking of its cargo β1AR. This work identifies a tribasic motif in the third intracellular loop of β1AR that is required for golgin-160 binding and characterizes the phenotypic consequences of mutating this binding motif. Hints on the mechanism behind golgin-160 influenced trafficking of β1AR have been obtained through the use of cargo trafficking synchronization techniques and analysis of golgin-160 localization using indirect immunofluorescence microscopy. Golgin-160 and -97 depletion experiments paired with live cell imaging and analysis of β1AR cell surface delivery provide further clues about β1AR trafficking at and beyond the *trans*-Golgi, and hint at a role for vesicle adaptor complexes and motor proteins in golgin-160 facilitated cargo trafficking. As alterations in β1AR surface levels, as with the surface levels of the other golgin-160-dependent cargo proteins, can lead to disease states, understanding of how golgin-160 modulates cargo trafficking could be of clinical importance. Finally, in the process of completing this work, a standard technique to synchronize protein trafficking was found to induce large disruptions in the localization and function of multiple Golgi resident proteins. Determining the mechanism behind these disruptions provides new insights into the connections between small GTPases and Golgi proteins.

Chapter 2

Three Basic Residues of Intracellular Loop 3 of the Beta-1 Adrenergic Receptor are Required for Golgin-160-Dependent Trafficking

Modified from Gilbert, C. E., Zuckerman, D. M., Currier, P. L., and Machamer, C. E. (2014). Int. J. Mol. Sci. *15*, 2929–2945.

Figures 2-2A and 2-4 were contributed by Dr. Carolyn Machamer, based on earlier work from David Zuckerman and Pamela Ronco.

Introduction

G protein-coupled receptors (GPCRs) are a large family of plasma membrane localized receptors with a characteristic seven transmembrane domain topology. Through activation of heterotrimeric G-proteins, GPCRs impact a multitude of normal cellular and disease processes and thus their modulation is of great interest. The regulation of receptor desensitization, internalization, and recycling back to the membrane has been extensively studied; less understood is the regulation of receptor biosynthesis and trafficking to the plasma membrane (reviewed in Dong *et al.*, 2007; Magalhaes *et al.*, 2012).

GPCR progression through the endoplasmic reticulum (ER) and Golgi is mediated by interactions with several classes of proteins. Several of these, including many PDZ (PSD-95, Discs-large, and ZO-1) containing proteins, interact with the C terminus of their GPCR binding partners, while others show specific binding to the third intracellular loops (Hu *et al.*, 2000; He *et al.*, 2004; Dong *et al.*, 2007; Cotecchia *et al.*, 2012). Recently, a highly conserved leucine in the first intracellular loop was shown to be critical for the ER export of multiple GPCRs through an unknown mechanism (Duvernay *et al.*, 2009). Receptor-activity-modifying proteins (RAMPs) not only promote ER exit of a subset of GPCRs, but can influence receptor specificity at the plasma membrane (Bouschet *et al.*, 2005; Dong *et al.*, 2007). GPCRs also show different requirements for Ras-like small GTPases during their trafficking (Wang and Wu, 2012). In this paper we focus on the atypical role of golgin-160 in influencing the initial delivery of the beta-1 adrenergic receptor (β1AR) to the plasma membrane.

β1AR is the primary beta adrenergic receptor in human cardiomyocytes and is responsible for the catecholamine-induced regulation of heart rate in the sympathetic "flight or fight" response. It also has been implicated in adipogenesis and memory formation; however, the majority of research has concentrated on its role in the heart as β1AR has been widely connected with heart disease (Soloveva *et al.*, 1997; Murchison *et al.*, 2004; Woo and Xiao, 2012). Both the downregulation and overstimulation of β1AR have been connected to myocyte apoptosis (Bristow *et al.*, 1993; Dash *et al.*, 2001; Port and Bristow, 2001). Until relatively recently, the bulk of research on the surface expression of β1AR has focused on its cycle of receptor desensitization, internalization, and recycling to the plasma membrane. This started to shift in 2004 when He *et al.* demonstrated that β1AR can be delayed at the Golgi when the Golgi resident PDZ-containing protein PIST (PDZ domain protein interacting specifically with TC10) is overexpressed (He *et al.*, 2004), and in 2006 Hicks *et al.* found that golgin-160 promotes trafficking of β1AR from the Golgi complex to the plasma membrane (Hicks *et al.*, 2006).

Golgins are a large family loosely characterized by their Golgi localization and extended coiled coil motifs and have traditionally been associated with maintenance of Golgi structure and assisting bulk flow of proteins through the organelle (Munro, 2011). Golgin-160 is a vertebrate-specific golgin that is one of only three golgins implicated in trafficking of specific cargoes (Lock *et al.*, 2005; Bundis *et al.*, 2006; Hicks *et al.*, 2006; Williams *et al.*, 2006; Lieu *et al.*, 2008). Hicks *et al.* demonstrated *in vitro* that the third intracellular loop of β1AR can interact with the N-terminal head domain of golgin-160 in a PIST-independent manner, and that depletion of golgin-160 from HeLa cells decreases

the steady state surface levels of exogenously expressed β1AR without affecting internalization rates. Surprisingly, given the steady state localization of golgin-160 to the *cis*-Golgi, this effect on trafficking occurs at or after the *trans*-Golgi network (Hicks *et al.*, 2006). While we initially proposed that golgin-160 might promote palmitoylation of β1AR, we later demonstrated that palmitoylation of β1AR was independent of golgin-160 and instead impacts receptor internalization, leaving the mechanism by which golgin-160 facilitates trafficking of β1AR unknown (Zuckerman *et al.*, 2011).

The specific interaction between golgin-160 and β1AR, in addition to being an unusual role for a golgin, suggests a novel mechanism of β1AR regulation independent of receptor desensitization and recycling. In this report, we further dissect the interaction between these two proteins and demonstrate that three basic residues in the third intracellular loop of β1AR are critical for binding to golgin-160. We further show that this binding is directly responsible for the efficient delivery of exogenously expressed β1AR from the *trans*-Golgi network to the cell surface.

Results

Three Basic Residues in Intracellular Loop 3 of β1AR Are Required for Direct Binding to Golgin-160

We previously showed that an *in vitro* transcribed and translated (IVTT) polypeptide consisting of the third cytoplasmic loop (L3, residues 249 to 325) of β1AR interacts with a region of the N-terminal head domain of purified GST-golgin-160, between residues 140 and 257 (Hicks *et al.*, 2006). To demonstrate that this interaction is direct, and not the result of other proteins present in the reticulocyte lysate, we performed binding assays with purified proteins. We used the NEB Intein Mediated Purification with an Affinity Chitin-binding Tag (IMPACT) system to create a purified, untagged golgin-160 head domain (residues 1 to 393) after intein cleavage. Using this method, we purified a protein that was detectable by immunoblotting with an antibody that recognizes the N-terminus of golgin-160 (Figure 2-1A). This untagged, purified golgin-$160_{(1–393)}$ was incubated with purified GST alone or GST-β1AR L3 that had been pre-conjugated to glutathione-Sepharose beads. Bound golgin-$160_{(1–393)}$ was detected using Coomassie blue staining (Figure 2-1B). Golgin-160 bound β1AR L3 specifically, indicating a direct interaction.

Further characterization of the golgin-160 and β1AR binding interaction required a more robust signal, so having demonstrated that the binding is direct we returned to the IVTT-generated proteins. We obtained the strongest binding readout using small segments of GST-tagged β1AR and IVTT [^{35}S]-labeled golgin-$160_{(1–393)}$. GST was fused to

Figure 2-1. Beta-1 adrenergic receptor (β1AR) binds directly to golgin-160$_{(1–393)}$. Representative gels for the purification of golgin-160$_{(1–393)}$ and its binding to β1AR are shown. (A) The NEB IMPACT system was used to create a purified, untagged golgin-160$_{(1–393)}$ following cleavage of the intein tag. DTT-induced cleavage caused enrichment of an approximately 60 kDa protein, which was specifically eluted off of the chitin column. This protein band could be detected using immunoblotting with an antibody to the N-terminus of golgin-160. Input, protein added to the chitin column; Cleaved, protein on the chitin column after addition of DTT but before elution; Eluate, protein released from the column after cleavage; *, golgin-160$_{(1–393)}$; **, GST fusion proteins; (B) The purified, untagged golgin-160 head domain was incubated with purified GST or GST-β1AR L3 pre-bound to glutathione-Sepharose 4B beads. The beads were washed and bound golgin-160$_{(1–393)}$ was detected by Coomassie blue staining after SDS-PAGE. Note that the samples in panel A were run on a 4%-12% gradient gel, whereas those in B were run on a 10% gel.

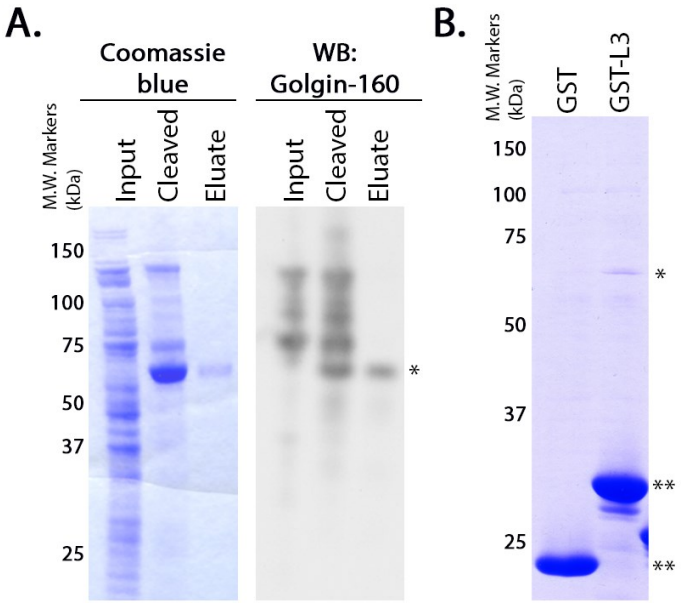
A.
Coomassie blue
WB: Golgin-160
M.W. Markers (kDa)
Input
Cleaved
Eluate
Input
Cleaved
Eluate
150
100
75
50
37
25
*
B.
M.W. Markers (kDa)
GST
GST-L3
150
100
75
50
37
25
*
**
**

the entire L3, the N-terminal half of L3 (residues 249 to 288, L3-NT), or the C-terminal half of L3 (residues 288 to 325, L3-CT). [^{35}S]-labeled golgin-160$_{(1–393)}$ was incubated with GST or the GST-L3 fusions pre-bound to glutathione-Sepharose and binding was detected by phosphorimaging. Golgin-160 binding was specific to L3-CT (Figure 2-2A). Human β1AR L3 contains three evolutionarily conserved basic residues, $K_{308}RR_{310}$. Through targeted mutagenesis we demonstrated that this cluster of three basic residues is required for interaction between β1AR and golgin-160: mutating the KRR sequence to three alanines (L3-CT/3A) eliminated binding *in vitro* (Figure 2-2A). Mutation of only two of these residues (RR_{310}) to alanines did not completely eliminate binding (data not shown). A schematic of this direct binding site on β1AR is shown in Figure 2-2B with the critical KRR residues highlighted in magenta. Figure 2-2C shows a schematic of golgin-160 with its β1AR binding region highlighted in green.

Full Length β1AR Interacts with Golgin-160 in a KRR-Dependent Manner

The *in vitro* binding was performed using small fragments of β1AR attached to large protein tags, so to test the relevance of these data we performed pull downs of the full length β1AR using lysates from transiently transfected HeLa cells. GST-golgin-160$_{(1–393)}$ was pre-conjugated to glutathione-Sepharose beads before being incubated with detergent lysates from cells transiently expressing full-length FLAG-tagged WT or 3A β1AR. β1AR bound to the golgin-160 head was detected by immunoblotting for the FLAG epitope (Figure 2-3A). The 3A mutant showed a 77.8% decrease in binding compared to WT (Figure 2-3B), supporting the *in vitro* data indicating a critical role for the KRR sequence

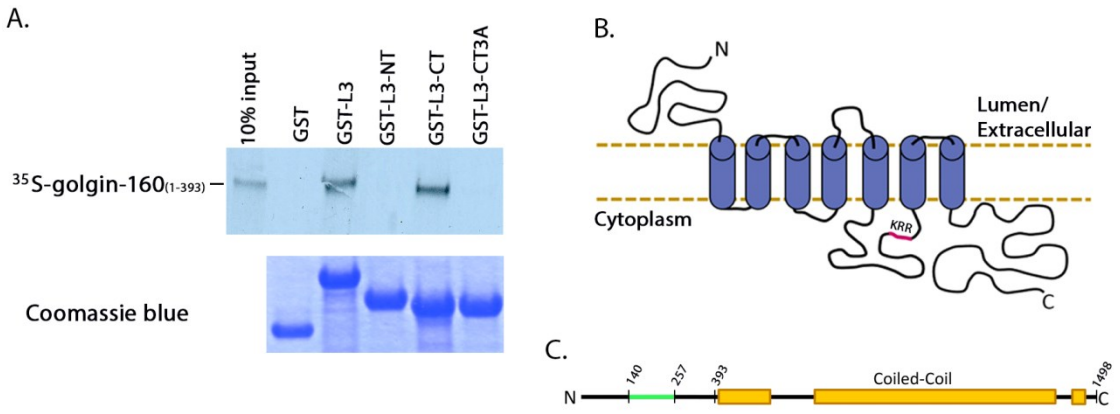

Figure 2-2. Three basic residues in the intracellular loop 3 of β1AR are required for binding to golgin-160. (A) Purified GST, GST-β1AR L3, GST-β1AR L3-NT, GST-β1AR L3-CT, or GST-β1AR L3-CT/3A were pre-bound to glutathione-Sepharose beads and incubated with [^{35}S]-labeled golgin-160$_{(1–393)}$. After washing the beads, bound golgin-160$_{(1–393)}$ was detected by phosphorimaging after SDS-PAGE. The input lane represents 10% of the starting material. The GST fusion proteins were visualized for equal loading with Coomassie blue staining; (B) The KRR residues are located in the third intracellular loop of β1AR, shown in magenta in this flattened schematic of the receptor; (C) The β1AR binding region between residues 140 and 257 of golgin-160 is shown in green (Hicks *et al.*, 2006). The coiled-coils characteristic of golgins are shown in orange.

in the interaction between these two proteins.

How does the mutation of only three residues almost completely disrupt binding? Human β1AR was modeled using Phyre2 with greater than 90% confidence for 87% of its residues using the recently crystallized turkey homologue as a template (Warne *et al.*, 2008). The predicted structure is displayed in Figure 2-3C with the KRR sequence highlighted in magenta. An expanded surface density model of intracellular loop 3 shows that the three basic residues are exposed on the surface of the loop. While the three-dimensional structure of golgin-160 is not known, the predicted globular head domain may form an acidic patch that can interact with this basic stretch, or alternatively the KRR residues may create a conformational state favorable for interaction with golgin-160.

Intra-Golgi Trafficking and Ligand-Induced Internalization of β1AR Are not affected by the 3A Mutation

Previous work demonstrated that golgin-160 does not impact trafficking of newly synthesized β1AR earlier than the *trans*-Golgi Network (TGN, (Hicks *et al.*, 2006)). However, recently a triple arginine motif in the third intracellular loop of the α-2B adrenergic receptor (α_{2B}AR) was found to mediate ER exit by influencing receptor interaction with the COPII-coated vesicle coat (Dong *et al.*, 2012). To investigate whether the 3A mutant affects the pre-TGN trafficking of β1AR, the O-glycosylation status of newly synthesized β1AR was examined. *O*-glycosylation is completed in the TGN, so a shift to a higher molecular weight "mature" form on

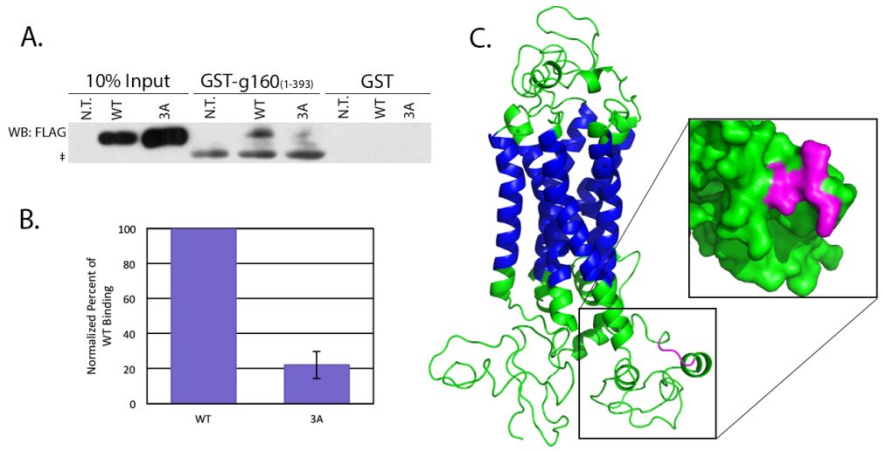

Figure 2-3. Full length β1AR interacts with golgin-160$_{(1–393)}$ in a KRR-dependent manner. (A) HeLa cells were either not transfected (N.T.) or transiently transfected with constructs encoding FLAG-β1AR WT or 3A. Lysates were prepared at 18 h post-transfection and incubated with GST- or GST-golgin-160$_{(1–393)}$-conjugated glutathione-Sepharose beads. Bound β1AR was detected by anti-FLAG immunoblotting. g160, golgin-160. The ‡ indicates nonspecific binding of the antibody to the GST-golgin-160 fusion protein; (B) Quantification of binding after normalization to input, $n = 7$, $p = 1.9 \times 10^{-7}$. Error bars represent standard deviation; (C) Structural model of human β1AR with an expanded region showing the surface filling model of intracellular loop 3. The KRR sequence is shown in magenta, the transmembrane regions are in blue. Structure prediction was performed using Phyre2 and modeled using PyMol.

denaturing gels indicates arrival of β1AR to this final Golgi compartment. A metabolic pulse-chase experiment was performed in cells expressing FLAG-β1AR WT or 3A. After a 15 min pulse label with [^{35}S]methionine and [^{35}S]cysteine, cells were harvested immediately (0 min) or after the indicated times of chase in unlabeled medium and β1AR was immunoprecipitated from the cell lysates. The shift from an immature to a mature, *O*-glycosylated form was visualized using phosphorimaging after SDS-PAGE and intensity of the bands measured. Three independent experiments were performed; a representative gel is shown in Figure 2-4A. The percent of β1AR that had reached the TGN was quantified by dividing the density of the mature band by the sum of the mature and immature band densities for each time point (Figure 2-4B). No difference in the rate of arrival at the TGN was observed between the WT and 3A forms of β1AR, indicating that β1AR 3A moves through the Golgi at the same rate as the wild type protein in spite of its reduced binding to golgin-160. Therefore, unlike α_{2B}AR, these three basic residues do not influence ER export.

Regulation of β1AR surface levels by endocytosis is well documented, in part due to beta adrenergic receptor agonists like isoproterenol (Iso), which stimulate receptor internalization (Sandnes *et al.*, 1987). After internalization, the receptor can either be diverted to the lysosome for degradation or recycled back to the plasma membrane. The third intracellular loop of β1AR contains a serine only two residues downstream from the KRR sequence that is critical for receptor recycling (Gardner *et al.*, 2004); because of this, we examined whether the 3A mutation had any effect on receptor recycling using an antibody internalization assay. HeLa cells transiently expressing FLAG-

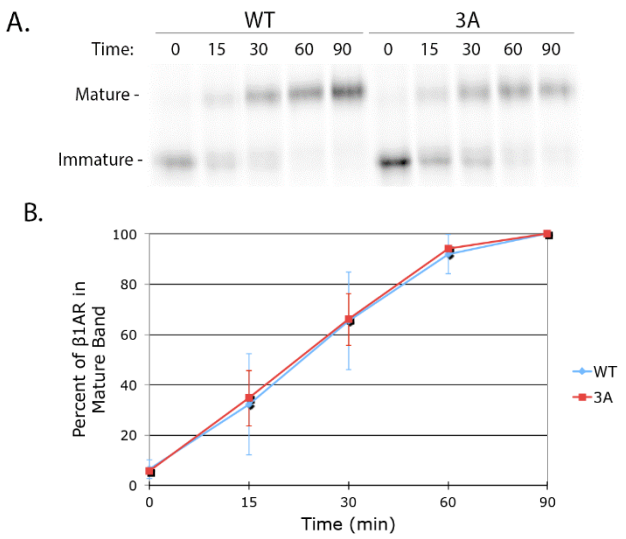

Figure 2-4. Trafficking of β1AR from the ER through the Golgi is not affected by the 3A mutation. (A) HeLa cells were transiently transfected with cDNAs encoding FLAG-β1AR WT or 3A. At 18 h post-transfection, cells were pulse-labeled for 15 min with [^{35}S]methionine and [^{35}S]cysteine, chased for 0–90 min, and lysed. β1AR was immunoprecipitated using anti-FLAG M2 affinity gel, separated by SDS-PAGE, and detected by phosphorimaging. A representative gel is shown. Passage through the *trans*-Golgi Network (TGN) was observed by a shift from an immature to a fully *O*-glycosylated (mature) band; (B) The percent of mature β1AR WT and 3A over 90 min. The percent mature was calculated for each individual time point by dividing the mature band density by the sum of the densities for the mature and immature bands. Error bars represent standard deviation, n=3.

tagged β1AR WT or 3A were fed anti-FLAG antibody with or without Iso for 30 min and the amount of internalized receptor was compared. Representative images are shown in Figure 2-5A. Internalization was quantified as the fold-increase in stimulated over unstimulated internalization in Figure 2-5B; no significant difference was seen between β1AR WT and 3A.

Taken together, the proper intra-Golgi trafficking of the 3A mutant (Figure 2-4) and normal internalization of the 3A mutant (Figure 2-5) indicate that disrupting the interaction between golgin-160 and β1AR does not affect the pre-TGN trafficking or plasma membrane internalization of β1AR, substantiating our golgin-160 depletion studies (Hicks *et al.*, 2006).

Steady State Surface Levels of β1AR 3A Are Decreased Compared to β1AR WT

Golgin-160 depletion by RNA interference causes a decrease in the steady state surface levels of exogenously expressed β1AR (Hicks *et al.*, 2006), so the binding-deficient 3A mutant was predicted to also have decreased surface levels. We first examined this qualitatively by differentially labeling the surface and internal pools of β1AR using indirect immunofluorescence microscopy (Figure 2-6A). The surface pool of the 3A mutant, labeled with anti-FLAG antibody in the cold prior to cell fixation and permeabilization, was reduced compared to WT. The internal pool, labeled using an anti-β1AR antibody post-fixation and permeabilization, appeared to be increased in the 3A mutant compared to WT. One explanation for decreased levels of protein at the

Figure 2-5. Internalization of β1AR from the plasma membrane is not affected by the 3A mutation. (A) Representative images of internalized β1AR WT or 3A following 30 min stimulation by Iso. HeLa cells expressing FLAG-tagged β1AR WT or 3A were serum starved for 3 h before receptor internalization was analyzed. Mouse anti-FLAG antibodies which recognize the exposed FLAG-tag were added to the serum free DMEM for 30 min, with or without the agonist Iso to induce internalization. Cells were then briefly acid washed to remove antibody from receptors still at the cell surface before they were fixed, permeabilized and labeled with a fluorescent secondary antibody to detect internalized antibody. The total internal pool of β1AR was detected using a rabbit antibody to the cytoplasmic C-terminus. Merge: red, anti-FLAG (internalized); green, anti-β1AR (total); blue, DNA stained with Hoechst 33258; (B) Internalization of β1AR WT or 3A was quantified as the fold-change of agonist-stimulated internalization over unstimulated. The fluorescent signal (integrated pixel density) was measured for each cell; only cells expressing similar levels of total β1AR were compared. Error bars represent standard deviation, $p = 0.327$.

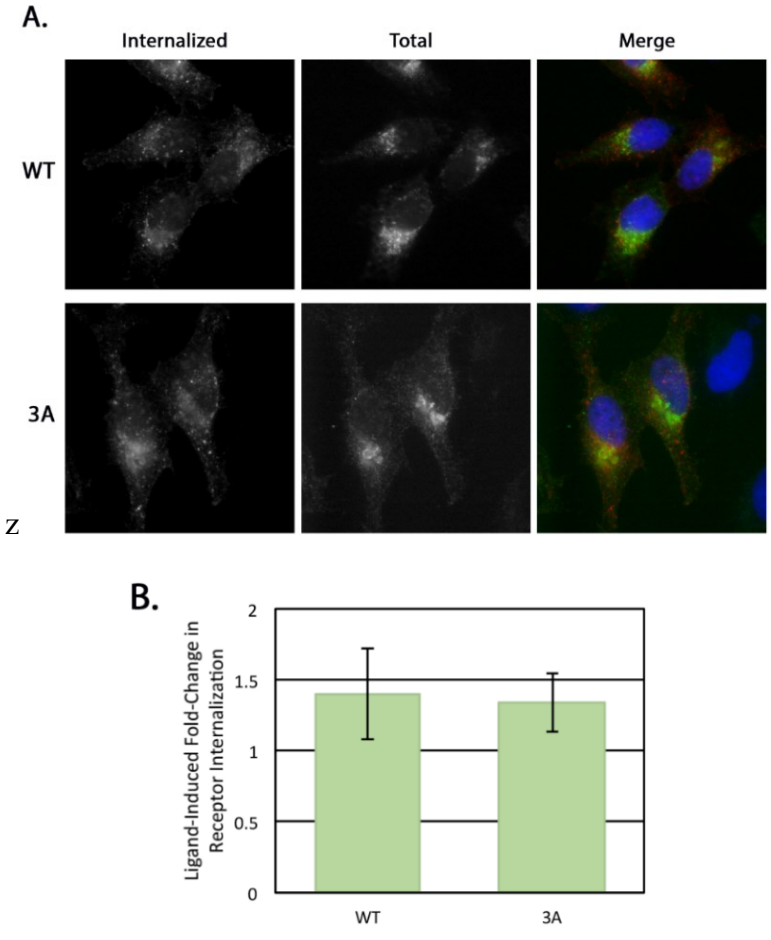
A.
Internalized
Total
Merge
WT
3A
B.
Ligand-Induced Fold-Change in Receptor Internalization
2
1.5
1
0.5
0
WT
3A

Z

plasma membrane is that β1AR 3A has a decreased half-life relative to that of the wild type protein. We ruled this out using both cycloheximide chase followed by immunoblotting and metabolic pulse-chase label followed by immunoprecipitation and phosphorimaging. The half-life of β1AR was 11.4 +/− 1.6 h and the half-life of the 3A mutant was 11.0 +/− 1.3 h using these two techniques. As the half-lives of both proteins were similar, we next compared the steady state surface levels of β1AR and β1AR 3A in a more quantifiable manner with a radiolabeled ligand binding assay. For this experiment, binding of [^{3}H]-labeled CGP-12177, a beta adrenergic receptor agonist, was assayed in cells expressing either β1AR WT or 3A. Surface levels were determined by quantifying cell-associated radioactivity after subtraction of background binding to non-transfected cells and normalization for total expression levels by immunoblotting. The 3A mutant bound 51% less ligand than WT, implying less than half the amount of the 3A receptor was present at the cell surface compared to WT (Figure 2-6B).

To ensure that the reduction in signal was not due to changes in the ligand binding site, we used Fluorescence Activated Cell Sorting (FACS) analysis to measure the surface pools of β1AR. HeLa cells transiently expressing FLAG-tagged β1AR WT or 3A for 16 h were surface labeled at 4°C using anti-FLAG antibody examined using FACS analysis. The mean fluorescence intensities of the two populations were compared as described (Hicks *et al.*, 2006). The 3A mutant had an average of 34% less receptor at the plasma membrane compared to WT β1AR (Figure 2-6C). The 17% difference seen in the ligand binding assay *versus* the FACS analysis may reflect a change in the ligand binding pocket induced by the mutation, or it may be because the ligand binding assays were

performed somewhat earlier post-transfection than the FACS analysis (14 h *vs.* 16 h). At 14 h, exogenously expressed β1AR may not have reached a steady state equilibrium at the plasma membrane. Nonetheless, these experiments both indicate that the 3A mutant is delivered less efficiently to the plasma membrane than the wild type protein. Further, the reductions seen in the 3A mutant surface levels are similar to the wild type β1AR surface levels after golgin-160 depletion (34% and 51% compared to 40%, (Hicks *et al.*, 2006)). This ability of the 3A mutant to phenocopy the effects of golgin-160 depletion on β1AR suggests that it is the lack of binding between golgin-160 and β1AR that causes the depletion phenotype.

Figure 2-6. Steady state surface levels of β1AR 3A are decreased compared to β1AR WT. (A) Representative images of surface and internal β1AR WT or 3A at 5 h post-transfection. Cells were labeled prior to fixation and permeabilization with anti-FLAG antibody to detect surface β1AR and then after fixation and permeabilization with anti-β1AR C-terminus antibody, allowing for differential labeling of the surface and internal pools. Merge: red, anti-FLAG (surface); green, anti-β1AR (internal); blue, DNA stained with Hoechst 33258; (B) Steady state surface levels of β1AR WT and 3A in transiently transfected HeLa cells were compared using radiolabeled ligand binding at 14 h post-transfection. After incubation with ligand for 3 h at 4°C, cells were washed, lysed, and cell-associated radioactivity was determined. The surface pool of β1AR WT or 3A was calculated after subtracting background binding on non-transfected cells and normalizing for total expression level by immunoblotting. Error bars represent standard deviation, $n = 3$, $p = 4.5 \times 10^{-6}$; (C) HeLa cells were co-transfected with expression plasmids encoding cytoplasmic GFP and either FLAG-β1AR WT or 3A. Sixteen h post-transfection, FACS analysis was performed to assess surface expression of β1AR. The median fluorescence intensity for β1AR was analyzed in GFP-positive cells to represent the average amount of β1AR at the plasma membrane. Error bars represent standard deviation, $p = 0.01$.

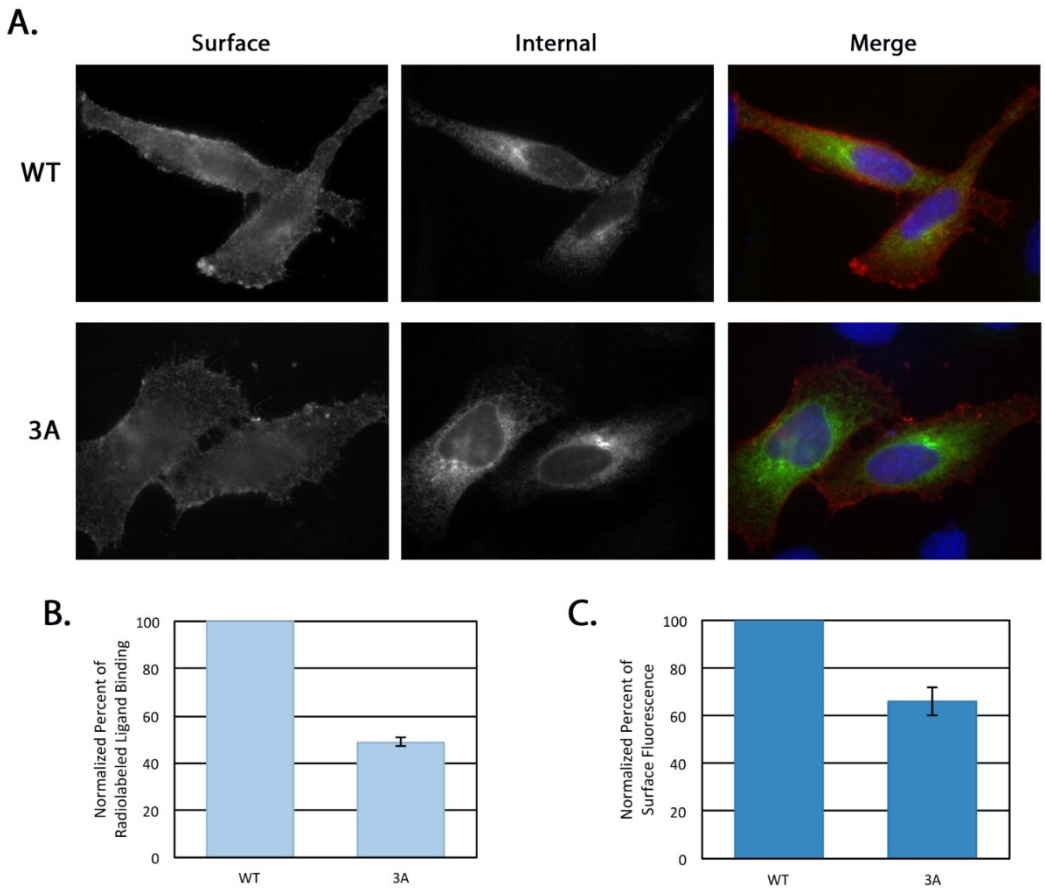
A.
Surface
Internal
Merge
WT
3A
B.
Normalized Percent of Radiolabeled Ligand Binding
100
80
60
40
20
0
WT
3A
C.
Normalized Percent of Surface Fluorescence
100
80
60
40
20
0
WT
3A

Discussion

Golgin-160 was the first protein described to positively impact β1AR trafficking from the Golgi to the plasma membrane. We previously demonstrated *in vitro* binding between these two proteins (Hicks *et al.*, 2006), but the interaction was largely uncharacterized. In this report, we have shown that golgin-160 can directly bind β1AR, that three basic residues in the third intracellular loop of β1AR are critical for the interaction, and that these residues are necessary for efficient β1AR trafficking from the Golgi to the plasma membrane in cells.

The third intracellular loop and C-terminus are the regions of greatest variance between the β1 and β2 adrenergic receptors. It is thought that the differences in protein interactions in these two domains account for many of the functional differences between the two receptors (Cotecchia *et al.*, 2012). The majority of proteins known to interact with β1AR bind to its C-terminal cytoplasmic tail via their PDZ domains and are involved in signal transduction and recycling from the plasma membrane (Cotecchia *et al.*, 2012). Previously, only endophilins SH3p4 and SH3p13 have been shown to bind to the third intracellular loop of β1AR. This binding depends on the Src homology SH3 domain and mediates receptor internalization and coupling with G_s (Tang *et al.*, 1999). Golgin-160 binding to the third intracellular loop may influence the interactions of these other proteins with β1AR. He *et al.* found that PSD-95 can compete for a binding site with PIST via their PDZ domains in order to modulate β1AR trafficking (He *et al.*, 2004); golgin-160 could be occluding a binding site in intracellular loop 3 in a similar manner.

Golgin-160 could also affect proteins binding to the C-terminal tail of β1AR. In 2007, Gardner *et al.* found that binding of a SAP97-AKAP79 protein scaffold to the C-terminus of β1AR was required for protein kinase A to phosphorylate a residue in loop 3, which is necessary for β1AR recycling to the plasma membrane (Gardner *et al.*, 2007). In an analogous fashion, golgin-160 may work cooperatively with other proteins that interact with the C-terminus of β1AR. At present, the influence of golgin-160 on other β1AR binding partners has not been studied.

To date, golgin-160 is the only protein demonstrated to interact directly with β1AR to regulate its Golgi to plasma membrane trafficking. This is an atypical role for a golgin: most golgins maintain Golgi structure or assist in global trafficking, for example by acting as vesicle tethers. Only two other golgins, *trans*-Golgi-localized golgin-97 and p230/golgin-245, have been implicated in trafficking of specific cargoes. Golgin-97 colocalizes with E-cadherin in post-Golgi transport carriers and golgin-97 depletion inhibits E-cadherin trafficking (Lock *et al.*, 2005). Similarly, golgin-245 colocalizes with tumor necrosis factor-α (TNF) in TGN tubules and depletion of golgin-245 prevents TNF localization to the plasma membrane (Lieu *et al.*, 2008). Golgin-160, in addition to its role in facilitating plasma membrane delivery of β1AR, can bind to the apical potassium channel ROMK and promote its delivery to the cell surface (Bundis *et al.*, 2006), and it is required for the proper localization of GLUT4 into insulin-responsive storage compartments (Williams *et al.*, 2006).

Because golgin-160 impacts efficient trafficking of β1AR and GLUT4 is mislocalized in its absence, we hypothesize that golgin-160 facilitates specialized sorting

of cargo at the TGN. The complexity of post-Golgi sorting has become more apparent in recent years. In non-polarized cells, it was once believed that proteins moved from the TGN to the plasma membrane by a single route, but it is now apparent that there are many routes to the cell surface (De Matteis and Luini, 2008). In polarized cells, not only have distinct apical and basolateral sorting pathways been demonstrated, but proteins headed for the same cell surface also segregate into separate transport pathways at the TGN based on their mode of regulation (Fölsch *et al.*, 2009; Mattila *et al.*, 2012; Arnspang *et al.*, 2013). Very little, however, is known about the composition of these various transport carriers or how this differential sorting occurs. We propose that golgin-160 plays a role in this sorting step, guiding cargo into vesicles so that specific cargo can be efficiently targeted. It is possible that golgin-160 accomplishes this directly by moving with cargo, or it could facilitate the interaction of its cargo with another protein, as proposed above. Both of these possibilities will be investigated by using the 3A mutant as a golgin-160-independent cargo protein. Since mutating only three basic residues dramatically interferes with this interaction, it may be that either a charged stretch or a three-dimensional conformation created by these three residues is critical for interaction with golgin-160. Our findings bring us closer to the identification of a binding motif, sequence-based or structural, among golgin-160 cargoes, which will then allow for a directed investigation into other potential cargoes including other GPCRs.

Neither depletion of golgin-160 nor disruption of its binding to β1AR completely disrupts β1AR localization—more than 50% of β1AR still makes it to the plasma membrane. This suggests that golgin-160 is playing a regulatory role, enhancing β1AR

surface expression. This method of regulation is possible as golgin-160 can itself be subject to regulatory control. Golgin-160 is recruited to the Golgi through binding of GTP-bound ARF1, which is in turn rapidly cycling on and off the Golgi (Presley *et al.*, 2002; Yadav *et al.*, 2012). Its localization may also be affected by interactions with dynein (Yadav *et al.*, 2012). Additionally, golgin-160 can undergo cleavage by caspase-2, -3, and -7 as well as phosphorylation by MLK3 (Mancini *et al.*, 2000; Cha *et al.*, 2004). All of these interactions and modifications could alter the localization or conformation of golgin-160, which could mediate interaction with β1AR. In the future, it will prove useful to study the dynamics of endogenous golgin-160 and β1AR movement in the context of cardiomyocytes to gain a better understanding of this putative regulatory cycle.

Materials and Methods

Cells and Transfection

HeLa cells were maintained in DMEM (Life technologies, Grand Island, NY, USA) with 10% Fetal Bovine Serum (Atlanta Biologicals, Flowery Branch, GA, USA) and 0.1 mg/mL Normocin (InvivoGen, San Diego, CA, USA) at 37 °C with 5% CO_2. Cells were grown in 35 mm dishes, 6 cm dishes, or 12-well plates depending on the experiment, and transfected with 3 µL X-tremeGENE9 DNA transfection reagent (Roche, Indianapolis, IN, USA) per 1 µg DNA.

Expression Constructs

Glutathione S-transferase (GST) fusion proteins of golgin-$160_{(1–393)}$ have been previously described (Hicks and Machamer, 2005). The untagged golgin-$160_{(1–393)}$ protein was constructed by polymerase chain reaction (PCR) amplifying residues 1–393 from the previously described pBluescript SK+ golgin-160 construct (Mancini *et al.*, 2000) and inserting a stop codon after residue 393, which was then inserted into New England Biolab's pTBY12 vector for purification using the IMPACT system (New England Biolabs, Beverly, MD, USA). Human FLAG-β1AR cDNA in pcDNA3 was provided by Randy Hall (Emory University, Atlanta, GA, USA). The 3A mutation, converting $K_{308}RR_{310}$ to $A_{308}AA_{310}$, was introduced using Quikchange mutagenesis (Stratagene, La Jolla, CA, USA). GST-tagged β1AR loop 3 (L3) was constructed by PCR amplification of residues 249 to 325 of β1AR and inserting the fragment into the pGEX-2T expression plasmid (GE

Healthcare, Little Chalfont, Buckinghamshire, UK). GST-β1AR L3 *N*-terminus (NT) was constructed by PCR amplifying residues 249 to 288 of β1AR, and the C-terminus (CT) likewise by PCR amplifying residues 288 to 325, followed by insertion into the pGEX-2T expression plasmid. GST β1AR L3CT with the 3A mutation was created by amplifying residues 288 to 325 from the β1AR 3A plasmid (described above), followed by insertion into the pGET-2T expression plasmid. The cytosolic GFP vector pEGFP C1 was obtained from Clontech (Mountain View, CA, USA).

Antibodies

Mouse monoclonal anti-FLAG was from Sigma-Aldrich (St. Louis, MO, USA). Rabbit anti-β1AR was obtained from Santa Cruz Biotechnology (Santa Cruz, CA, USA). Rabbit anti-golgin-160 was previously described (Mancini *et al.*, 2000). R-Phycoerythrin-conjugated IgG goat anti-mouse was from Jackson ImmunoResearch Laboratories Inc. (West Grove, PA, USA). Alexa Fluor 568 anti-mouse IgG and Alexa Fluor 488 anti-rabbit IgG were from Life Technologies. Horseradish peroxidase (HRP)-conjugated secondary antibodies were from GE Healthcare.

In Vitro *Binding*

GST-fusion proteins were grown in *Escherichia coli* BL21 cells (Stratagene) as previously described (Hicks and Machamer, 2005). GST or the GST-fusion proteins were purified from the soluble fraction of the cell lysates according to manufacturer instructions using glutathione-Sepharose 4B beads (GE Healthcare). The purified proteins (5 μg each) were

diluted in PBS and rebound to glutathione-Sepharose 4B beads by incubating them overnight at 4 °C with rotation. Untagged golgin-160$_{(1\text{-}393)}$ was purified using the NEB IMPACT system as described by the manufacturer (New England Biolabs, Beverly, MD, USA). To confirm the purity and identity of the resulting protein, the eluate was separated on NuPAGE 4%–12% Bis-Tris Gel (Invitrogen, Carlsbad, CA, USA) and was detected by Coomassie blue staining or immunoblotted with rabbit anti-golgin-160. Purified golgin-160$_{(1–393)}$ in the elution buffer (20 mM HEPES pH 8.5, 500 mM NaCl, 1 mM EDTA, 50 mM DTT) was added to the conjugated GST-fusion proteins and incubated 4–6 h at 4 °C. After washing, protein remaining attached to the glutathione-Sepharose beads was eluted, separated by SDS-PAGE (10% gel) and detected by Coomassie blue staining.

For the binding assays using *in vitro* transcribed and translated golgin-160, the GST-fusion proteins were purified and 3 µg of each was rebound to glutathione Sepharose beads as above. IVTT [^{35}S]-labeled golgin-160$_{(1–393)}$ was prepared following the manufacturer's instructions and as previously described (Promega, Madison, WI, USA, (Hicks *et al.*, 2006)). Golgin-160 was then diluted in binding buffer (25 mM HEPES, 125 mM KOAc, 5 mM EDTA, 0.5% Nonidet P-40 (NP-40), 1 mM DTT) and incubated with the GST-fusion proteins for 2 h at 4 °C. After washing, bound golgin-160 was eluted and separated by SDS-PAGE followed by phosphorimaging on a PharosFX molecular imager (Bio-Rad, Hercules, CA, USA).

Pull Downs from Cell Lysates

HeLa cells grown to 70% confluency were left untransfected, or transfected with 0.5 μg of either pcDNA/WT or 3A β1AR. After incubating for an additional 16–18 h, cells were lysed in a potassium acetate lysis buffer (125 mM potassium acetate, 25 mM HEPES pH 7.1, 1 mM DTT, 1% NP-40, protease inhibitor cocktail). The soluble fraction of the lysed cells was incubated 2 h at 4 °C with 10 μg GST alone or GST-tagged golgin-$160_{(1–393)}$ that had been pre-conjugated to glutathione-Sepharose 4B beads. After washing the beads twice with lysis buffer, protein bound to the beads was separated by SDS-PAGE and β1AR was detected by immunoblotting with anti-FLAG antibody followed by ECL. The amount of protein in the input and pull down bands was measured after imaging on a VersaDoc Imaging System Model 5000 (Bio-Rad, Hercules, CA, USA) using Quantity One volume analysis tools (Bio-Rad, Hercules, CA, USA). Percent bound was calculated after first normalizing 3A and WT to their input and significance was calculated using a heteroscedastic two-tailed Student's t-test.

Modeling of β1AR

The nucleotide sequence of the human β1AR mRNA was obtained from NCBI for the *Homo sapiens* adrenoceptor beta 1 (ADRB1) mRNA (Accession number NM_000684). The corresponding amino acid sequence was submitted for intensive modeling to the Protein Homology/analogY Recognition Engine (PHYRE) V 2.0 server (Structural Bioinformatics Group, London, UK). The resulting predicted protein structure was then visualized using PyMOL (Schrödinger, Portland, OR, USA).

Metabolic Pulse-Chase and Immunoprecipitation

HeLa cells grown to 70% confluency were transiently transfected with 0.5 µg pcDNA/FLAG-β1AR WT or 3A. At 15–18 h post-transfection, cells were pulse labeled for 15 min with [^{35}S]methionine and [^{35}S]cysteine. For following movement of β1AR to the TGN, cells were chased for 0–90 min and lysed on ice for 5 min in 1% NP-40, 0.4% deoxycholic acid, 50 mM Tris pH 8, 62.5 mM EDTA pH 8, with protease inhibitor cocktail (Sigma-Aldrich). For determination of the half-life of β1AR, cells were chased for 0, 3, 6, or 9 h and lysed as described above. β1AR was immunoprecipiated with anti-FLAG-M2 affinity gel (Sigma-Aldrich, St. Louis, MO, USA), and after washing, the samples were eluted and separated by SDS-PAGE. The density of protein bands was measured using Quantity One volume analysis tools (Bio-Rad, Hercules, CA, USA) after phosphorimaging as described above.

Receptor Internalization

HeLa cells at 70% confluency on coverslips in 35 mm dishes were transfected with 0.5 µg of either pcDNA/FLAG-β1AR WT or 3A. After 16–18 h the medium was switched to serum-free DMEM for 3 h. For the internalization assay, 1 µg/mL mouse anti-FLAG antibody was added to the serum-free medium with or without 10 uM isoproterenol (Iso, Sigma-Aldrich) for 30 min at 37 °C. Cells were then washed with PBS and left untreated or remaining surface antibody was removed with an acid wash (0.5 M NaCl, 0.5% HOAc, pH 1) for 1 min at room temperature. Cells were then fixed and permeabilized as previously described (Hicks *et al.*, 2006) and the internal pool of β1AR

detected using the rabbit anti-β1AR C-terminal antibody described above. Alexa Fluor 568 anti-mouse IgG and Alexa Fluor 488 anti-rabbit IgG were used for secondary labeling and Hoechst 33258 was used as a DNA stain. Cells with similar rabbit anti-β1AR signal intensity were selected for comparison and all images were taken on the same day with the same exposure on an Axioskop microscope (Zeiss, Thornwood, NY, USA) equipped with epifluorescence using an ORCA-03G charge-coupled device camera (Hamamatsu, Japan) using iVision software (BioVision Technologies, Exton, PA, USA). The integrated pixel density of the anti-FLAG signal for each cell was determined using Image J (National Institutes of Health, Bethesda, MD, USA) and was normalized to background fluorescence. Statistical analysis was performed using a two-tailed heteroscedastic Student's *t*-test.

Surface Immunofluorescence

HeLa cells grown to 70% confluency on coverslips in 35 mm dishes were transfected with 0.5 μg of either pcDNA/FLAG-β1AR WT or 3A. After 5 h the cells were rinsed in ice cold PBS and incubated on ice with mouse anti-FLAG antibody for 15 min. Cells were then fixed and permeabilized as previously described (Hicks *et al.*, 2006) and the internal pool of β1AR detected using the rabbit anti-β1AR *C*-terminal antibody described above. Alexa Fluor 568 anti-mouse IgG and Alexa Fluor 488 anti-rabbit IgG were used for secondary labeling and Hoechst 33258 was used as a DNA stain. All images were taken on the same day with the same exposure on an Axioskop microscope (Zeiss, Thornwood,

NY, USA) equipped with epifluorescence using an ORCA-03G charge-coupled device camera using iVision software (version 4.5.1, BioVision Technologies, Exton, PA, USA).

Cycloheximide Chase

HeLa cells were grown to 70% confluency in 35 mm dishes and were transfected with 0.5 µg of either pcDNA/FLAG-β1AR WT or 3A. After 16 h the cells were rinsed in PBS and incubated with DMEM containing 100 µg/mL cycloheximide (Calbiochem, La Jolla, CA, USA). After 0, 2, 4, 6, and 8 h, cells were lysed on ice for 5 min in 1% NP-40, 0.4% deoxycholic acid, 50 mM Tris pH 8, 62.5 mM EDTA pH 8, with protease inhibitor cocktail. Soluble protein was separated by SDS-PAGE and immunoblotted with rabbit anti-β1AR antibody.

Radiolabeled Ligand Binding

HeLa cells at 70% confluency on 12-well plates were transfected with 0.12 µg pcDNA/β1AR WT or 3A per well in triplicate. Nontransfected cells were used to determine background binding. After 14 h, cells were washed in cold PBS and incubated with 10 nM [^{3}H]-labeled CGP-12177 (PerkinElmer Life Sciences, Waltham, MA, USA) diluted in KRH buffer (136 mM NaCl, 4.7 mM KCl, 1.25 mM $MgSO_4$, 1.25 mM $CaCl_2$, 20 mM HEPES, pH 7.4, and 2 mg/mL BSA) for 3 h at 4 °C. Cells were then washed in PBS and lysed as described above. Cell-associated radioactivity was determined using a Beckman Coulter LS6500 scintillation counter (Brea, CA, USA). Total expression level was determined by immunoblotting lysate prepared from a parallel transfected dish with

anti-FLAG antibody followed by ECL. Three independent experiments (each done in triplicate) were averaged. Statistical analysis was performed using a two-tailed heteroscedastic Student's *t*-test.

FACS Analysis

HeLa cells growing in 6 cm dishes to 70% confluency were co-transfected with 1.5 µg cytosolic GFP (pEGFP-C1) and 0.5 µg of either pcDNA/FLAG-β1AR WT or 3A. After 16-18 h, cells were harvested by trypsinization before being washed twice with DMEM and resuspended at (5–10) × 10^6 cells/mL in blocking solution (1% BSA in PBS). After blocking for 30 min on ice the cells were incubated 1 h on ice with monoclonal mouse anti-FLAG diluted in blocking solution. Cells were washed in PBS and then were incubated 1 h on ice in phycoerythrin-labeled goat anti-mouse IgG, also diluted in blocking solution. Cells were washed again in PBS before being resuspended in serum-free DMEM and analyzed using a FACSCalibur flow cytometer (Becton Dickinson, Franklin Lake, NJ, USA). The mean phycoerythrin fluorescence intensity of cells expressing GFP was calculated for each sample using CellQuest Pro software (Becton Dickinson). Significance was determined using a two-tailed heteroscedastic Student's *t*-test.

Chapter 3

Golgins influence Post-Golgi Trafficking of the Beta-1 Adrenergic Receptor

Introduction

Protein processing through the secretory pathway can be divided into three general stages: synthesis, modification, and then delivery of proteins to their final destination. Recent reviews have emphasized the complexity of this final step, both in sorting proteins into appropriate carriers for post-Golgi delivery, and in successfully transporting those carriers to their target membrane (Anitei and Hoflack, 2011). One family of proteins, the golgins, has been implicated in supporting bulk protein trafficking through and out of the Golgi, particularly through their roles as vesicle tethers (Gillingham and Munro, 2016; Witkos and Lowe, 2017). Three golgins (golgin-160, p230/golgin-245, and golgin-97) have been reported to have the ability to promote the trafficking of specific subsets of cargo proteins (Lock *et al.*, 2005; Hicks *et al.*, 2006; Lieu *et al.*, 2008).

Golgin-97 and p230 are both GRIP (golgin-97, RanBP2α, Imh1p, and p230/golgin-245) domain containing golgins that localize to the *trans*-Golgi network (TGN) through interaction with ADP ribosylation factor-like GTPase 1 (ARL1; Munro, 2005). But despite having similar targeting mechanisms, GRIP domain containing golgins do not heterodimerize with each other and separate into distinct subdomains of the TGN (Gleeson *et al.*, 2004). This could explain previous findings that golgin-97 colocalizes with and promotes the trafficking of E-cadherin, but does not influence the surface delivery of tumor necrosis factor α (TNF) while p230 facilitates the surface delivery of TNF but does not colocalize in tubules containing E-cadherin (Lock *et al.*, 2005; Lieu *et al.*, 2008).

The third atypical golgin, golgin-160, has been implicated in the trafficking of three proteins: the glucose transporter type 4 (GLUT4), renal outer medullary potassium channel (ROMK), and beta-1 adrenergic receptor (β1AR; Bundis *et al.*, 2006; Hicks *et al.*, 2006; Williams *et al.*, 2006). Golgin-160 is localized to the *cis*-Golgi in an ADP-ribosylation factor 1 (ARF1) and Golgi Brefeldin A Resistant Guanine Nucleotide Exchange Factor 1 (GBF1) dependent manner, yet it affects the post-Golgi trafficking of GLUT4 and β1AR (Hicks *et al.*, 2006; Williams *et al.*, 2006; Yadav *et al.*, 2012). In cells depleted of golgin-160, GLUT4 bypasses the *trans*-Golgi and GLUT4 storage vesicles and is delivered directly to the plasma membrane (Williams *et al.*, 2006). β1AR has a decreased rate of arrival at the plasma membrane but unaffected intra-Golgi trafficking in cells lacking golgin-160 (Hicks *et al.*, 2006).

β1AR is the main adrenergic receptor in human cardiomyocytes (Wallukat, 2002). A G protein coupled receptor (GPCR), its localization, sensitization, and internalization is highly regulated by phosphorylation (Gardner *et al.*, 2004, 2006, 2007). Both increased and decreased function of β1AR at the cell surface have been associated with heart disease, and it is the main cellular target of the commonly used beta blocker medications (Bristow *et al.*, 1993; Port and Bristow, 2001; Woo and Xiao, 2012). Interestingly, recent reports have demonstrated that β1AR not only signals from the plasma membrane, but that β1AR at the Golgi can also be activated by ligands to initiate a signal cascade (Irannejad *et al.*, 2017).

In this chapter, we investigated the mechanism behind the golgin-160 facilitated trafficking of β1AR. We found that β1AR trafficking through the Golgi-induces changes in golgin-160 localization that may be required for the function of golgin-160, and investigate the impact of golgin-160 depletion on post-Golgi vesicle dynamics. We also demonstrate that β1AR anterograde trafficking is likely not facilitated by golgin-97 or p230.

Results

Golgin-160 loses its Golgi localization when β1AR is constitutively expressed

Golgin-160 facilitates the trafficking of β1AR through a currently unknown mechanism (Hicks *et al.*, 2006; Gilbert *et al.*, 2014). As we investigated this role of golgin-160, we discovered that constitutive expression of β1AR in HeLa cells led to a 25% decrease in Golgi localized golgin-160 (Figure 3-1A and C). Golgin-160 is an ARF1 effector protein that is peripherally and dynamically associated with Golgi membranes (Yadav *et al.*, 2012). At the *cis*-Golgi, ARF1 is activated by its GEF, GBF1. If golgin-160 was dispersing from Golgi membranes due to a decrease in the levels of ARF1-GTP, supplying an excess of GBF1 could increase the cellular pool of ARF1-GTP and prevent golgin-160 dispersal. However, we did not observe any protective effect of co-transfecting GBF1 and β1AR (23% decrease, Figure 3-1B and C). We therefore hypothesize that loss of golgin-160 localization on Golgi membranes could be required for its function in promoting β1AR cell surface delivery, and not merely a consequence of altering the ARF1 nucleotide binding state.

Loss of golgin-160 localization occurs as β1AR reaches a golgin-97 containing TGN compartment

We next wanted to understand the timing of golgin-160 dispersal in order to elucidate its role in β1AR trafficking. Synchronization of cargo trafficking at distinct compartments within the secretory pathway allows for precise control of when proteins reach specific stages of the pathway. Because the commonly used synchronization

Figure 3-1: Golgin-160 loses its Golgi localization when constitutive β1AR is expressed, and this is not rescued by GBF1 overexpression. Representative images of HeLa cells transfected with (A) β1AR alone or (B) β1AR and GBF1 for 18 h. Cells were labeled with rabbit anti-golgin-160 and mouse anti-GM130, followed by Alexa Fluor 488 anti-rabbit IgG and Alexa Fluor 546 anti-mouse IgG. Arrows indicate the Golgi regions of β1AR expressing cells. (C) Quantification of golgin-160 dispersal. The GM130 signal was used to outline the Golgi region in each cell, and the amount of golgin-160 fluorescent signal was measured within the Golgi and divided by the total golgin-160 fluorescence in the cell to obtain the percent of golgin-160 at the Golgi. Each fluorescence intensity value was normalized to nontransfected cells. Two independent experiments were performed, and n=39-43 cells were quantified per condition. $p<0.001$ for all comparisons of untransfected to transfected conditions, but the difference between β1AR alone and β1AR + GBF1 was not significant.

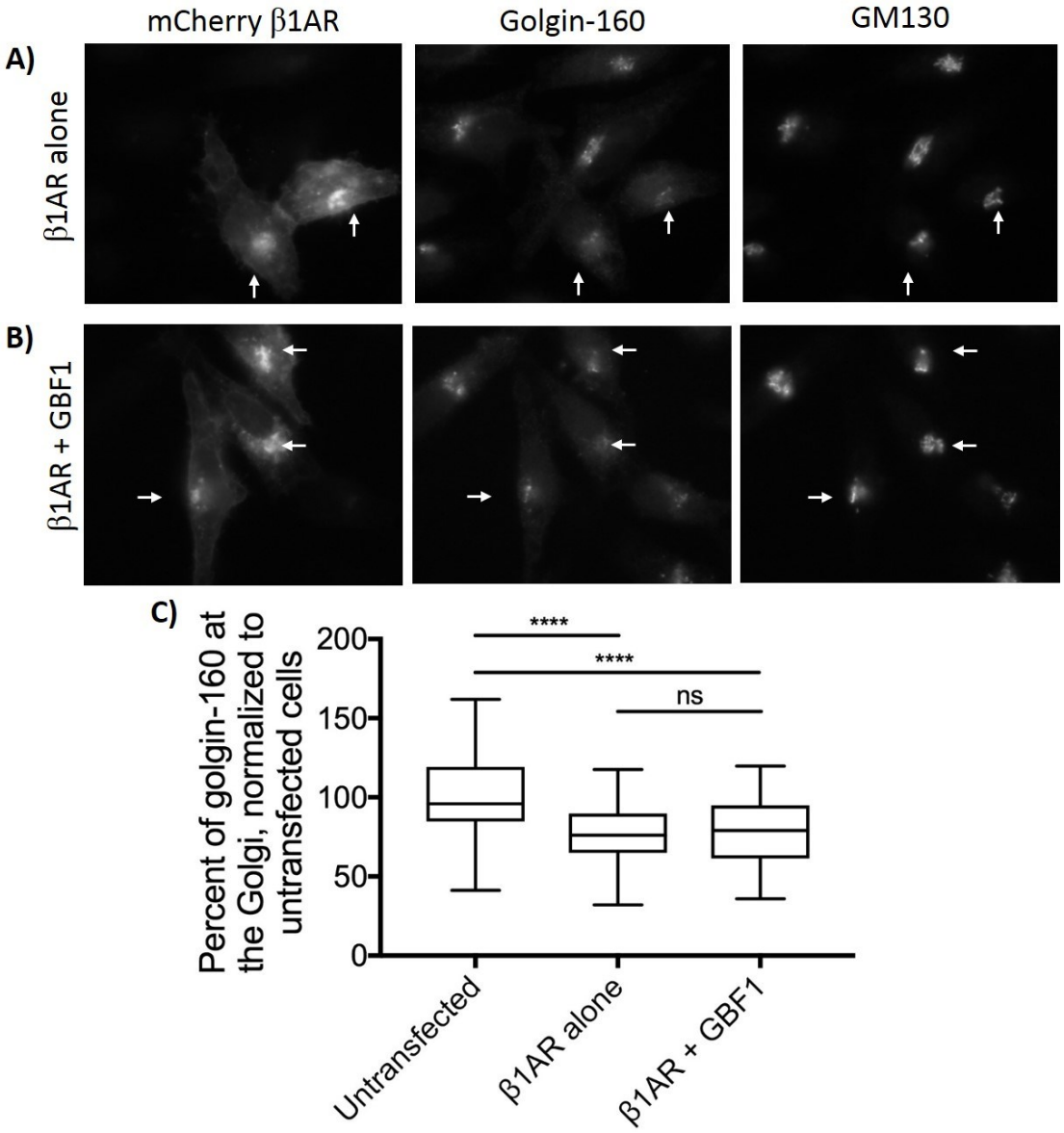
mCherry β1AR
Golgin-160
GM130
A)
β1AR alone
B)
β1AR + GBF1
C)
Percent of golgin-160 at the Golgi, normalized to untransfected cells
200
150
100
50
0
****
****
ns
Untransfected
β1AR alone
β1AR + GBF1

technique, 20°C and 16°C cold temperature blocks, caused golgin-160 to become cytoplasmic (see Chapter 4), we investigated alternative means of synchronization.

The Retention Using Selective Hooks (RUSH) system, developed by the Perez lab (Boncompain *et al.*, 2012), uses the relative affinities of streptavidin, streptavidin binding peptide (SBP), and biotin to regulate protein trafficking. This system utilizes three components: a Hook protein (here, we utilized the ER-localized major histocompatibility complex (MHC) class II invariant chain (Ii), abbreviated MHCII below) that is fused with streptavidin, a cargo protein of interest (here, mCherry-tagged β1AR) that has a SBP tag added to its luminal N-terminus, and membrane permeable biotin. The Hook and β1AR are encoded on a bicistronic plasmid, and upon plasmid transfection and expression, the Hook streptavidin interacts with the β1AR SBP, retaining β1AR in the ER. Biotin can outcompete the SBP tag for streptavidin binding, causing β1AR to be released to traffic through the secretory system normally (schematic in Figure 3-2A). Transient transfection of HeLa cells with the RUSH β1AR plasmid led to an accumulation of β1AR in the ER in the absence of biotin (Figure 3-2B). After a 30 min treatment with 10 μM biotin, β1AR was observed to localize to the Golgi by indirect immunofluorescence microscopy. Surface staining using an antibody against β1AR at these two conditions revealed that no β1AR was localized at the plasma membrane. After 1 h biotin treatment, β1AR could be observed at the plasma membrane by surface staining.

Using the RUSH system, we were able to gain temporal understanding of golgin-160 dynamics during β1AR trafficking. Due to the convoluted, intertwined ribbon

Figure 3-2: The RUSH system allows for a synchronized bolus of β1AR to travel through the Golgi. (A) Schematic of synchronized β1AR trafficking using the RUSH system. Interactions between and localizations of the mCherry-SBP-tagged β1AR construct (blue), the streptavidin MHCII ER hook (red), golgin-160 (green), and biotin (yellow) are drawn in the absence of biotin, and in the presence of biotin over time as β1AR travels through the Golgi and into post-Golgi vesicles. (B) HeLa cells transfected with RUSH β1AR for 20 h were treated with 10 uM biotin for 0, 30, or 60 min. Surface β1AR was labeled with a mouse anti-mCherry antibody on intact cells, and the total β1AR fluorescence was detected using a rabbit β1AR specific antibody, followed by labeling with Alexa Fluor 488 anti-mouse IgG and Alexa Fluor 546 anti-rabbit IgG.

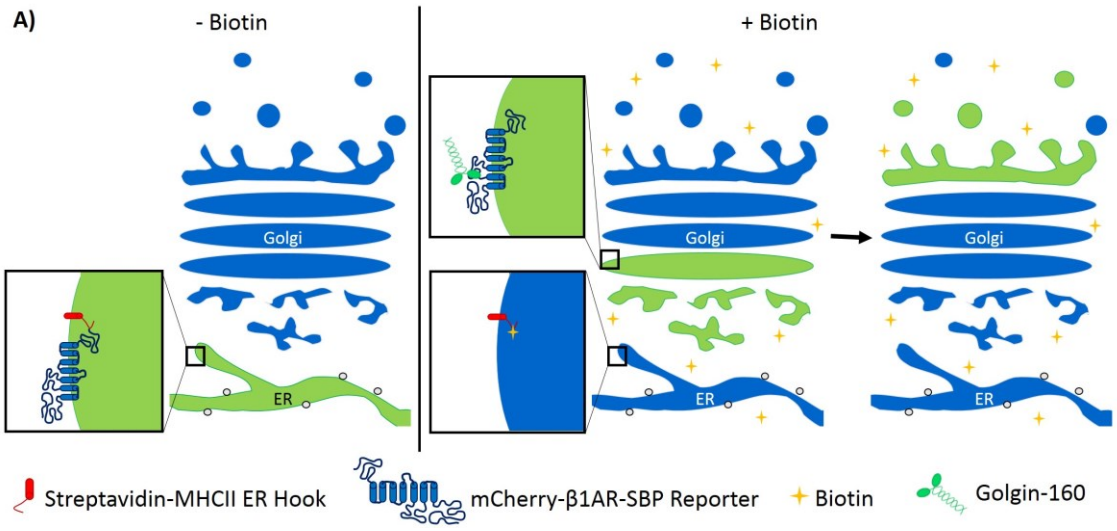
A)
- Biotin
+ Biotin
Golgi
ER
Streptavidin-MHCII ER Hook
mCherry-β1AR-SBP Reporter
Biotin
Golgin-160

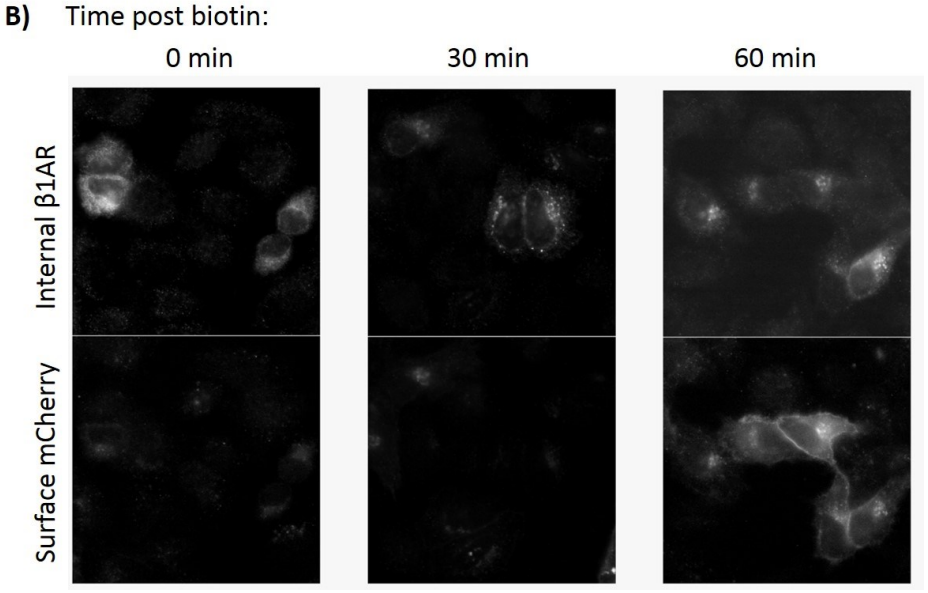
B)
Time post biotin:
0 min
30 min
60 min
Internal β1AR
Surface mCherry

structure of the mammalian Golgi, colocalization can be difficult to accurately measure in the intact Golgi by light microscopy. To simplify this, we added 1 μg/mL nocodazole to HeLa cells expressing RUSH β1AR. Nocodazole disrupts the microtubule network and causes the Golgi to separate into ministacks. These ministacks still contain *cis*, medial, and *trans* cisternae, but are no longer laterally tethered to other Golgi stacks and are diffusely localized through the cell. β1AR can still traffic to the plasma membrane in nocodazole treated cells, though trafficking is slower than in untreated cells (Figure 3-3A). β1AR reached Golgi ministacks within 20 minutes of biotin addition, where it colocalized with golgin-160 in *cis*-Golgi cisternae. At 40 minutes post biotin, β1AR localized to cisternae marked by the *trans*-Golgi protein, golgin-97. At this time, loss of membrane-associated golgin-160 was observed. β1AR colocalization with golgin-97 and the loss of golgin-160 membrane localization was still observed 60 minutes post biotin addition, but by 80 minutes post biotin addition β1AR was observed at the plasma membrane and golgin-160 was once again observed on Golgi membranes. This indicates that golgin-160 becomes dispersed from Golgi membranes after β1AR has passed through the *cis*-Golgi, and can return to the *cis*-Golgi either after a set period of time (between 20-40 minutes in the absence of an intact microtubule network) or after β1AR has left the *trans*-Golgi.

RUSH synchronized β1AR traveled sequentially from golgin-160 containing cisternae to golgin-97 containing cisternae. Pearson's r colocalization coefficient was measured for β1AR and each of the golgins, and a spike in the colocalization of β1AR and golgin-160 occurred 20 minutes after biotin addition, while colocalization with

Figure 3-3: Golgin-160 loses membrane localization as β1AR localizes with golgin-97 at the *trans*-Golgi network. (A) Golgin-160 (green) loses Golgi localization during β1AR (blue) trafficking 40 min after biotin addition, and recovers after 80 min biotin treatment when β1AR has left the Golgi and reached the PM. β1AR colocalizes with golgin-97 (red) 40-60 min post biotin addition. Insets of the small boxed regions depict the localizations of two proteins per box for clarity. Left inset: comparing golgin-160 and golgin-97 localization. Center inset: Comparing golgin-160 and β1AR localization. Right inset: comparing β1AR and golgin-97. (B) Quantification of the Pearson's r correlation coefficient between β1AR and either golgin-160 or golgin-97 over the first 60 minutes of trafficking. (C) β1AR does not colocalize with another *trans*-Golgi golgin, p230 in a similar assay to that performed in (A). Left inset: enhanced view of the boxed region for clarity. Right inset: comparing only β1AR and p230 localization in the boxed region. For all images, mCherry fluorescence was used to identify β1AR localization, rabbit anti-golgin-160 and either mouse anti-golgin-97 or -p230 followed by labeling with Cy5 anti-rabbit IgG and Alexa Fluor 488 anti-mouse IgG were used to determine golgin localization. Microscopy was performed in one (for C) or two (for A) independent experiments. n>30 cells were analyzed per condition.

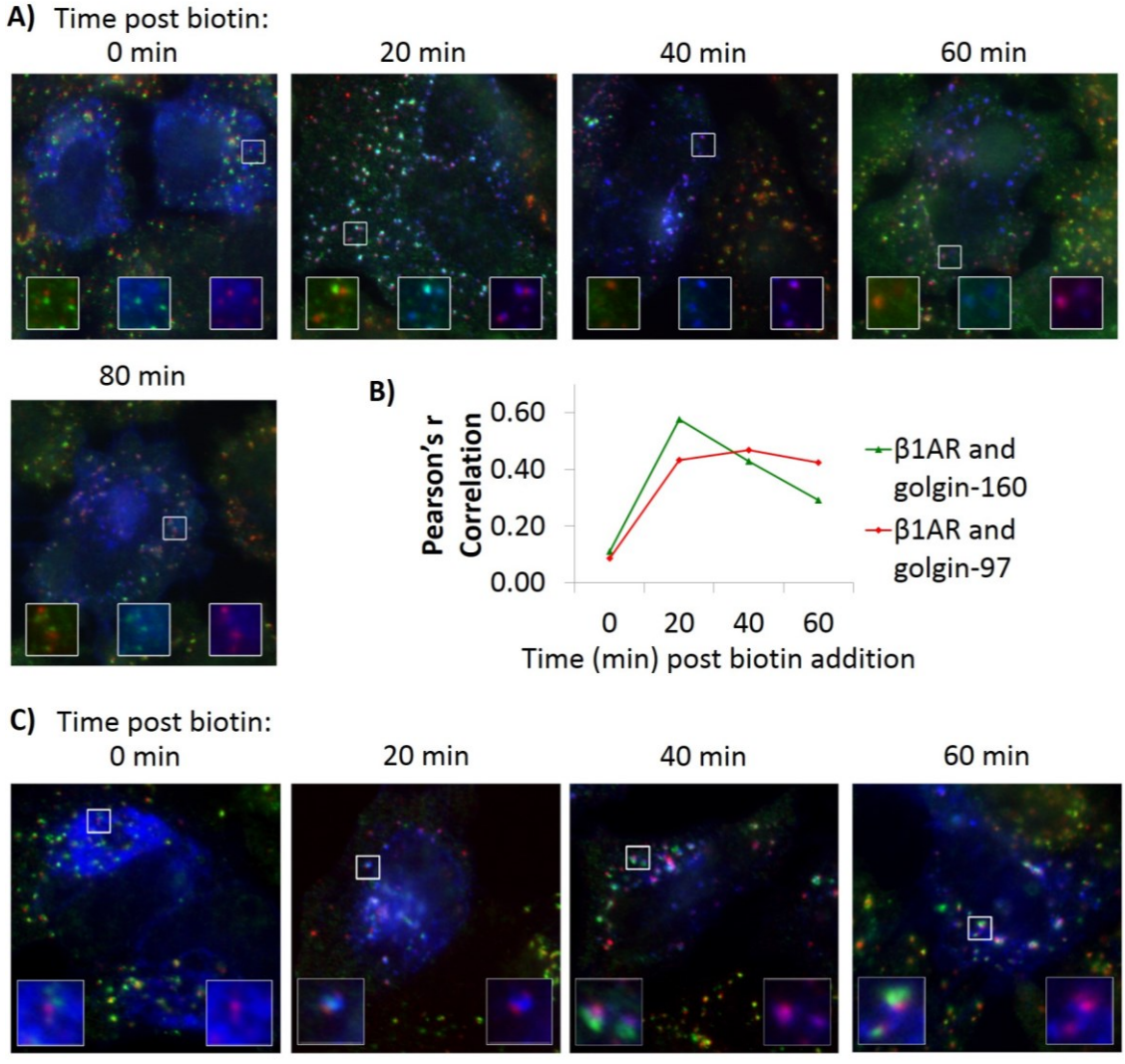
A) Time post biotin:
0 min
20 min
40 min
60 min
80 min
B)
Pearson's r Correlation
0.60
0.40
0.20
0.00
0
20
40
60
Time (min) post biotin addition
β1AR and golgin-160
β1AR and golgin-97
C) Time post biotin:
0 min
20 min
40 min
60 min

golgin-97 continued to increase and reached a plateau 40 minutes post biotin (Figure 3-3B). The packaging of cargo proteins at the *trans*-Golgi is a complex process, and part of this packaging can involve separating cargo proteins into subdomains based on their transport machinery. To see if β1AR was being specifically sorted into golgin-97 containing subdomains, we compared the localization of β1AR to another golgin, p230. Like golgin-97, p230 is localized at the *trans*-Golgi through interaction with the small GTPase ARL1, however these proteins are known to localize to separate TGN subdomains (Gleeson *et al.*, 2004). Using indirect immunofluorescence microscopy to examine the localization of β1AR and p230 during trafficking using the RUSH system, we did not observe any significant colocalization between the two proteins after biotin addition (Figure 3-3C).

Golgin-97 does not promote anterograde trafficking of β1AR

Golgin-97 has reported functions in both anterograde trafficking from and retrograde trafficking to the Golgi. We did not detect direct binding between β1AR and golgin-97 (data not shown), but that did not rule out indirect or transient interactions between these two proteins. We utilized RNAi depletion to determine which role, if any, golgin-97 is playing in β1AR trafficking. In HeLa cells, RNAi depletion of golgin-97 was variable, ranging from 65% to 80% decrease in the amount of golgin-97 protein, measured by Western blotting (Figure 3-4A). RNAi depletion of golgin-160 alone and double depletion of golgin-160 and golgin-97 were also performed, resulting in >70-80% depletion of each protein in each condition.

For each depletion condition, the amount of steady state β1AR at the plasma membrane was measured by indirect immunofluorescence microscopy and flow cytometry. By immunofluorescence, at 18 h post transfection with N-terminally FLAG-tagged β1AR, intact cells were labeled with anti-FLAG antibody to selectively mark the surface pool of β1AR. Cells were then permeabilized and total β1AR was detected using a C-terminal antibody (Figure 3-4B). The fluorescence intensity of each signal was used to measure the amount of β1AR at the cell surface, which was then normalized to the total amount of β1AR per cell. The percent of β1AR at the plasma membrane is reported in Figure 3-4C. Flow analysis was also used to measure the amount of β1AR at the plasma membrane. HeLa cells were co-transfected with constitutive FLAG-tagged β1AR and cytoplasmic GFP. Live cells were immunostained with anti-FLAG and labeled with a phycoerythrin conjugated secondary antibody at 18 h post transfection. Flow cytometry analysis was then performed to assess surface expression of β1AR. The mean fluorescence intensity for β1AR was determined in GFP-positive cells to represent the average amount of β1AR at the plasma membrane and all values were normalized to control β1AR surface levels (Figure 3-4D). Depletion of golgin-160 led to a decrease (26% by immunofluorescence and flow) in the steady state surface levels of β1AR, as expected. Unexpectedly, depletion of golgin-97 led to an increase in surface levels of β1AR (27% by immunofluorescence, 13% by flow). Double depletion of golgin-160 and golgin-97 has a less severe defect in β1AR surface levels than golgin-160 depletion alone (only a 10% decrease by immunofluorescence, 20% by flow). This suggests that golgin-97 is not promoting β1AR surface delivery as it does for E cadherin, but is instead.

Figure 3-4: Depletion of golgin-97 leads to an increase in β1AR steady state surface levels. (A) Golgin-97 and golgin-160 were either singly or double depleted from HeLa cells, as described in the Materials and Methods section. Separation of proteins from cell lysates by SDS-PAGE followed by Western blotting was performed. Membranes were probed with rabbit anti-golgin-160, mouse-anti-golgin-97, and mouse-anti-actin, followed horseradish peroxidase (HRP) conjugated secondaries and ECL. (B) Immunofluorescence microscopy of the surface pool of β1AR transiently transfected into control or golgin depleted cells. Surface β1AR (red) was detected using a mouse-anti-FLAG antibody against the extracellular FLAG-tag on intact cells. Rabbit-anti-β1AR (green) was used after cells were permeabilized, followed by labeling with Alexa Fluor 488 anti-rabbit IgG and Alexa Fluor 546 anti-mouse IgG. (C) Surface levels of β1AR were quantified as described in Materials and Methods. One experiment was performed for surface immunofluorescence of β1AR surface levels and n>30 cells were quantified, $p<0.029$ when comparing golgin-97 depletion to golgin-160 or double depletion, all other comparisons were not significant. (D) Flow analysis was performed on live, intact HeLa cells 18 h post co-transfection of constitutive FLAG- β1AR and cytoplasmic GFP. GFP was used to identify transfected cells, and β1AR levels were detected by flow analysis after immunostaining live cells with mouse anti-FLAG followed by phycoerythrin anti-mouse IgG. Two independent experiments were performed analyzing β1AR surface levels by flow cytometry. The difference between golgin-160 and double depletion was not significant, $p<0.001$ for all other comparisons.

A)

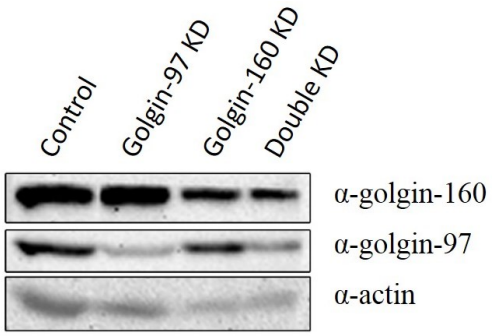

B)

RNAi depletion:

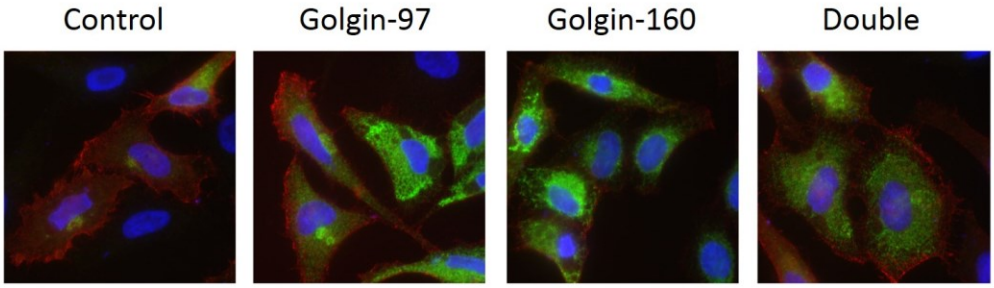

C)

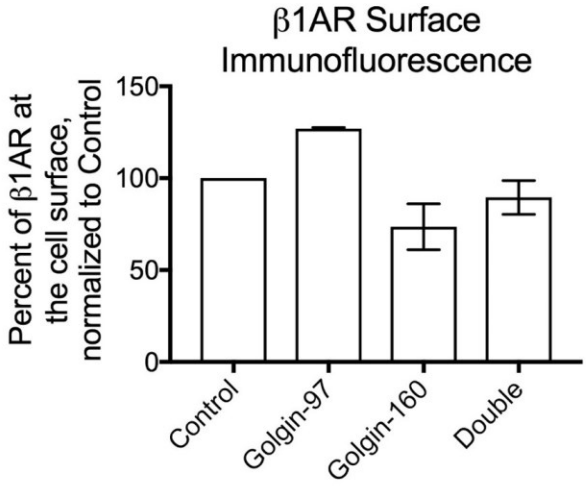

D)

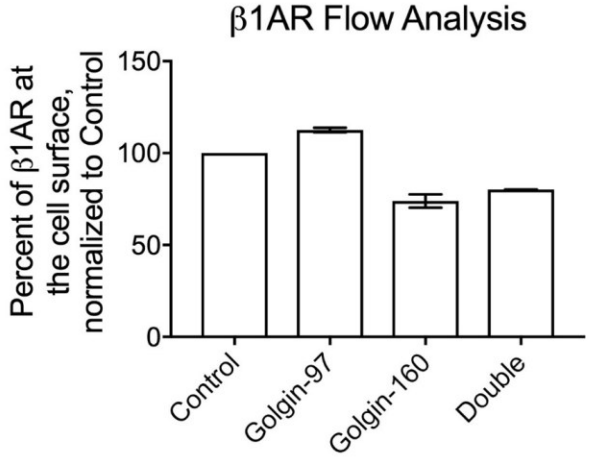

involved in modulating β1AR surface levels through regulation of β1AR retrograde trafficking

Golgin-160 impacts dynamics of β1AR containing vesicles

While static time points can be informative, the RUSH synchronization system allows for easy manipulation of cargo trafficking in conjunction with live cell imaging. In order to examine the influence of golgin-160 on the post-Golgi trafficking of β1AR, control HeLa cells or cells depleted of golgin-160 by RNAi were transfected with the RUSH β1AR construct. Between 20-22 h post transfection, cells were treated with biotin and imaged on the 3i Spinning Disk confocal microscope. To capture rapid vesicle trafficking, stacks encompassing the majority of the cell were taken once every 1.4-1.8 seconds at low (40 ms) exposure to prevent photobleaching and toxicity. Vesicle tracking was then performed using Imaris.

Several distinct vesicle movement phenotypes were observed in cells depleted of golgin-160 compared to control cells (Figure 3-5A-D). An early hypothesis for how golgin-160 was affecting β1AR trafficking was that β1AR containing vesicles might move faster towards the plasma membrane in the presence of golgin-160; however we did not observe this (Figure 3-5E). Instead, in the absence of golgin-160, β1AR-containing vesicles moved less persistently; vesicles paused at an intermediate location between the Golgi and plasma membrane (Figure 3-5C). After stalling, vesicles could continue in the same direction, or they occasionally reversed direction to return towards the cell center (Figure 3-5D). These differences can be seen in two measurements, track

displacement length and track length, as well as two calculated measurements called track straightness and speed variation (Figure 3-5E and F). Track displacement length measures the straight line distance between the beginning of the vesicle track and the end, whereas track length measures the total distance travelled by each vesicle. The track displacement was almost doubled in golgin-160 depleted cells, indicating that β1AR containing vesicles were moving farther away from the Golgi before reaching their final destination. The track length tripled, which could be due to vesicles changing direction. This is supported by the decrease in track straightness (Figure 3-5F), which is calculated by dividing the track displacement by the length, in cells depleted of golgin-160. The vesicle pausing behavior is measured by the parameter speed variation, which is calculated by dividing the speed standard deviation by the average speed. As the speed of vesicles did not change significantly (Figure 3-5E), the increase in speed variation observed in golgin-160 depleted cells is due to the increase in the variability (standard deviation) of vesicle speed displayed by the vesicles.

Figure 3-5: Live cell imaging reveals aberrant post-Golgi vesicle dynamics in cells depleted of golgin-160. (A) Live cell imaging of control or golgin-160 depleted HeLa cells transfected with RUSH β1AR were taken on a 3i Spinning Disk confocal microscope and vesicles were tracked using Imaris. Tracks created for representative cells from each condition are displayed. Tracks are color coded by vesicle speed. (B) One representative vesicle from the control cell is shown (white arrow) moving directly from the Golgi to the plasma membrane (panels go right to left). Time post biotin addition is shown in the top left corner of each panel. (C) One representative vesicle from the golgin-160 depleted cell that shows vesicle pausing. The top left panel shows the overall track of the vesicle, for clarity. The other panels (read top to bottom) show the path of the vesicle (white arrow) over time. Time post biotin addition is shown in the top left. Images representing the end of a pause include a notation on the duration of the pause by the time stamp, and a vesicle that reversed direction to travel towards the cell interior is highlighted. (D) A track from another vesicle from the golgin-160 depleted cell, this one showing the vesicle reversal phenotype. Layout is as in (C). The time when the vesicle reverses direction highlighted. (E) The minimum and maximum vesicle speed as well as the track length and displacement length for the tracked vesicles were determined using Imaris. (F) Two calculated metrics, track straightness and speed variation, were calculated for each tracked vesicle. Three independent live cell imaging experiments were performed and 24-28 individual tracks were measured per condition, using two cells per condition.

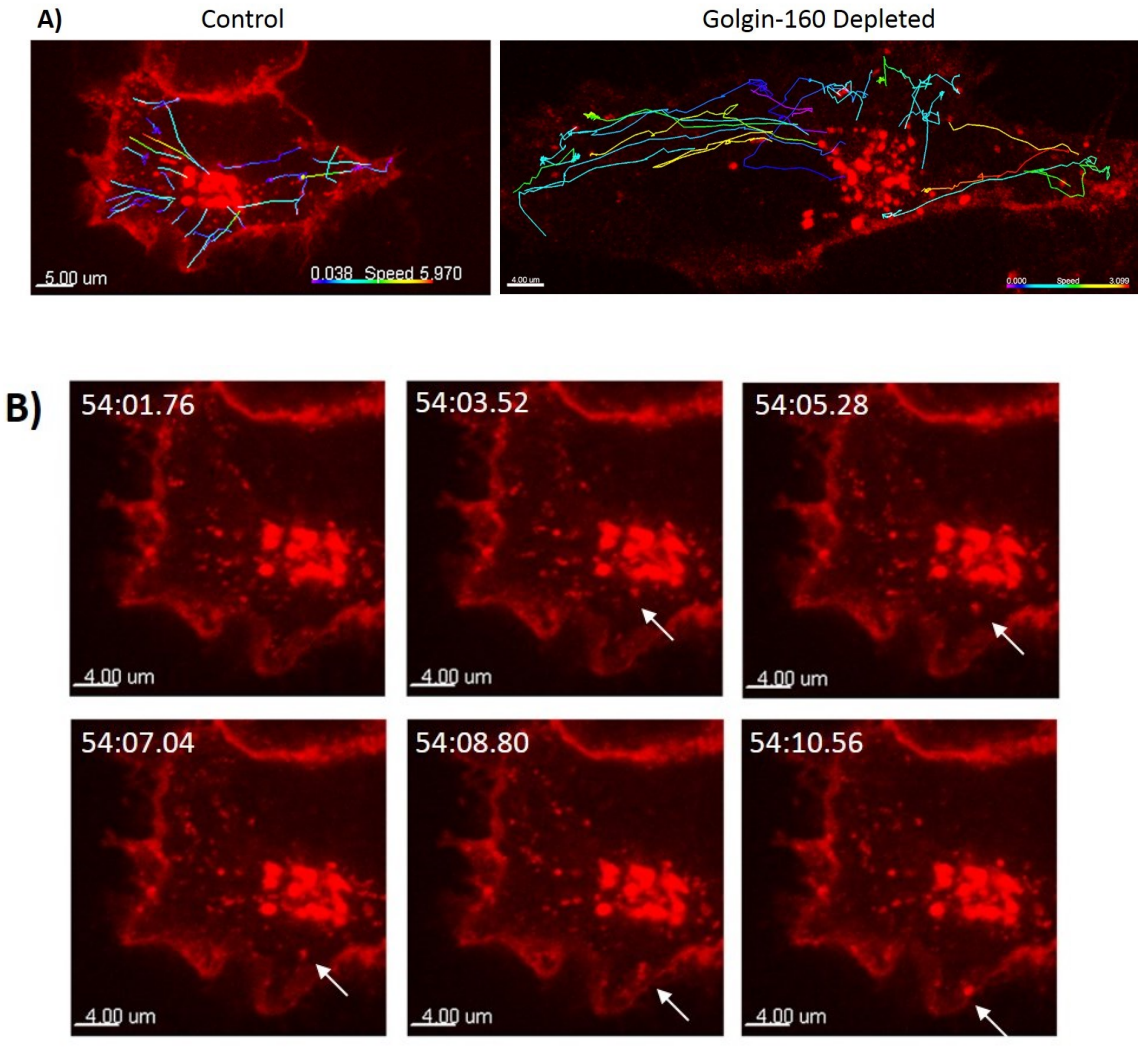
A)
Control
Golgin-160 Depleted
5.00 um
0.038 Speed 5.970
4.00 um
0.000 Speed 3.099
B)
54:01.76
54:03.52
54:05.28
54:07.04
54:08.80
54:10.56
4.00 um

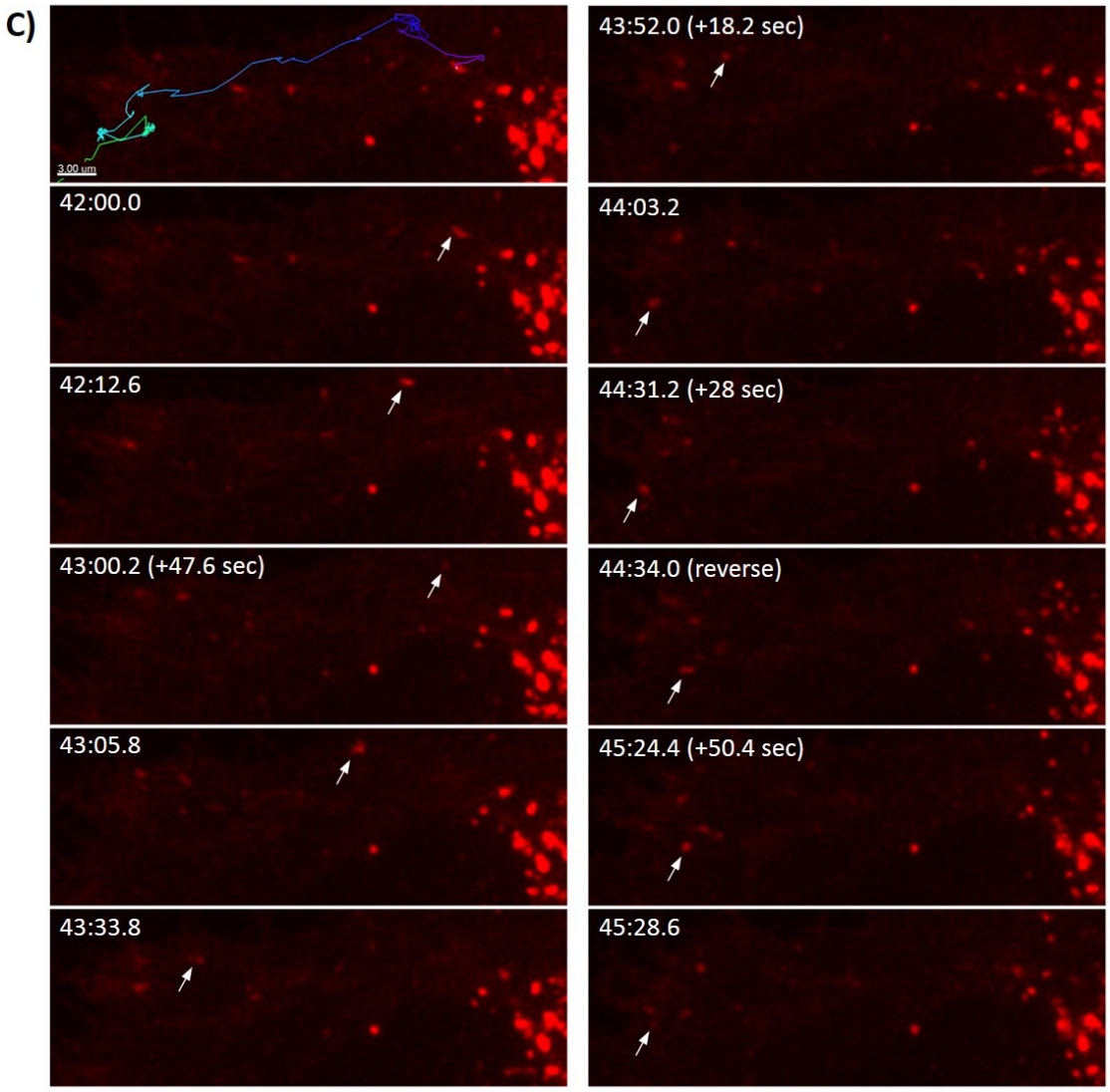
C)
3.00 um
42:00.0
42:12.6
43:00.2 (+47.6 sec)
43:05.8
43:33.8
43:52.0 (+18.2 sec)
44:03.2
44:31.2 (+28 sec)
44:34.0 (reverse)
45:24.4 (+50.4 sec)
45:28.6

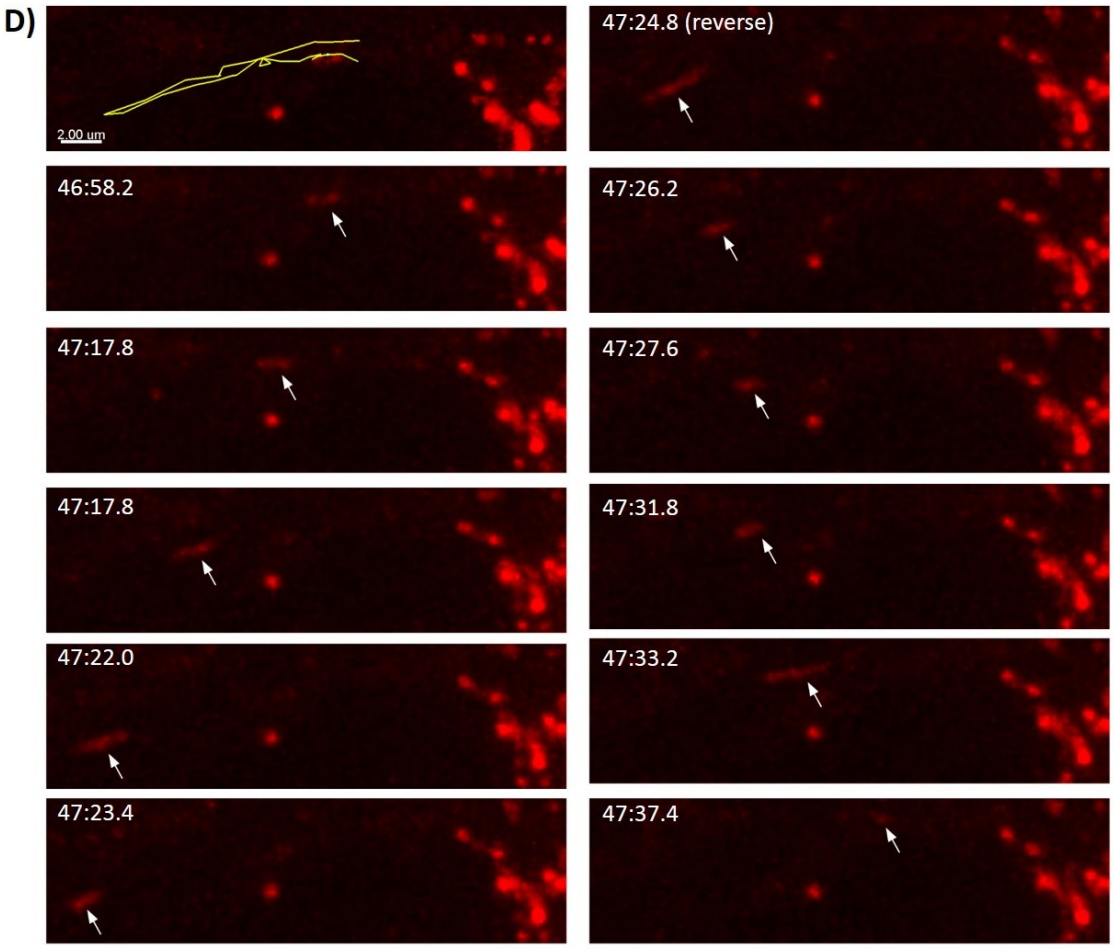
D)
2.00 um
47:24.8 (reverse)
46:58.2
47:26.2
47:17.8
47:27.6
47:17.8
47:31.8
47:22.0
47:33.2
47:23.4
47:37.4

E)

	Control	Golgin-160 Depleted
Min Speed (um/s)	0.04	0.01
Max Speed (um/s)	0.23	0.28
Track Displacement Length (um)	6.92	13.14
Track Length (um)	11.9	34.47

F)

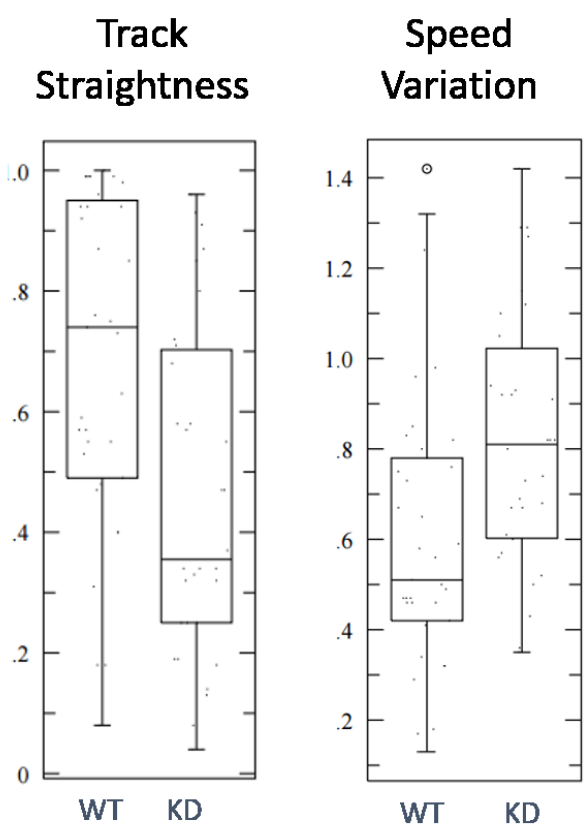

Discussion

The golgin family of proteins supports Golgi structure and function throughout the eukaryotic domain. Recently, numerous golgins have been implicated in promoting vesicle tethering at the Golgi. Here, we investigated the impact of three atypical golgins on β1AR trafficking.

Efficient β1AR trafficking to the plasma membrane has been shown to be dependent on golgin-160 (Hicks *et al.*, 2006). In investigating the mechanism behind this phenotype, we discovered that golgin-160 disperses from Golgi membranes in cells constitutively expressing β1AR (Figure 3-1A-C). Using the RUSH system to synchronize β1AR trafficking out of the ER, we determined the timing behind this change in localization in nocodazole treated cells. Golgin-160 dispersed from Golgi membranes after β1AR left the *cis*-Golgi, and returned to Golgi membranes after β1AR left the *trans*-Golgi. Golgin-160 is recruited by the active, GTP-bound form of the GTPase ARF1 (Yadav *et al.*, 2012). However, overexpression of the ARF1 GEF GBF1 did not prevent golgin-160 dispersal (Figure 3-1B-C), indicating that it is unlikely that ARF1-GTP depletion at the *cis*-Golgi causes the loss of golgin-160 localization, or the delay in golgin-160 recovery to the Golgi. We therefore hypothesize that the loss of golgin-160 binding to Golgi membranes is important for golgin-160 facilitated trafficking of β1AR.

The golgin-160 targeting information resides in its N-terminus between residues 172-257 (Hicks and Machamer, 2002), and the N-terminal domain (residues 1-496) can bind directly and specifically to ARF1-GTP (Yadav *et al.*, 2012). Interestingly, this same

region binds to β1AR (residues 140-257, Hicks *et al.*, 2006). This may indicate that golgin-160 is handed off from ARF1-GTP to β1AR upon β1AR arrival to the *cis*-Golgi. As golgin-160 is never observed to travel with β1AR into the *trans*-Golgi or post-Golgi vesicles (Figure 3-3), we hypothesize that golgin-160 is released into the cytoplasm upon β1AR trafficking to the medial or *trans*-Golgi. The delay in golgin-160 recovery to Golgi membranes could be due to slow diffusion kinetics, or possibly a transient masking of golgin-160 localization motifs. Changes to golgin-160 localization based on interactions with other proteins is not novel: the golgin-160 N-terminus contains a cryptic nuclear localization signal that is unmasked due to secretory stress-induced caspase cleavage (Mancini *et al.*, 2000; Hicks and Machamer, 2002; Maag *et al.*, 2005). While the recovery of golgin-160 to Golgi membranes indicates that golgin-160 is not being cleaved or degraded after β1AR binding, golgin-160 is a phosphorylated protein (Misumi *et al.*, 1997; Cha *et al.*, 2004), and it could be imagined that changes in N-terminal phosphorylation (or in another post translational modification, or protein conformation) could result in a transient masking of the ARF1-interacting domain.

While golgin-160 does not localize with β1AR at the TGN, β1AR does selectively localize with the *trans*-Golgi protein golgin-97, and not with p230 (Figure 3-3). Golgin-97 was previously reported to colocalize with E cadherin in *trans*-Golgi tubules, and depletion of golgin-97 caused a reduction in E cadherin surface levels (Lock *et al.*, 2005). In contrast, depletion of golgin-97 here led to a small but consistent increase in the steady state surface levels of β1AR (Figure 3-4C and D). Golgin-97 has also been implicated in tethering retrograde endosome derived vesicles to the TGN (Munro, 2011;

Wong and Munro, 2014); golgin-97 promoting β1AR recycling to the Golgi would be more consistent with the phenotype observed here.

Delivering proteins efficiently and accurately to their final destination requires several complex series of protein interactions. At the TGN, cargo proteins must be sorted into the correct vesicle type (clathrin-dependent, -independent, or pleiomorphic tubule-like carriers), often through interactions with coat or adaptor proteins (Gleeson *et al.*, 2004; Anitei and Hoflack, 2011). Newly formed vesicles must then be transported along microtubules to their destination membrane. This process often requires cargo adaptors, multiprotein motor adaptor scaffolds, and molecular motors. There has been some evidence that motor proteins can bind directly to some cargo proteins, but the importance of multiprotein scaffolds in linking cargo and motor is being increasingly highlighted (Akhmanova and Hammer, 2010). There are several known scaffolding proteins, including the rab7-interacting lysosomal protein (RILP) and huntingtin proteins.

The initial "selective recruitment" model, in which anterograde trafficking vesicles would attach to plus end (cell periphery) directed kinesins and retrograde vesicles would bind minus end-directed dynein, was complicated by the discovery that many vesicles simultaneously bind to both dynein and kinesins. These led to the "tug of war" model, in which vesicles are constantly being pulled in opposite directions. However, many vesicles do not show the frequent direction reversals that such a model would predict. This is addressed by the "coordination model" in which both types of

motors are constantly attached to vesicles, but the scaffold complex regulates which motor is engaged. Huntingtin is an example of this model. It forms a complex that can bind to both dynein and kinesin, and phosphorylation of huntingtin may determine which motor is functional at any time (Caviston and Holzbaur, 2009; Fu and Holzbaur, 2014).

β1AR containing vesicles in cells depleted of golgin-160 lost their processive movement. Instead, they exhibited multiple pausing events and direction reversals (Figure 3-5C-D). This phenotype may indicate that the scaffold complex in β1AR containing vesicles was disrupted without golgin-160. This could be through altering the scaffold protein state (for example, huntingtin phosphorylation state changes vesicle direction) or through altering the scaffold protein's ability to localize on the vesicle. RILP promotes retrograde lysosome to TGN trafficking by interacting with Rab7-GTP, which is activated on late endosomes, and then recruits dynein and dynactin. RILP membrane interaction is stabilized by another protein, ORP1L (oxysterol-binding protein-like 1), which is a cholesterol sensor, therefore tying scaffold and motor recruitment to the lipid composition of a membrane (Fu and Holzbaur, 2014). GPCR binding to Rabs or Rab-modifying proteins has been shown to modulate GPCR endocytosis and recycling to the plasma membrane (Hamelin *et al.*, 2005; O'Keeffe *et al.*, 2008; Lachance *et al.*, 2011), and Rab8 can bind to the C-terminal tail of several GPCRs to promote their anterograde Golgi to plasma membrane transport (Wang and Wu, 2012).

The mechanism behind how the *cis*-Golgi localized golgin-160 facilitates β1AR trafficking from the *trans*-Golgi to the plasma membrane is still unclear. We have yet to identify any post-translational modifications on β1AR that depend on the presence of golgin-160; instead, here we present data that suggests that golgin-160 is important for incorporating β1AR into processive, directional vesicles. This could be through altering the ability of β1AR to recruit multiprotein scaffolds, either directly or through other proteins like cargo adaptors or small GTPases. Altering interactions with these scaffold complexes could result in altered vesicle interactions with motor proteins, potentially resulting in the stalled, reversible movements of vesicles described here. Future work analyzing the coat and trafficking components associated with β1AR containing vesicles in the presence and absence of golgin-160 may provide more insight into how golgin-160 can alter vesicle trafficking without being associated with β1AR containing vesicles.

Materials and Methods

Cell Culture

HeLa cells were maintained in DMEM (Life technologies, Grand Island, NY, USA) with 10% Fetal Bovine Serum (Atlanta Biologicals, Flowery Branch, GA, USA) and 0.1 mg/mL Normocin (InvivoGen, San Diego, CA, USA) at 37 °C with 5% CO_2.

Expression constructs and transfection

Human FLAG-β1AR cDNA in pcDNA3 was provided by Randy Hall (Emory University, Atlanta, GA, USA). The cytosolic GFP vector pEGFP C1 was obtained from Clontech (Mountain View, CA, USA). The mCherry β1AR construct was created by subcloning β1AR into a mCherry backbone. The RUSH GFP backbone was provided by Franck Perez (Institut Curie, Centre de Recherche, Paris, France). The RUSH β1AR plasmid was created by removing the GFP tag from the RUSH backbone and subcloning in mCherry β1AR. HA-GBF1 was provided by Dr. Elizabeth Sztul (University of Alabama at Birmingham, Birmingham, AL, USA). The GBF1 coding region was subcloned into the pEGFP C1 backbone. Plasmids were verified by sequencing. All transfections were done with X-tremeGENE9 DNA transfection reagent (Roche, Indianapolis, IN, USA) as per manufacturer protocols.

Antibodies

Mouse monoclonal anti-FLAG and mouse-anti-mCherry were from Sigma-Aldrich (St. Louis, MO, USA). Rabbit anti-β1AR C terminus was obtained from Santa Cruz

Biotechnology (Santa Cruz, CA, USA). Rabbit anti-golgin-160 was previously described (Mancini *et al.*, 2000). R-Phycoerythrin-conjugated IgG goat anti-mouse was from Jackson ImmunoResearch Laboratories Inc. (West Grove, PA, USA). Mouse anti golgin-97 and mouse anti-p230 were obtained from BD Transduction Laboratories (San Jose, CA, USA). Alexa Fluor 568 anti-mouse IgG, Alexa Fluor 488 anti-mouse, Alexa Fluor 568 anti-rabbit, and Alexa Fluor 488 anti-rabbit IgG were from Life Technologies. Cy5-conjugated AffiniPure Donkey anti-rabbit IgG was obtained from Jackson ImmunoResearch Laboratories, Inc. (West Grove, PA, USA). Horseradish peroxidase (HRP)-conjugated secondary antibodies were from GE Healthcare (Little Chalfont, Buckinghamshire, UK).

Golgin-160 dispersal

HeLa cells grown to 70% confluence on autoclaved coverslips in 35 mm dishes were transfected with 0.5 ug mCherry β1AR alone, or co-transfected with 0.5 ug HA-GBF1 for 16 h. Cells were then fixed in 3% paraformaldehyde and permeabilized in 0.02% saponin (CalBiochem/Sigma) and 10 mM glycine (Sigma) in phosphate buffered saline (PBS; Sap/PBS/gly buffer). Coverslips were incubated 15 min in anti-golgin-160 and anti-GM130 primary antibodies diluted in Sap/PBS/gly buffer with 1% bovine serum albumin (BSA). Cells were washed 2 times with Sap/PBS/gly buffer before being incubated in Alexa Fluor 568 anti-mouse IgG and Alexa Fluor 488 anti-rabbit IgG diluted as above. Cells were washed again before being incubated for 3 min in 0.1 µg/mL Hoechst 33258 diluted in PBS. Coverslips were then mounted in glycerol with 0.1 M N-propyl gallate. Coverslips were imaged on an Axioskop microscope (Zeiss, Thornwood, NY, USA)

equipped for epifluorescence using an ORCA-03G charge-coupled device camera (Hamamatsu, Japan) using iVision software (BioVision Technologies, Exton, PA, USA).

To quantify dispersal, the GM130 stain was used to identify a Golgi region of interest. The golgin-160 fluorescence intensity within the Golgi region ROI and in an ROI encompassing the whole cell was then measured using FIJI (National Institutes of Health, Bethesda, MD, USA). The percent of golgin-160 within the Golgi region was calculated by dividing the Golgi intensity measurements by the whole cell measurements for each cell. Data was normalized to non-transfected cells imaged on the same coverslip by dividing the individual values for percent at the Golgi by the average non-transfected percent at the Golgi. In the box and whisker plot, the center bar represents the mean, the box extends from the 25^{th} to the 75^{th} percentiles, and the whiskers extend to the minimum and maximum values. Data are from two independent experiments; 39-43 cells were quantified for each condition.

β1AR Trafficking Time Course

HeLa cells plated on coverslips in 35 mm dishes were transfected with 0.5 ug RUSH β1AR. After 18 h, cells were pre-treated with 1 ug/mL nocodazole for 2 h before 10 uM biotin was added for the indicated amount of time. Cells were then fixed and permeabilized in saponin as described above. Cells were incubated in anti-golgin-160 and either anti-golgin-97 or anti-p230 primary antibodies. Cy5 anti rabbit and Alexa Fluor 488 anti-mouse were used to label the golgins, and mCherry fluorescence was used to identify β1AR localization. Imaging was performed as described above.

Quantification of Pearson's R coefficient to measure colocalization was done using the Coloc 2 plugin on FIJI. Only early time points were measured for colocalization, as signal from plasma membrane localized β1AR at 80 min post-biotin addition covered the entire cell, artificially increasing the colocalization coefficient by appearing to "colocalize" with Golgi structures.

Double depletion analyses

Synthetic siRNA-4 duplex for golgin-160 depletion was obtained from Dharmacon Research Inc. (Lafayette, CO, USA) and was previously described (Hicks *et al.*, 2006). Control scramble (SR30005) and golgin-97 (GOLGA1 SR301868A) Trilencer-27 siRNA constructs were obtained from OriGene (Rockville, MD, USA). HeLa cells were plated on 35 or 60 mm dishes 6-8 hours prior to siRNA addition. A final concentration of 13.5 nM siRNA-4 was mixed with 5 nM g97 A RNA. For single depletion experiments and for controls, scrambled RNA was added to make up a final concentration of 18.5 nM (13.5 + 5 nM). Cells were transfected with Oligofectamine (Invitrogen, Carlsbad, CA, USA) according to manufacturer protocols for 18-20 hours. Fresh media was added and cells were grown for an additional 24 h. Experimental dishes were then plated from the initial knockdown plates. For each experiment, one 35 mm dish was plated at $3x10^5$ cells/mL for lysates to compare depletion effectiveness. After 48 h, cells were lysed in detergent solution (1% NP-40, 0.4% deoxycholic acid, 50 mM Tris pH 8, 62.5 mM EDTA pH 8 with protease inhibitors) and proteins were separated by SDS-PAGE. Golgin-160, golgin-97, and actin were detected by immunoblotting with antibody against each protein followed by ECL. The amount of each protein in each sample was measured after

imaging on a VersaDoc Imaging System Model 5000 (Bio-Rad, Hercules, CA, USA) using Quantity One volume analysis tools (Bio-Rad, Hercules, CA, USA). Percent depleted was calculated after first normalizing each sample to actin, and then values were normalized to the control sample.

Surface Immunofluorescence

For RUSH β1AR surface immunofluorescence experiments, cells at 70% confluency on coverslips in 35 mm dishes were transfected with 0.5ug RUSH β1AR. After 20 h transfection, 10 uM biotin, from a 40 mM stock diluted in serum free DMEM and 0.22 μm filter sterilized, was added to cells for the time indicated. After the indicated amount of time, cells were incubated on ice in anti-mCherry diluted in cold PBS for 15 min. Cells were then fixed in 3% paraformaldehyde for 10 min and permeabilized in 0.05% Triton X-100 for 3 min. Cells were washed in PBS/gly, (the Sap/PBS/gly buffer described above without saponin) for 5 min then incubated for 15 min in anti- β1AR antibody diluted in 1% BSA in PBS/gly. Cells were washed in PBS/gly and then incubated in Alexa Fluor 488 anti-mouse IgG and Alexa Fluor 568 anti-rabbit IgG, diluted in 1% BSA in PBS/gly as above. Nuclei were stained with Hoechst 33258 and images were taken as described above.

For golgin depletion experiments, cells were plated on coverslips in 35 mm dishes. 24 hours after plating, cells were transfected with 0.5 ug FLAG-β1AR. After 16 h, cells were washed with ice cold PBS and stained with mouse anti-FLAG for 15 min in 1% BSA in PBS on ice. Cell fixation, permeabilization, and internal primary antibodies were done the same as the RUSH β1AR surface immunofluorescence. Cells were washed in PBS/gly and

then incubated in Alexa Fluor 568 anti-mouse IgG and Alexa Fluor 488 anti-rabbit IgG, diluted as above. Nuclei were stained with Hoechst 33258 and images were taken as described above. Surface fluorescence was measured by measuring the fluorescence intensity of each cell for each image, and dividing the surface intensity by the total intensity. Data were normalized to control cells by dividing individual cell percent at the surface by the average percent from control cells.

Flow Analysis of β1AR Surface Levels

For flow analysis, three 60 mm dishes were plated per condition. After 24 h, cells were co-transfected with 1.5 ug cytosolic GFP and 0.5 ug FLAG β1AR. After 16 hr expression, cells were harvested by trypsinization and washed twice with DMEM. Cells were resuspended at $5x10^6$ cells/mL in blocking solution (1% BSA in PBS) and incubated for 30 min on ice. Cells were then incubated for 1 h on ice with anti-FLAG antibody diluted in blocking solution. Cells were washed in cold PBS and were then incubated 1 h on ice in phycoerythrin-labeled goat anti-mouse IgG diluted in blocking solution. After a final wash in cold PBS, cells were resuspended in serum free DMEM and analyzed using the FACSCalibur flow cytometer (Becton Dickinson, Franklin Lake, NJ, USA). The mean phycoerythrin fluorescence intensity of cells expressing GFP was calculated for each sample using CellQuest Pro software (Becton Dickinson). Data represents two independent experiments.

Live cell imaging and vesicle tracking

HeLa cells were plated on uncoated 35 mm glass bottom dishes No. 1.0 (MatTek Corporation, Ashland, MA, USA). After 24 h, cells were transfected with RUSH mCherry-β1AR for 20 h. Immediately before imaging, 10 µM biotin was added to the dishes. Imaging was done on a 3i Marianis/Yokogawa Spinning Disk Confocal microscope outfitted with an environmental chamber heated to 37^{o}C with 5% CO_2. Images were taken once every 1.4-1.8 seconds at low (40 ms) exposure. Between 4-10 cells were imaged per dish and were selected based on similar, moderate β1AR expression level. Each cell could be imaged for 7-15 min before photobleaching and phototoxicity impeded analysis. Vesicle tracking was performed on Imaris 8.1 (Bitplane, Oxford Instruments, Zurich, Switzerland). Two cells were selected for vesicle tracking based on ability to reliably track vesicles from Golgi to the plasma membrane. Manual tracking was performed using the Imaris spot detection and tracking tools. For golgin-160 depleted cells, 28 vesicles were tracked; 24 were tracked for control cells. The metrics described in Figure 3-5 were measured using the Imaris spots tracking tool.

Statistical Analysis

Statistical analyses were obtained using GraphPad Prism version 7.00 for Mac OS X (GraphPad Software, La Jolla, CA, USA). For all experiments, one-way ANOVA followed by Tukey's multiple comparisons test were performed.

Chapter 4

Commonly used trafficking blocks disrupt ARF1 activation and the localization and function of specific Golgi proteins

Modified from Gilbert, C. E., Sztul, E., and Machamer, C. E. (Submitted 2017).

Introduction

The ARF family of proteins consists of five small GTPases that are critical for the function of the secretory pathway through their interactions with effector proteins (reviewed in D'Souza-Schorey and Chavrier, 2006; Donaldson and Jackson, 2011). The ARFs play semi-redundant but essential roles in cargo transit throughout the secretory system through their functions as molecular switches, which result from their GTPase cycles (Volpicelli-Daley *et al.*, 2005). The *cis*-Golgi role of ARF1 has been well studied. After activation by its guanine nucleotide exchange factor (GEF), GBF1, the Golgi membrane-bound ARF1-GTP recruits COPI coat complexes to interact with cargo proteins (reviewed in Jackson, 2014). The ARF GTPase activating protein (ARFGAP)-stimulated hydrolysis of GTP by ARF1 is required for the recruitment of cargo into COPI coated vesicles and the subsequent removal of those coats (Teal *et al.*, 1994; Nickel *et al.*, 1998; Pepperkok *et al.*, 2000; Lee *et al.*, 2005).

ARF1-GTP can recruit several other effector proteins, one of which is golgin-160 (also called GOLGA3 and GCP-170). Found only in vertebrates, golgin-160 has been reported to promote Golgi structure as well as facilitate the proper targeting and efficient trafficking of specific cargo proteins (Hicks *et al.*, 2006; Yadav *et al.*, 2009). Many golgins promote bulk cargo movement through the Golgi, by acting as tethers or maintaining Golgi structure (Munro, 2011). Golgin-160's trafficking role is unique because it only promotes the trafficking of a small, specific subset of cargos. We previously found that loss of golgin-160 causes GLUT4 to traffic directly to the plasma membrane, bypassing its proper localization to insulin sensitive vesicles (Williams *et al.*,

2006). We also reported that golgin-160 directly binds to the beta-1 adrenergic receptor (β1AR), and that depletion of golgin-160 decreases β1AR steady state surface levels as well as the rate of arrival of the receptor at the plasma membrane (Hicks *et al.*, 2006; Gilbert *et al.*, 2014). Intriguingly, the *cis*-localized golgin-160 affects the rate of β1AR trafficking at a post-*trans*-Golgi step (Hicks *et al.*, 2006). These findings led us to become interested in how the localization of golgin-160 impacted its function in protein trafficking.

Synchronization of cargo exit from a specific compartment is a commonly used tool to study protein trafficking at distinct stages of the secretory pathway. Several new synchronization techniques have been developed in the last several years, however they require protein modifications which can have unintended effects on trafficking or localization (reviewed in Boncompain and Perez, 2013; Roboti *et al.*, 2013; Feng and Arnold, 2016). One of the oldest and most broadly useful techniques is the use of cold temperature blocks, which allows for synchronization of untagged, endogenous cargo proteins. First reported in 1983, it was shown that incubating cells at 20^{o}C leads to a total block in cargo trafficking at the *trans*-Golgi network (TGN), while an incubation at 15-16^{o}C leads to retention of cargo proteins in the early Golgi or ER-Golgi intermediate compartment (ERGIC; Matlin and Simons, 1983; Saraste and Kuismanen, 1984; Saraste and Svensson, 1991). While some data, like the inability of brefeldin A (BFA) to collapse the Golgi into the ER at these temperatures (Lippincott-Schwartz *et al.*, 1990), suggest that these blocks may be due to inhibiting membrane dynamics, the exact mechanism behind these temperature blocks has never been elucidated.

In this study, we attempted to utilize cold temperature blocks to study golgin-160's role in cargo trafficking at distinct compartments of the secretory pathway. However, we found that these temperatures disrupt golgin-160 localization at the Golgi. This led us to analyze the effects of cold temperature shifts on ARF1 (the protein responsible for recruitment of golgin-160 to Golgi membranes) and other Golgi-localized proteins.

Results

Golgin-160 disperses from Golgi membranes in cells subjected to 20 or 16°C trafficking blocks

We and other groups have reported that golgin-160 facilitates the trafficking of specific cargo proteins (Bundis *et al.*, 2006; Hicks *et al.*, 2006; Williams *et al.*, 2006; Gilbert *et al.*, 2014). To dissect golgin-160's role in this process, we attempted to employ two commonly used temperature blocks to stop cargo trafficking at different subcompartments of the Golgi complex. However, when we assessed the localization of golgin-160 by indirect immunofluorescence microscopy in HeLa cells after incubation for 3 h at 20 or 16°C, we found that golgin-160 signal was lost from the Golgi region (Fig. 4-1A). To quantify this effect, we defined the Golgi region using the fluorescence of another *cis*-Golgi-localized peripheral membrane protein, GM130, and measured the golgin-160 fluorescence intensity within both the Golgi region and the whole cell. The percent of the signal within the Golgi region was calculated and the values were normalized to those in cells kept at 37°C. Surprisingly, there was a progressive loss of golgin-160 localization at the lower temperatures, with a 40% decrease in golgin-160 at the Golgi at 20°C, and a 48% decrease at 16°C (Figure 4-1B).

It was possible that the loss of Golgi-localized golgin-160 could be due to protein degradation. However, a Western blot of lysates from HeLa cells incubated at 37, 20, or 16°C showed no difference in golgin-160 levels after normalizing to actin (Figure 4-2).

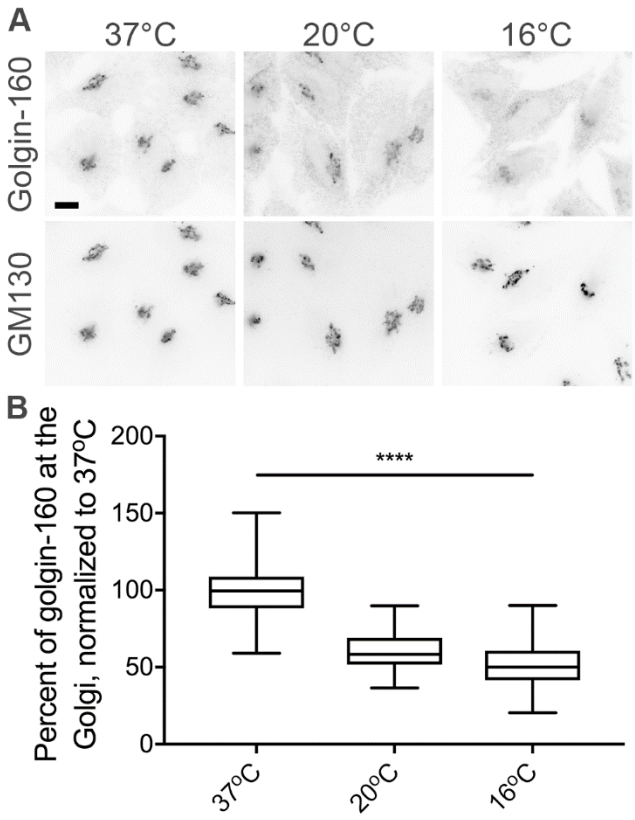

Figure 4-1: Two temperature blocks lead to dispersal of golgin-160 from Golgi membranes. (A) Representative images of HeLa cells incubated for 3 h at 37, 20, or 16°C for 3 h are shown. Cells were labeled with rabbit anti-golgin-160 and mouse anti-GM130, followed by AlexaFluor488 anti-rabbit IgG and Alexa Fluor 546 anti-mouse IgG. Scale bar, 10 µm. (B) Quantification of golgin-160 dispersal. The GM130 signal was used to outline the Golgi region in each cell, and the amount of golgin-160 fluorescent signal was calculated within the Golgi and divided by the total golgin-160 fluorescence in the cell to obtain the percent of golgin-160 at the Golgi. Each fluorescence intensity value was normalized to that at 37°C. More than 160 cells from 3 separate experiments were quantified for each temperature. $P<0.001$ for all comparisons.

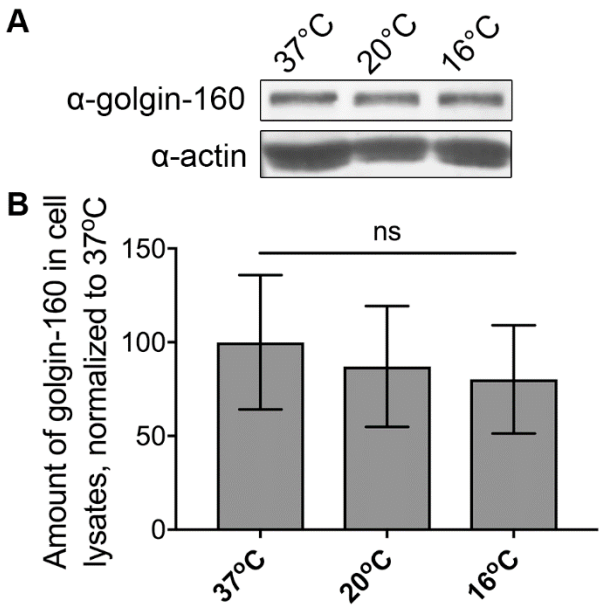

Figure 4-2: Loss of golgin-160 localization at cold temperatures is not due to protein degradation. (A) Lysates of HeLa cells incubated at 37, 20, or 16°C for 3 h were analyzed by Western blot with rabbit anti-golgin-160 or mouse anti-actin, followed by 680RD donkey anti-rabbit IgG or 680RD donkey anti-mouse IgG. (B) Golgin-160 signal was first normalized to actin and then to the 37°C control. ns, not significant by ANOVA (p=0.23), n=5.

Thus, it appears that cold temperatures cause the release of golgin-160 from the membranes into a cytosolic pool.

Manolea *et al.* discovered that exogenously expressed GFP-tagged ARF3 loses its Golgi localization upon shifting cells to 20^{o}C. This relocation to the cytoplasm was nearly complete within 20 minutes, and ARF3 Golgi localization could be restored within 20 minutes of shifting cells back to 37^{o}C (Manolea *et al.*, 2010). Thus, we examined the kinetics of golgin-160 dispersal, and whether the effect was reversible. Golgin-160 dispersal was not as rapid as that reported for ARF3: after 30 minutes at 16^{o}C, Golgi localized golgin-160 decreased by only 32%, compared to 48% after 3 h (Figure 4-3). Golgin-160 localization also recovered more slowly than that of ARF3: when HeLa cells incubated for 3 h at 16^{o}C were shifted back to 37^{o}C for 30 minutes, golgin-160 still had a 12% decrease in Golgi localization compared to cells kept at 37^{o}C for the entire time course (Figure 4-3B).

ARF1 activation status but not its localization is altered at cold temperatures

Golgin-160 localization at the Golgi is dependent on the activation status of the small GTPase ARF1 (Yadav *et al.*, 2012). We predicted that the temperature blocks might cause golgin-160 dispersal by affecting ARF1 activation. Thus, we determined the relative amount of GTP-bound ARF1 in HeLa cells incubated at 37, 20, or 16^{o}C using an effector GGA3-based pull down kit (see Materials and Methods). We observed a 30% decrease in the amount of GTP-bound ARF1 in cells incubated for 3 h at 20^{o}C, and a 60% decrease at 16^{o}C, when compared to cells incubated at 37^{o}C (Figure 4A-B). After a 3 h

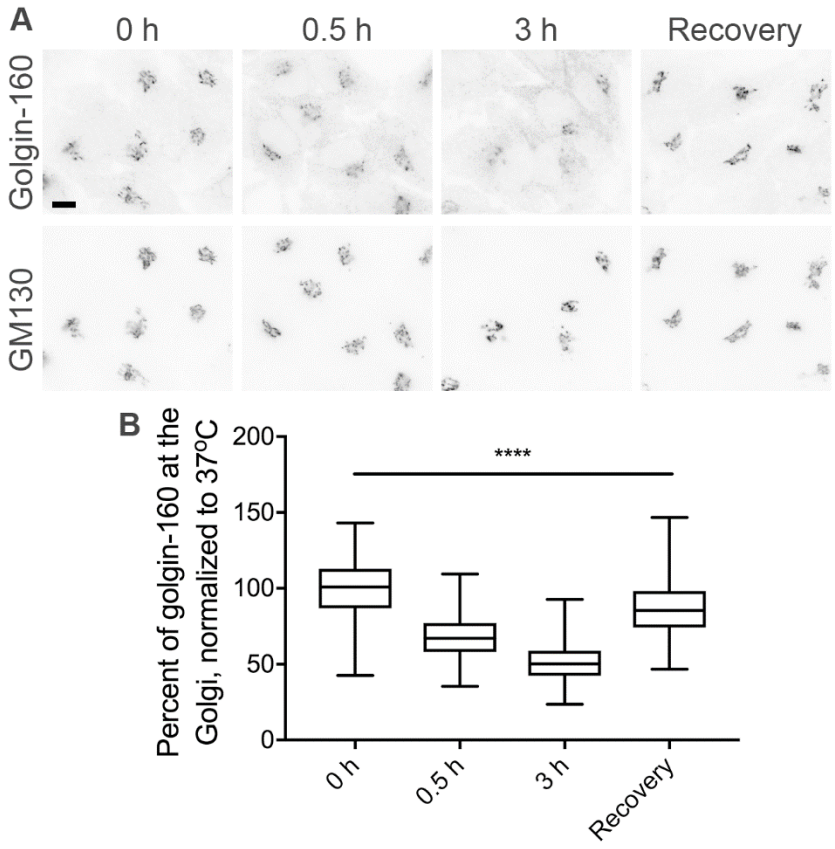

Figure 4-3: Golgin-160 disperses from and recovers to the Golgi slowly during temperature shifts. (A) HeLa cells were shifted from 37°C to 16°C for 0, 0.5 or 3 h. For recovery, cells were incubated 3 h at 16°C and then returned to 37°C for 0.5 h. Cells were labeled with rabbit anti-golgin-160 and mouse anti-GM130, followed by AlexaFluor488 anti-rabbit IgG and Alexa Fluor 546 anti-mouse IgG. Scale bar, 10 µm. (B) Quantification of the percent of golgin-160 signal in the Golgi region was calculated as in Figure 4-1. More than 170 cells from 3 separate experiments were analyzed for each temperature condition. P<0.001 for all conditions.

incubation at 16°C, a 30 minute recovery at 37°C restored levels of activated ARF1, with only an 11% decrease in ARF1-GTP levels compared to control cells maintained at 37°C. We observed a wide range of biological variability in this assay, but the progressive loss of GTP-bound ARF1 at cold temperatures and the ability to restore ARF1-GTP levels after a recovery period correlated with the progressive decrease and restoration of Golgi-localized golgin-160 (Figure 4-1B and 4-3B).

Manolea *et al.* (2010) also examined the localization of GFP-tagged ARF1 at 20°C and found that ARF1, unlike ARF3, was insensitive to this temperature shift and did not dissociate from the Golgi. We confirmed that GFP-tagged ARF1 does not disperse from Golgi membranes at 20°C, and also observed no change in GFP-ARF1 localization at 16°C, despite the decrease in cellular ARF1-GTP levels (Figure 4-4C).

While activated ARF1-GTP is canonically the predominant form of ARF1 thought to be stably associated with Golgi membranes, the dominant inactive ARF1 T31N mutant (that mimics the inactive ARF1-GDP) is also Golgi localized, possibly through stabilized interaction with GBF1 (Niu *et al.*, 2005; Szul *et al.*, 2005). The Golgi localization of ARF1-GFP observed by fluorescence microscopy at cold temperatures, coupled with the decrease in cellular ARF1-GTP levels, suggest that the Golgi-localized ARF1 could be stabilized on Golgi membranes in its GDP bound form. This predicts that the decrease in golgin-160 localization should be prevented by providing activated ARF1 to the cells. To test this, we expressed the ARF1 Q71L mutant, which mimics the active ARF1-GTP bound protein (Teal *et al.*, 1994). ARF1 Q71L prevented golgin-160 dispersal at both 20°C and 16°C (Figure 4-5A). While non-transfected cells in the same coverslip had a

Figure 4-4: ARF1-GTP levels decrease during cold temperature shifts and recover after return to 37°C, but GFP-ARF1 localization does not change. (A) Representative Western blot of active (GTP-bound) ARF1. The input and pull down (PD) samples were run side by side. HeLa cells were incubated at 37, 20, or 16°C for 3 h before being lysed. For the recovery sample, cells were incubated at 16°C for 3 h before being shifted back to 37°C for 0.5 h. Active ARF1 was removed from lysates using agarose beads conjugated with the ARF1-GTP binding domain of GGA3. (B) The amount of active ARF1 was analyzed by Western blot and was normalized first to input and then to the 37°C control. For the recovery time point n=3; n=5 for all other conditions. When analyzed using an ANOVA and post hoc Tukey test, $p=0.08$ comparing 37°C and 16°C, $p>0.2$ for all other comparisons. (C) HeLa cells expressing GFP-ARF1 WT for 16-17 h were shifted to 20 or 16°C for 3 h and the GFP signal was visualized after fixation. Scale bar, 10 μm.

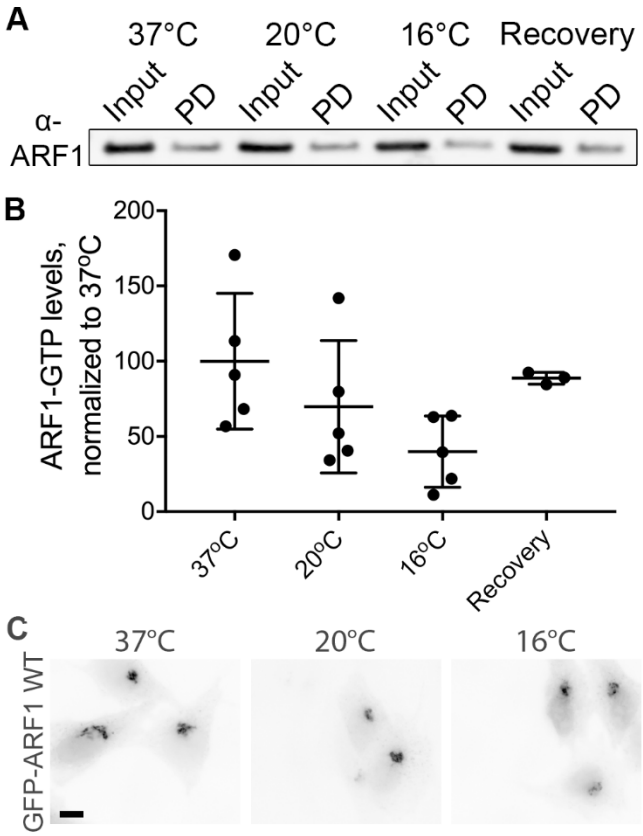
A
37°C
20°C
16°C
Recovery
Input
PD
Input
PD
Input
PD
Input
PD
α-
ARF1
B
ARF1-GTP levels,
normalized to 37°C
200
150
100
50
0
37°C
20°C
16°C
Recovery
C
37°C
20°C
16°C
GFP-ARF1 WT

decrease in golgin-160 Golgi localization by 28 and 44%, ARF1 Q71L transfected cells had reductions of only 11 and 26%, respectively (Figure 4-5B). Thus, it appears that the cold-induced dissociation of golgin-160 from Golgi membranes is due to reduced levels of ARF1 activation.

Cold temperatures affect the function of the ARF1 activator GBF1

GBF1 depletion experiments have indicated that GBF1 is required for ARF1 activation to facilitate golgin-160 recruitment (Yadav *et al.*, 2012). Thus, we examined the distribution of endogenous GBF1 in cells incubated at lower temperatures. As shown in Figure 4-6A, GBF1 displayed increased Golgi localization at 20^{o}C and 16^{o}C. The increased level of Golgi-associated GBF1 is consistent with the Golgi-localized ARF1 being in an inactive form as GBF1 is stabilized on membranes in the presence of the ARF1-GDP, and is released from membranes when ARF1 becomes activated by binding GTP (Szul *et al.*, 2005). The increased localization of GBF1 and inactive form of ARF1 at the Golgi during cold treatments suggests that the catalytic activity of GBF1 might be inhibited at lower temperatures.

To further probe this point, we expressed GFP-tagged GBF1 and assessed its ability to support golgin-160 localization in the cold. We did not observe any protective effect of overexpressing GBF1 on golgin-160 dispersal at lower temperatures (Figure 4-6B). When normalized to cells incubated at 37^{o}C, the Golgi localization of golgin-160 decreased by ~27 and ~41% at 20^{o}C and 16^{o}C, respectively, in both GBF1 transfected and non-transfected cells (Figure 4-6C). This suggests that GBF1, while localized to the

Figure 4-5: The active ARF1 Q71L mutant can prevent golgin-160 dispersal from the Golgi at lower temperatures. A) HeLa cells expressing GFP-ARF1 Q71L for 16-17 h were shifted to 20 or 16^{o}C for 3 h. GFP fluorescence was used to identify transfected cells and golgin-160 and GM130 localization was determined by indirect immunofluorescence with rabbit anti-golgin-160 and mouse anti-GM130, followed by AlexaFluor488 anti-rabbit IgG and Cy5 anti-mouse IgG. Scale bar, 10 μm. Arrows indicate transfected cells. B) The percent of golgin-160 at the Golgi was calculated in both transfected (T) and non-transfected (NT) cells for each experiment as described in Figure 4-1. For each population of cells (T and NT), values were normalized to 37^{o}C. The differences between temperatures were significant for both T and NT populations ($p<0.001$ for all comparisons). Expression of ARF1 Q71L was protective, with a significant difference between ARF1 Q71L transfected and non-transfected cells at both 20^{o}C and 16^{o}C ($p<0.001$). More than 135 cells from 4 separate experiments were analyzed for each temperature and transfection condition.

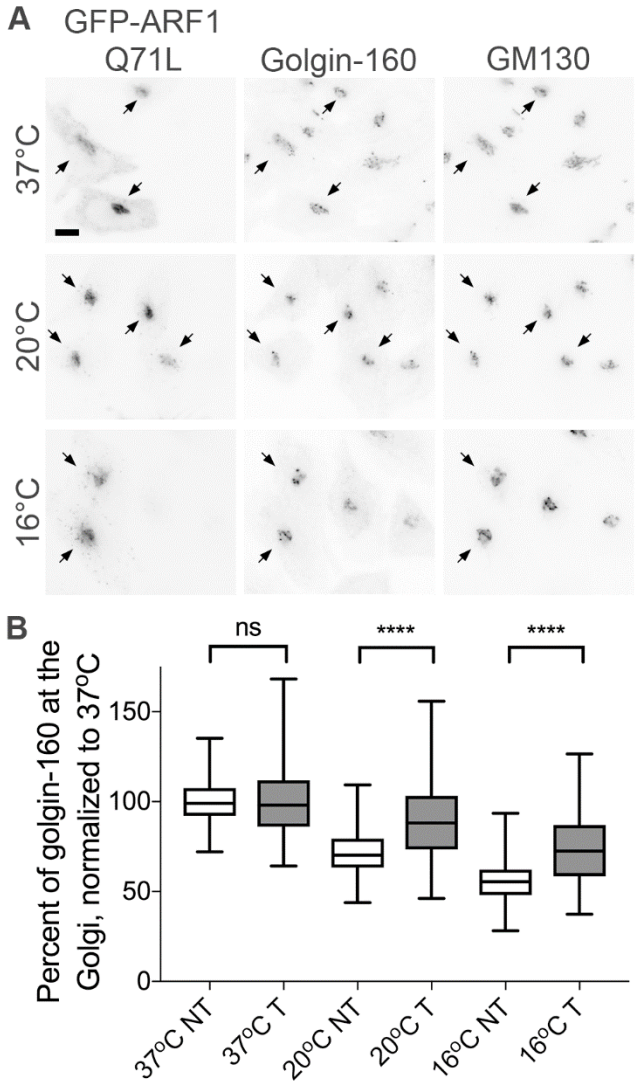
A
GFP-ARF1
Q71L
Golgin-160
GM130
37°C
20°C
16°C
B
ns
****
****
Percent of golgin-160 at the Golgi, normalized to 37°C
150
100
50
0
37°C NT
37°C T
20°C NT
20°C T
16°C NT
16°C T

Figure 4-6: GBF1 overexpression does not prevent golgin-160 dispersal from the Golgi at lower temperatures. (A) HeLa cells were shifted to 20 or 16^{o}C for 3 h, followed by staining with mouse anti-GBF1 and AlexaFluor 546 anti-mouse IgG. Scale bar, 10 µm. Arrows indicate transfected cells. (B) HeLa cells expressing GFP-GBF1 A795E for 16-17 h were shifted to 20 or 16^{o}C for 3 h. Microscopy and analysis was performed as in Figure 4-5B) The differences in golgin-160 Golgi localization between temperatures were significant ($p<0.001$ for all comparisons), however there were no significant differences between the GBF1 transfected and NT populations at each temperature. More than 135 cells from 4 separate experiments were analyzed for each temperature and transfection condition.

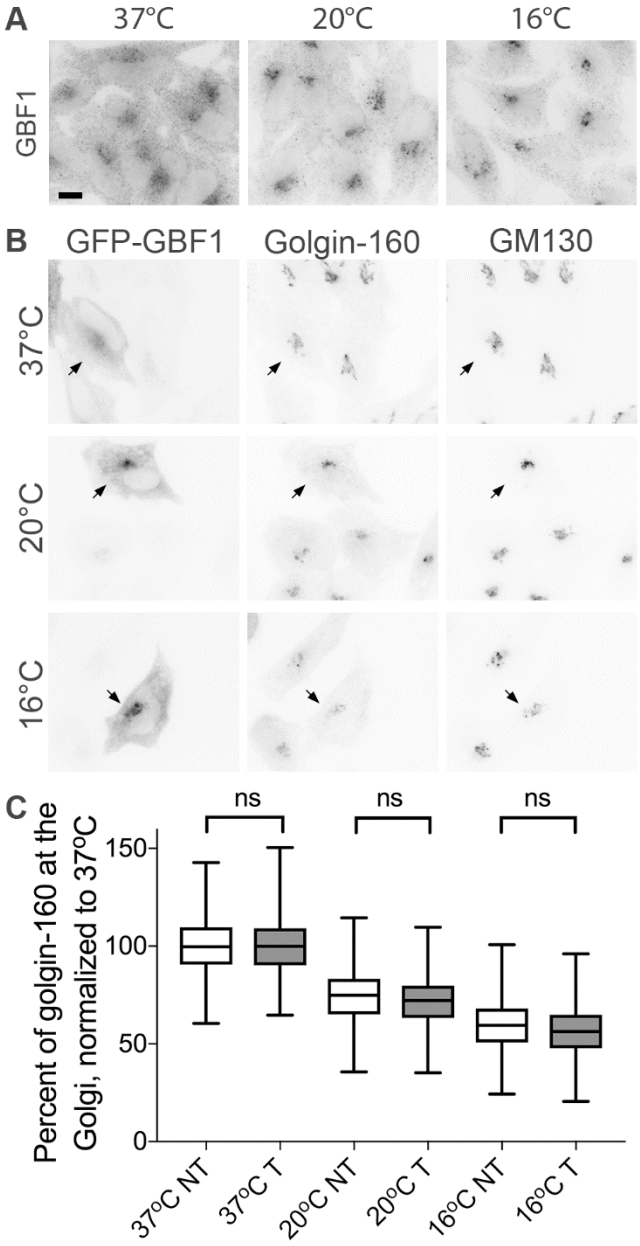
A
37°C
20°C
16°C
GBF1
B
GFP-GBF1
Golgin-160
GM130
37°C
20°C
16°C
C
ns
ns
ns
Percent of golgin-160 at the Golgi, normalized to 37°C
150
100
50
0
37°C NT
37°C T
20°C NT
20°C T
16°C NT
16°C T

Golgi at cold temperatures, is not functioning to promote conversion of ARF1-GDP to its GTP bound form.

Numerous Golgi localized proteins have disrupted localization at cold temperatures

Our finding of decreased ARF activation at lower temperatures led us to examine the distribution of other ARF-dependent as well as ARF-independent Golgi proteins at 20^{o}C and 16^{o}C. β-COP is a subunit of the COPI coat complex, which is recruited by activated ARF1 to the *cis*-Golgi (Donaldson *et al.*, 1992). Unexpectedly, and in contrast to golgin-160, β-COP had slightly increased Golgi localization at 20^{o}C and 16^{o}C (Figure 4-7A). This was surprising since increased Golgi localization of β-COP has been reported with an increase in activated ARF1 (Teal *et al.*, 1994; Saitoh *et al.*, 2009). β-COP could also be detected in large extra-Golgi puncta at lower temperatures (Figure 4-7A). Punctate β-COP and altered ARF GTPase activity have previously been associated with punctate GM130 and ERGIC53 (Volpicelli-Daley *et al.*, 2005; Saitoh *et al.*, 2009), but those phenotypes were not observed here (Figures 4-1 and 4-7B, respectively).

Cold-induced changes in cellular localization extend beyond the ARF-dependent protein family, as multiple ARF-independent proteins also had altered localization in the cold (Table 4-1 and Supplemental Figure 4-1). While we do not currently know how these proteins are affected by cold temperature shifts, our data suggest that caution should be taken when interpreting results obtained using these methods.

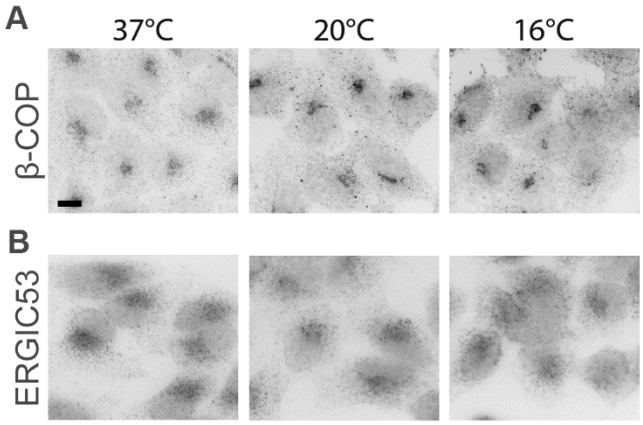

Figure 4-7: β-COP but not ERGIC53 has altered localization in the cold. HeLa cells were shifted to 20 or 16°C for 3 h, followed by staining with either (A) mouse anti-β-COP or (B) mouse anti-ERGIC53 followed by Alexa Fluor 546 anti-mouse IgG. Scale bar, 10 µm.

Protein Name	Localization	ARF Dependent?	Change at lower temperatures?
ERGIC53	ERGIC	No	No change
Golgin-160	CGN	ARF1	Decrease
β-COP	CGN	ARF1	Increase; puncta at 20°C
GBF1	CGN and TGN	No	Increase
p115	CGN	No	No change
GM130	CGN	No	No change
Giantin	Medial	No	No change
AP-1	TGN	ARF1/3	Increase
GGA2	TGN	ARF1/3	No change
GGA3	TGN	ARF1/3	Increase at 20°C
BIG1	TGN	ARF4/5	No change
BIG2	TGN	ARF4/5	Decrease at 16°C
Golgin-97	TGN	No	Puncta
GCC1	TGN	No	Variable decrease
GCC2	TGN	No	No change
p230	TGN	No	Increase; puncta

Table 4-1: Numerous Golgi-localized proteins show disrupted localization patterns during cold shifts. Multiple Golgi-localized proteins were analyzed by indirect immunofluorescence microscopy after incubation at 37, 20, or 16°C for 3h. Sub-Golgi localization and ARF dependence does not correlate to cold shift phenotypes. TGN, trans-Golgi network; CGN, cis-Golgi network; ERGIC, ER-Golgi intermediate compartment

Discussion

We previously reported that golgin-160 is a *cis*-Golgi concentrated golgin that facilitates the post-Golgi trafficking of several specific cargo proteins (Hicks *et al.*, 2006; Williams *et al.*, 2006; Gilbert *et al.*, 2014). In our attempts to further characterize the function of golgin-160, we utilized two common cold temperature blocks to synchronize protein trafficking. We report here that these temperature blocks lead to the disruption of not only golgin-160's localization (Figure 4-1), but the localization and function of multiple Golgi resident proteins, including ARF1, several ARF1-dependant proteins and numerous ARF1-independent proteins (Figure 4-7, Table 4-1, and Supplemental Figure 4-1).

ARF1 has many effector proteins, including golgin-160, which facilitate ARF1's critical roles in promoting anterograde and retrograde trafficking at the Golgi. At the *cis*-Golgi, the balance between the active ARF1-GTP and the inactive ARF1-GDP is maintained both by its GEF, GBF1, and multiple GAPs. Disruption of this balance has a negative impact on trafficking through the secretory pathway: overexpression of the activated Q71L mutant and the triple depletion of the semi-redundant ARFGAP1, 2, and 3 both lead to blocks in trafficking through the Golgi (Zhang *et al.*, 1994; Claude *et al.*, 1999; Saitoh *et al.*, 2009). It has been reported that wild-type ARF1 and the active ARF1 Q71L mutant can bind to the N-terminus of golgin-160 *in vitro* (Yadav *et al.*, 2012), which contains its Golgi targeting information (Hicks and Machamer, 2002). Here, we demonstrated that the degree and timing of dispersal of golgin-160 from Golgi membranes directly correlates with the ARF1-GTP levels in cells (Figures 4-1, 4-3, and 4-

4). This suggests the possibility that in addition to causing the dispersal of golgin-160, a decrease in ARF1 activity could cause the block in protein transport observed at cold temperatures. However, it is likely not the only contributing factor. The BFA-induced collapse of the Golgi into the ER is blocked at 20^{o}C and 16^{o}C, which indicates that decreased membrane dynamics also could be impacting vesicle or cisternae fission and fusion events (Lippincott-Schwartz *et al.*, 1990).

Typically, only GTP-bound ARF1 has high membrane affinity, therefore the decrease in ARF1-GTP at cold temperatures should correlate with a loss of Golgi localized ARF1. However, we saw no changes in ARF1-GFP localization in the cold (Figure 4-4). These data agree with the finding described by Manolea *et al.* (2010), where the cold induced dispersal of ARF3 was due to two unique amino acids in the ARF3 N-terminus. The corresponding amino acids on ARF1 had in fact previously been implicated in stabilizing ARF1 contact with membranes (Antonny *et al.*, 1997), and substituting these ARF1 residues with those from ARF3 caused ARF1 to gain temperature sensitivity (Manolea *et al.*, 2010). Therefore, we propose that ARF1 localization is separable from its nucleotide binding status at cold temperatures, possibly due to stabilized interactions between the ARF1 N-terminus and Golgi membranes. Furthermore, stabilized ARF1-GDP on Golgi membranes is not unique to cold temperatures. ARF1-GDP is bound by GBF1 on Golgi membranes, and both inhibition of GDP release from or GTP incorporation into ARF1 lead to stabilized ARF1-GBF1 interactions on Golgi membranes (Szul *et al.*, 2005). This stabilized interaction could explain the increased GBF1 Golgi localization in the cold (Figure 4-6). We

hypothesize that increased GBF1 does not lead to increased levels of ARF1-GTP because GBF1 is inactive at these temperatures. This was demonstrated by the observation that overexpression of GBF1 does not prevent golgin-160 dispersal (Figure 4-6), whereas directly expressing the active ARF1 mutant, ARF1 Q71L, can protect golgin-160 from cold-induced dispersal (Figure 4-5).

ARFGAPs also play a role in regulating ARF nucleotide state. While we have not investigated the multiple ARFGAPs reported to act on ARF1, the ARF1 GTPase cycle could be affected by inhibition of ARFGAPs in conjunction with inhibition of ARF GEFs at cold temperatures; it would not be surprising that multiple enzymes are inhibited at lower temperatures. Decreased ARFGAP activity could explain the stabilized β-COP localization at the Golgi (Figure 4-7), as ARFGAP-stimulated ARF1 GTPase activity is not required for the initial COPI coat recruitment to the Golgi, only for cargo-containing vesicles to be formed (Teal *et al.*, 1994; Nickel *et al.*, 1998; Lee *et al.*, 2005). Punctate β-COP localization similar to that seen in Figure 4-7 has been reported in two opposing conditions: increased active ARF1-GTP due to triple depletion of ARFGAP1, 2, and 3 and loss of ARF1 due to double depletion of ARFs (both ARF1 and ARF3, and ARF1 and ARF5) (Volpicelli-Daley *et al.*, 2005; Saitoh *et al.*, 2009). However, all depletion experiments resulted in additional phenotypes not observed here, notably ERGIC53 and GM130 puncta. We hypothesize that a simultaneous decrease in the activity of both the ARFGAPs and GBF1 could result in both β-COP being maintained on vesicle coats and Golgi membranes, and a decrease in the levels of ARF1-GTP. Interestingly, two other papers that examined Golgi protein localization in the cold reported increased ERGIC-53

Golgi localization and loss of β-COP from membranes at 15°C (Klumperman *et al.*, 1998 and Martínez-Alonso *et al.*, 2005, respectively). These various discrepancies could be due to several factors, including differences between acutely reducing protein function as demonstrated here (Figure 4-4A-B), depletion of protein over several days (Volpicelli-Daley *et al.*, 2005; Saitoh *et al.*, 2009), and differences in cell types used and methodology (Klumperman *et al.*, 1998; Martínez-Alonso *et al.*, 2005). It could also indicate that the stabilization of β-COP on the Golgi and in extra-Golgi puncta observed here may be through a more complex mechanism that we have yet to fully understand.

In addition to golgin-160, other ARF-dependent proteins have altered localization during cold shifts (Table 4-1). Like β-COP, multiple coat proteins had increased Golgi localization at cold temperatures. Intriguingly, we found that the *trans*-Golgi clathrin coat adaptor complex and ARF effector AP-1, like β-COP, had increased Golgi localization at cold temperatures (Table 4-1 and Supplemental Figure 4-1). As ARF3 (which has a semi-redundant role in vesicle coating and trafficking at the *trans*-Golgi with ARF1; Shin *et al.*, 2004; Dong *et al.*, 2010) is most likely dissociated from the Golgi at these temperatures (Manolea *et al.*, 2010), and we have shown here that ARF1 has decreased activity (Figure 4-4), we would predict that AP-1 would have decreased Golgi localization in the cold. It has been shown, however, that AP-1 binding to a cargo sorting signal enhances subsequent cargo binding and stabilizes AP-1 binding to ARF1-GTP (Lee *et al.*, 2008). The high concentration of cargo proteins induced by trapping cargo at the *trans*-Golgi, in addition to altered Golgi membrane dynamics, may allow for stable association of cargo adaptors like AP-1 on Golgi membranes even when levels of ARF1-

GTP are reduced. This cargo-induced or -stabilized recruitment of coat proteins is not unique to AP-1. GGA2 and GGA3 are two *trans*-Golgi localized proteins which also have enhanced recruitment to the Golgi in the presence of overexpressed cargo, even in the presence of BFA when ARF1 should be inactive (Hirst *et al.*, 2007). Interestingly, GGA2 localization does not change in the cold, while GGA3 has increased Golgi localization only at 20^{o}C (Table 4-1 and Supplemental Figure 4-1). The GGA3 localization phenotype could be due to cargo being trapped at the *trans*-Golgi at 20^{o}C, compared to at the *cis*-Golgi at 16^{o}C, though why it is different from GGA2 has yet to be explored.

Several of the proteins examined in Table 4-1 with altered localization in the cold are recruited to the Golgi independently of ARF activity. This indicates that multiple mechanisms or regulators of protein localization may be impacted by cold temperature shifts. What is particularly interesting is that proteins that contain similar localization signals (e.g. the GRIP domain containing proteins golgin-97, p230, GCC1, and GCC2) have distinct localization phenotypes at cold temperatures. Previous work examining Golgi structure at cold temperatures demonstrated that glycosylation enzymes and several SNARE and Rab proteins involved in intra-Golgi transport rapidly localized to Golgi-derived tubules in cells shifted to 15^{o}C, as well (Martínez-Alonso *et al.*, 2005, 2007a, 2007b). Overall, these data support the idea of a complex system of protein and membrane interactions being disturbed at lower temperatures.

Cold temperature trafficking blocks are undeniably useful due to their ability to stop all cargo proteins in specific subcompartments of the Golgi complex, which is why they are still in use 3 decades after their initial discovery (Park *et al.*, 2011; Lavieu *et al.*,

2013, 2014; Jensen *et al.*, 2014; Farr *et al.*, 2015). However the effect of these blocks on Golgi function itself has not been studied in depth. While we cannot state that a decrease in GBF1 or ARFGAP function is the sole mechanism by which these trafficking blocks work, altering the activity of ARF1 has been associated with complete cargo trafficking blocks (Zhang *et al.*, 1994; Saitoh *et al.*, 2009). The effects of the cold temperature blocks on golgin-160 localization are reversible; however while cargo trafficking immediately restarts at permissive temperatures, it takes more than 30 minutes for golgin-160 to completely recover its Golgi localization. Therefore, the trafficking roles of mislocalized proteins like golgin-160 may not be fully reconstituted immediately after return to 37^{o}C.

Though more specialized in scope, several new techniques to synchronize cargo trafficking have been developed in the past few years. The RUSH system can block a protein of interest in a specific secretory compartment (Boncompain *et al.*, 2012), the IM-LARIAT system combines optogenetics and protein aggregation to reversibly sequester vesicles and inhibit trafficking at various stages throughout the secretory system (Nguyen *et al.*, 2016), and the CUTE system controls cargo movement by reversible masking of transport signals (Abraham *et al.*, 2016). Additionally, improvements in microscopy and photoactivatable constructs allow for visual pulse chases to be performed in cells. Genetic editing techniques are also allowing for the introduction of tagged proteins that are expressed at endogenous levels. These techniques may provide better methods of synchronization of cargo proteins in the future.

Supplemental Figure 4-1: Numerous ARF-dependent and -independent proteins have disrupted localization patterns during cold shifts. Multiple Golgi-localized proteins were analyzed by indirect immunofluorescence microscopy after incubation at 37, 20, or 16oC for 3h. The cells were labeled with primary antibodies, as described in the Materials and Methods section, followed by Alexa Fluor 488 anti-rabbit IgG or Alexa Fluor 546 anti-mouse IgG. Scale bar, 10 µm. Proteins have been categorized by their response to cold shifts, for clarity.

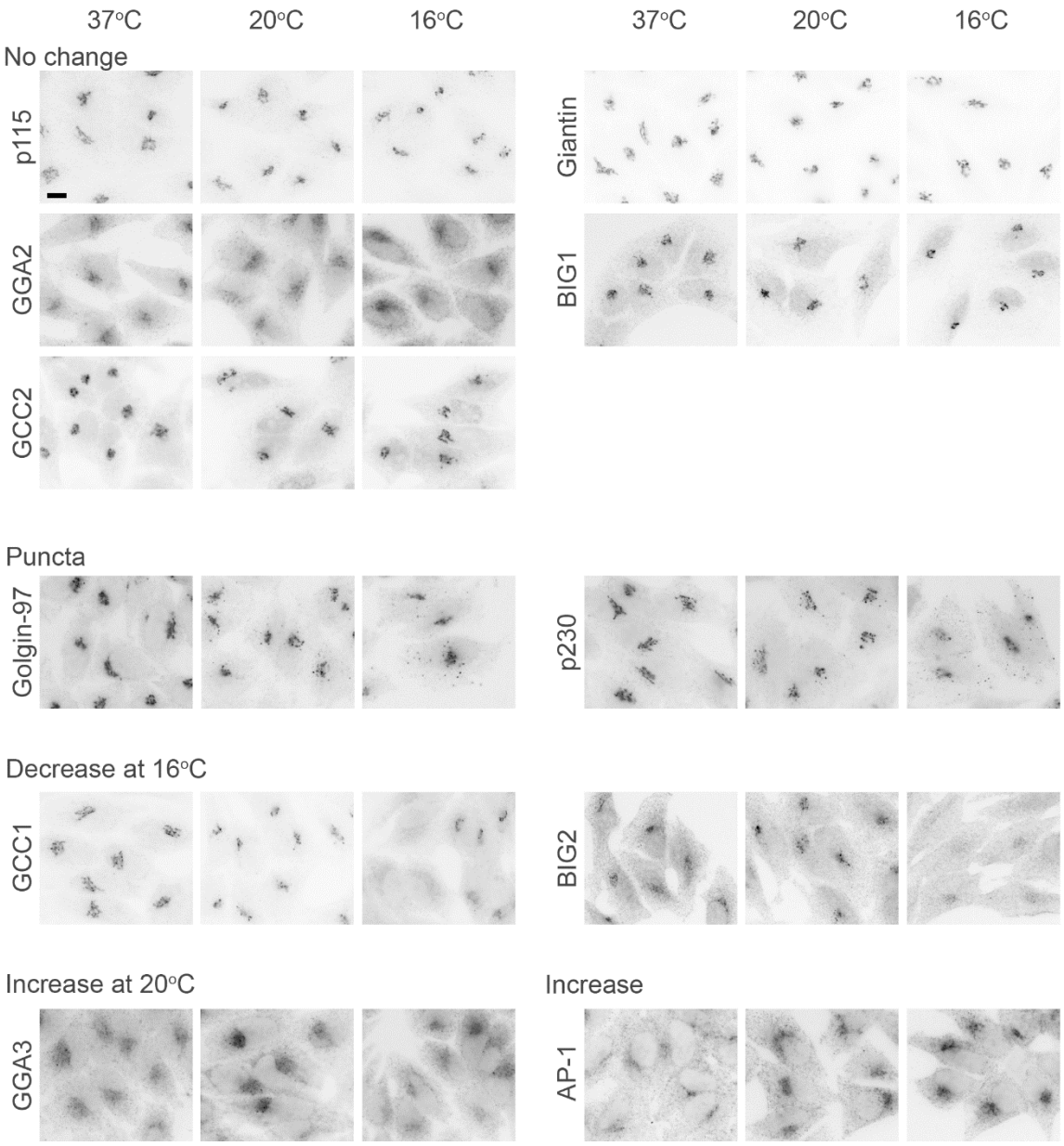
37°C
20°C
16°C
37°C
20°C
16°C
No change
p115
Giantin
GGA2
BIG1
GCC2
Puncta
Golgin-97
p230
Decrease at 16°C
GCC1
BIG2
Increase at 20°C
Increase
GGA3
AP-1

Materials and Methods

Cell Culture

HeLa cells (ATCC CCL-2) were maintained in Dulbecco's Modified Eagle's Medium (DMEM; Life technologies, Grand Island, NY, USA) supplemented with 10% fetal bovine serum (Atlanta Biologicals, Flowery Branch, GA, USA) and 0.1 mg/mL Normocin (InvivoGen, San Diego, CA, USA) at 37^{o}C with 5% CO_2. The cells were authenticated by STR profiling in the Johns Hopkins Genetics Resources Facility, and are tested for mycoplasma contamination every 6 months.

Expression Constructs and Transient Transfection

The plasmid encoding GFP-ARF1 WT was obtained from Addgene (#39554; Cambridge, MA, USA). The Q71L mutation was introduced via Quikchange mutagenesis and confirmed by sequencing (Stratagene, La Jolla, CA, USA), using the following mutagenic primers: 5'-GACGTGGGTGGCCTGGACAAGATCCGG-3' and its complement, 5'-CCGGATCTTGTCCAGGCCACCCACGTC-3'. The Venus-GBF1 A795E construct was previously described (Lanke *et al.*, 2009). The A795E mutation provides resistance to BFA but otherwise this construct behaves similarly to WT (Lanke *et al.*, 2009). The GBF1 A795E coding region was subcloned into the pEGFP N1 backbone (Clontech, Mountain View, CA, USA).

Transfection was performed using the X-tremeGENE 9 DNA transfection reagent (Roche, Indianapolis, IN) in accordance with the manufacturer's protocol. For all transfection experiments, 35 mm dishes of HeLa cells were transfected with 0.2 μg of plasmids

encoding GFP-ARF1 WT or GFP-ARF1 Q71L, or 0.5 μg of the plasmid encoding GFP-GBF1 A795E. Experiments were performed 16-17 h post transfection.

Antibodies

Rabbit anti-golgin-160 N-terminal head domain was previously described and validated (Chandran and Machamer, 2008). Rabbit anti-golgin-160 C-terminus was also previously described and validated (Hicks and Machamer, 2002). Mouse anti-GBF1, -GM130, -GGA2, -GGA3, -p115, and -p230 were obtained from BD Transduction Laboratories (San Jose, CA, USA). Mouse anti- β-COP, -actin (A3853), -ERGIC-53, and -AP-1 (gamma adaptin) were obtained from Sigma-Aldrich (St. Louis, MO, USA). Rabbit anti-GCC1 and -GCC2 were obtained from Atlas Antibodies (Bromma, Sweden). Mouse anti-golgin-97 was obtained from Molecular Probes/Thermo Fisher Scientific (Rockford, IL, USA). Rabbit anti-giantin was obtained from Covance/BioLegend (San Diego, CA, USA). Mouse anti-ARF1 was obtained from Cell Biolabs, Inc. (San Diego, CA, USA). Rabbit anti-BIG1 and -BIG2 were previously described (Lowery *et al.*, 2013). Alexa Fluor 568 anti-mouse IgG and Alexa Fluor 488 anti-rabbit IgG were from Life Technologies (Grand Island, NY, USA). Cy5-conjugated AffiniPure Donkey anti-rabbit IgG was obtained from Jackson ImmunoResearch Laboratories, Inc. (West Grove, PA, USA). IRDye 680RD goat anti-mouse IgG and 680RD donkey anti-rabbit IgG were obtained from LI-COR, Inc. (Lincoln, NE, USA).

Temperature Shifts

For all temperature shifts, cells were placed in normal growth medium containing 20 mM HEPES (Cellgro, Manassas, VA, USA) that had been pre-chilled to 20 or 16^{o}C. Dishes were parafilmed closed and placed in water baths set to 20 or 16^{o}C for 3 h (or the indicated time). For recovery at 37^{o}C, after cells were first incubated at 16^{o}C for 3 h, the medium was exchanged for media lacking HEPES that had been pre-warmed at 37^{o}C and cells were returned to a 37^{o}C incubator with 5% CO_2.

Indirect Immunofluorescence Microscopy and Quantification

Cells were plated on 15 or 35 mm dishes with coverslips for 24 h before transfection with GBF1 or ARF1 constructs, or 48 h for analysis of endogenous proteins, before temperature shifts were performed. At the indicated times post temperature shift, cells were fixed with 3% paraformaldehyde in PBS for 10 min at room temperature. For most antibodies, cells were permeabilized for 10 min with 0.02% saponin (CalBiochem/Sigma) and 10 mM glycine (Sigma) in phosphate buffered saline (PBS; Sap/PBS/gly buffer). Coverslips were incubated 15 min in primary antibody diluted in Sap/PBS/gly buffer with 1% bovine serum albumin (BSA). Cells were washed 2 times with Sap/PBS/gly buffer before being incubated in secondary antibody diluted as above. Cells were washed again before being incubated for 3 min in 0.1 μg/mL Hoechst 33258 diluted in PBS. Coverslips were then mounted in glycerol with 0.1 M N-propyl gallate.

Several antibodies (BIG1, BIG2, β-COP) required permeabilization in 0.5% Triton X-100 in PBS/10 mM glycine for 3 min. For these antibodies, coverslips were washed in

PBS/glycine buffer without saponin, and antibodies were also diluted in PBS/glycine with 1% BSA.

Coverslips were imaged on an Axioskop microscope (Zeiss, Thornwood, NY, USA) equipped for epifluorescence using an ORCA-03G charge-coupled device camera (Hamamatsu, Japan) using iVision software (BioVision Technologies, Exton, PA, USA). All images are shown inverted for better visualization of cytoplasmic localization. For quantification of golgin-160 localization, regions of interest (ROI) were created around the Golgi region using the GM130 image as well as around the whole cell, and the integrated pixel density of the golgin-160 signal in each ROI was determined using FIJI (National Institutes of Health, Bethesda, MD, USA). For each experiment, control images where fluorescent light was blocked from reaching the camera (no photon controls) were also taken to account for variations in camera light detection. Adjusted integrated pixel densities for each ROI were calculated by subtracting the pixel density measured in the control images from the corresponding experimental image pixel densities. To calculate the percent of golgin-160 at the Golgi, the adjusted integrated pixel density at the Golgi was divided by that of the whole cell. This percent was then normalized to 37^{o}C by dividing each individual percent by the average percent at 37^{o}C. For endogenous protein quantification, 3 independent experiments were performed and between 180-300 cells were quantified per condition. For transfected cell experiments, 4 independent experiments were performed and between 130-190 cells were quantified per condition. For all box and whiskers plots, the center bar represents the mean, the

box extends from the 25th to the 75th percentiles, and the whiskers extend to the minimum and maximum values.

Golgin-160 expression levels

HeLa cells were seeded on 35 mm dishes and allowed to grow for 48 h before being shifted to 20 or 16^{o}C as described above. After 3 h, cells were washed with PBS twice and then lysed on ice for 10 min in lysis buffer (1% NP-40, 0.4% DOC, 50 mM Tris, pH 8.0, 62.5 mM EDTA, pH 8.0) containing protease inhibitors. The lysate was separated by SDS-PAGE (10% acrylamide) and golgin-160 and actin were detected by immunoblotting after transfer to Immobilon-FL PVDF (EMD Millipore, Billerica, MA, USA), by near-infrared fluorescent imaging on the Odyssey CLx Imaging System (LI-COR, Lincoln, NE, USA). The amount of protein in each lane was measured using Quantity One volume analysis tools (Bio-Rad, Hercules, CA, USA). The graph represents the mean value of 5 independent replicates, and the error bars represent standard deviation.

Active ARF1-GTP Pull Down

The amount of active ARF1-GTP in HeLa cells at each temperature condition was determined using the ARF1 Activation Assay kit (Cell Biolabs, Inc., San Diego, CA, USA). In brief, three 6 cm dishes of HeLa cells were incubated at each condition, 37, 20, or 16^{o}C, for 3 h as described above. Three recovery dishes were incubated at 16^{o}C for 3 h before being returned to 37^{o}C for 0.5 h. The cells were then lysed on ice using the kit lysis buffer with protease inhibitors for 10 min. After clarification of the lysate, 10% input was removed and the remaining lysate was added to 40 μL of GGA3 protein

binding domain (PBD) agarose bead slurry. The lysates and beads were rotated for 1 h at 4^{o}C before the beads were washed 3 times in lysis buffer. The beads were resuspended in 40 μL SDS-PAGE loading sample buffer (0.1 M Tris, pH 6.8, 0.04% SDS, 30% glycerol, 0.1% bromophenol blue) with 4% BME and boiled for 3 min at 95^{o}C. The input and 50% of the pull down for each condition were then separated on a 4-12% NuPAGE Bis/Tris gel (Thermo Fisher Scientific), transferred to PVDF, and analyzed for ARF1 via Western blotting. Blots were imaged on the Odyssey CLx Imaging System and the amount of protein in each lane was measured using Image Studio (LI-COR, Lincoln, NE, USA). n=3 for the recovery condition, and n=5 for all other conditions. The center line on the scatter plot represents the mean and the error bars represent the standard deviation.

Statistical Analysis

Graphs and statistical analyses were obtained using GraphPad Prism version 7.00 for Mac OS X (GraphPad Software, La Jolla, CA, USA). For all experiments, one-way ANOVA followed by Tukey's multiple comparisons test were performed. For the microscopy data, outliers were identified using Prism's Robust Regression and Outlier removal (ROUT) tool with Q set to 1%. Between 0-1 outliers (out of 130-300 measurements) per condition were identified per experiment and removed.

Conclusions

The objective of this thesis was to understand how the *cis*-Golgi localized protein, golgin-160, was affecting the post-Golgi trafficking of its cargo protein, β1AR. In the pursuit of that goal, we have characterized the binding interaction between these two proteins and have identified three basic residues on the third intercellular loop of β1AR that are critical for this interaction. We have also discovered that golgin-160 is temporarily displaced from Golgi membranes when a bolus of β1AR exits the *cis*-Golgi. While our analysis is complicated by the discovery that golgin-160 localization is artificially disrupted by a commonly used synchronization technique, new technologies are providing alternative strategies to modulate cargo trafficking. One such technique, the RUSH system, allowed us to examine the dynamics of β1AR trafficking in post-Golgi vesicles in the absence of golgin-160. These vesicles could move at similar speeds to those from cells containing golgin-160, but they had defects in maintaining processive movement. This suggests the intriguing possibility that golgin-160 may be altering interactions between β1AR containing vesicles and multiprotein scaffolding complexes that link vesicles to motor proteins.

The N-terminal head domain of golgin-160 contains multiple localization signals and protein interaction domains. The same region, encompassing residues 140-257, is the site for ARF1-GTP binding and β1AR binding, and also contains a cryptic nuclear localization signal that can be revealed after secretory stress-induced cleavage by caspases (Hicks and Machamer, 2002; Hicks *et al.*, 2006; Yadav *et al.*, 2012). ARF1-GTP is required for Golgi membrane localization of golgin-160 (Yadav *et al.*, 2012), therefore

our data showing that expression of β1AR induces loss of golgin-160 Golgi localization fit with a model in which golgin-160 changes from binding ARF1-GTP to β1AR. Golgin-160 does not disperse until after β1AR has left the *cis*-Golgi, which suggests that the multipass transmembrane β1AR maintains its interaction with golgin-160 until it leaves that compartment. Determining what changes dictate golgin-160 binding to β1AR and release will be very informative for understanding the localization changes and mechanism of golgin-160 promoted trafficking. The RUSH system could be used in conjunction with proteomics assays to study the cleavage and post translational modification state of golgin-160 at distinct stages during β1AR trafficking, and the effects of any changes to golgin-160 on the binding between these two proteins could be analyzed.

The RUSH system in conjunction with improvement in microscopes and image analysis packages will also improve our understanding of how golgin-160 is impacting vesicle dynamics. The lattice light sheet microscope can image the entire cell depth quickly, and improvements to heating chambers and CO_2 delivery, as well as optimizing fluorophore tags for improved signal to noise ratios, would make it an attractive system to image vesicle movements from the Golgi to the plasma membrane. Biochemical work to identify the cargo adaptors and scaffold complexes associated with β1AR containing vesicles in the presence and absence of golgin-160 could also provide mechanistic insight to how golgin-160 is affecting vesicle trafficking.

It is interesting to note that golgin-160 is only found in vertebrates, and only affects a small (that we are aware of) subset of the proteins that pass through the Golgi.

Has golgin-160 evolved to fulfill a purpose not required in non-vertebrates? The three known golgin-160-dependent cargo proteins are multipass transmembrane proteins that can have deleterious effects when their localization to the plasma membrane is altered, and therefore their localization needs to be tightly regulated. And yet golgin-160 effects them in different ways – promoting β1AR and ROMK delivery to the plasma membrane, but preventing GLUT4 from traveling directly to the plasma membrane from the medial Golgi. Perhaps a unifying characteristic of these cargo proteins might be altered localization in response to cell stresses. Golgin-160 is cleaved early in response to secretory stress-induced apoptosis (Mancini *et al.*, 2000). There may be a benefit to altering the localization of these particular proteins under stress conditions, for example by rapidly increasing glucose entry by having GLUT4 bypass GSVs, or increasing the amount of intracellular β1AR signaling. There may in fact be a connecting feature between these proteins that will only be revealed as improvements in protein trafficking assays allow us to identify more golgin-160-dependent cargo proteins.

An increasing number of protein tag or modification based synchronization systems, like the RUSH system, are being developed. Our work demonstrating that the commonly used temperature block method of protein synchronization causes significant changes to the localization and function of Golgi proteins proves that these alternate systems are necessary to gain an accurate understanding of protein trafficking through the secretory system. Golgin-160 becomes cytoplasmic when these blocks are used, and therefore is likely not performing its Golgi-based function. While golgin-160 can recover to the Golgi after cells are returned to 37^{o}C, it is not an immediate recovery. In contrast,

synchronized cargo immediately begins trafficking through the secretory pathway, and therefore golgin-160 may still be predominantly cytoplasmic when cargo proteins are passing through the *cis*-Golgi. It is therefore possible that there are additional proteins with golgin-160 facilitated trafficking that have remained undiscovered, as the assays used to test protein requirements for cargo trafficking may have essentially been performed in golgin-160 depleted cells.

The changes in golgin-160 localization at reduced temperatures are due to preventing the activation of ARF1 through inhibition of GBF1, and another lab has reported that ARF3 is also mislocalized and likely inactive at cold temperatures. This could explain why numerous proteins at both the *cis*- and *trans*-Golgi also have altered localization in response to cold shifts. Why ARF-independent proteins are also affected by cold shifts is currently unknown, but could be through altering the function or activity of other GTPases that are critical to protein trafficking through the secretory system. Regardless of the precise mechanism, the data presented here indicate that results obtained using these methods need to be critically assessed and verified. Using alternate methods may lead to the discovery of more golgin-160 dependent cargo proteins, which will help to further elucidate the mechanism of golgin-160 facilitated cargo trafficking.

Appendix A

GBF1 and the GBF1-ARNO Chimera GARG can

Promote Golgin-160 Localization and β1AR Trafficking

Results

GBF1 (Golgi Brefeldin A Resistant Guanine Nucleotide Exchange Factor 1) is a large GEF that facilitates ADP-ribosylation factor 1 (ARF1) activation (Gillingham and Munro, 2007). Golgin-160 is an ARF1 effector, and depletion of GBF1 causes loss of golgin-160 Golgi localization (Yadav *et al.*, 2012). The lab of Dr. Elizabeth Sztul at the University of Alabama at Birmingham generated a chimera of two ARF1 GEFs, the large GEF GBF1 and the pleckstrin homology (PH) domain containing ARF GEF ARNO (ARF nucleotide-binding site opener, also known as cytohesin-2) (Nawrotek *et al.*, 2016). The chimera, called GBF1-ARNO-GBF1 or GARG, consists of the GBF1 A795E backbone (a mutation which confers brefeldin A, BFA, resistance) with the sec7 catalytic domain of ARNO. The purpose of these experiments was to characterize both the ability of GBF1 to support the localization and function of golgin-160, and examine how altering the sec7 domain (with the ARNO mutant) affects this ability.

BFA inhibits the large ARF GEFs, including GBF1, and treating cells with BFA also leads to loss of golgin-160 localization, as well as the general collapse of the Golgi into the ER (Lippincott-Schwartz *et al.*, 1990; Yadav *et al.*, 2012). We confirmed the loss of golgin-160 localization in the presence of BFA, as well as the loss of Golgi structure seen by the redistribution of giantin in BFA treated cells. We also demonstrated that the BFA resistant GBF1 mutant, GBF1 A795E, could prevent the mislocalization of both golgin-160 and giantin, indicating that the Golgi structure and the activity of ARF1 were restored in GBF1 A795E transfected cells (Figure A-1A). Immunofluorescence

microscopy of golgin-160 and giantin demonstrated that cells expressing GARG also maintained intact Golgi structures in the presence of BFA (Figure A-1B).

We next tested the ability of GBF1 to support not just the localization but also the function of golgin-160. Golgin-160 promotes the efficient trafficking of the beta-1 adrenergic receptor (β1AR) to the plasma membrane. Using the retention using selective hooks (RUSH, described in Chapter 3) system, we demonstrated by immunofluorescence microscopy that β1AR trafficking to the plasma membrane was inhibited in the presence of BFA (Figure A-2A). This inhibition was relieved by co-expression of the GBF1 A795E mutant (Figure A-2B). This observation was confirmed using a radiolabeled ligand binding assay. [3H]-CGP-12177 is a tritiated β1AR-specific cell impermeable ligand. HeLa cells expressing β1AR alone or β1AR and GBF1 A795E were pre-treated for 45 min with BFA before 10 uM biotin was added to release RUSH β1AR from the ER. An increase in the surface levels of β1AR over time was observed only in cells co-expressing GBF1 A795E (Figure A-2C). A smaller scale experiment showed that GARG could also promote β1AR trafficking to the plasma membrane in the presence of BFA (Figure A-2D).

Finally, we had previously observed that expression of constitutively expressed β1AR leads to a decrease in Golgi localized golgin-160, and that this phenotype could not be prevented by expression of GBF1 (discussed in Chapter 3, Figure 3-1). GARG could not prevent this β1AR-induced loss of golgin-160 localization, either (Figure A3-A and B, β1AR alone and GBF1 transfected data from Figure 3-1 replicated here for comparison).

Figure A-1: GBF1 A795E and GARG both maintain Golgi structure and golgin-160 recruitment to Golgi membranes in BFA-treated cells. HeLa cells transiently transfected for 16 h with (A) GFP-GBF1 A795E or (B) GFP-GARG were either left untreated (-BFA) or treated with 0.5 mg/mL BFA for 45 min (+BFA) before the localization of the GFP constructs, endogenous and transfected GBF1, golgin-160, and giantin were assessed by immunofluorescence microscopy. GFP was used to identify transfected cells, and cells were labeled with mouse anti-GBF1, and rabbit anti-golgin-160 or -giantin, followed by Cy5 anti-rabbit IgG and Alexa Fluor 568 anti-mouse IgG. Arrows indicate transfected cells.

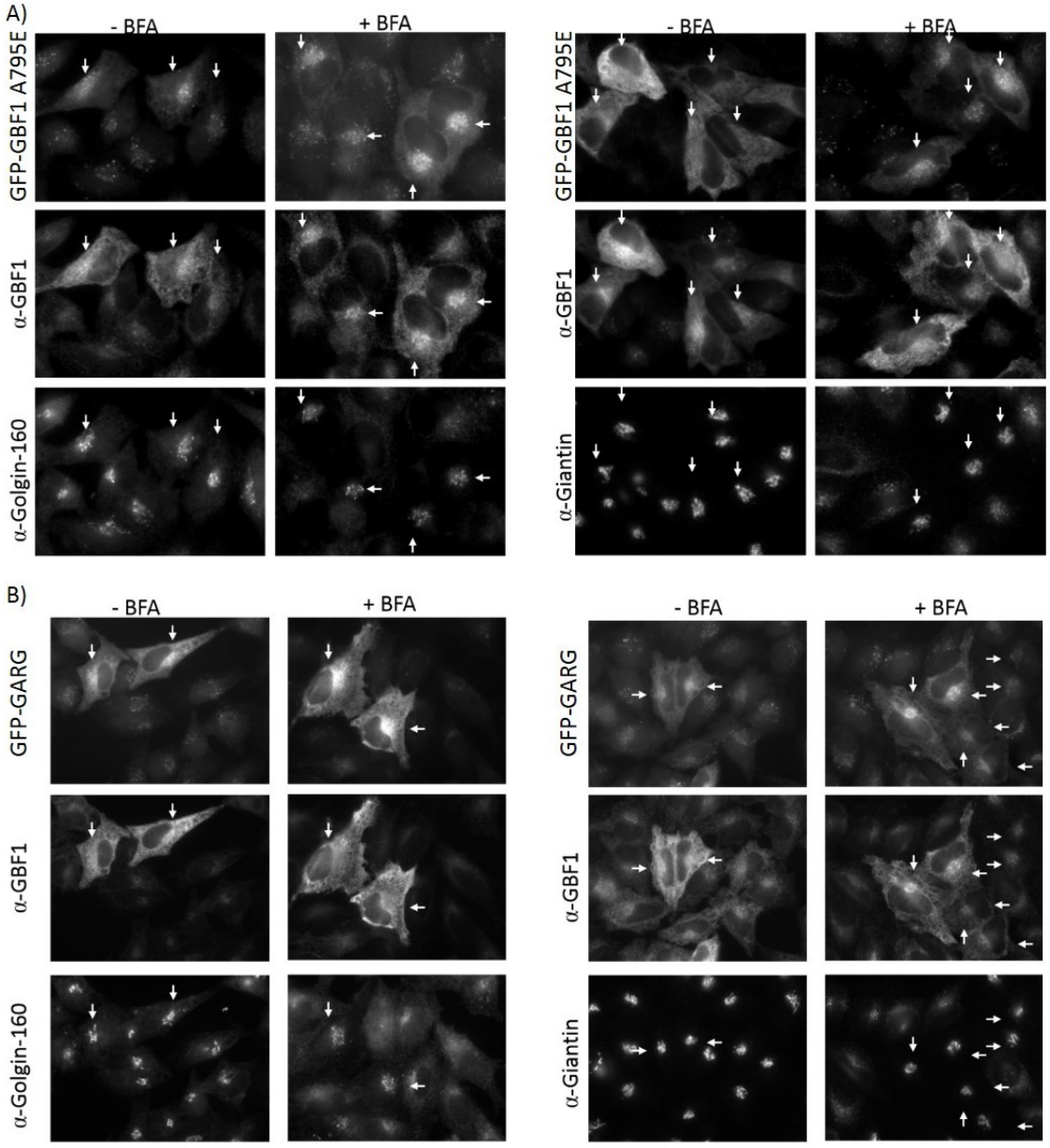
A)
- BFA
+ BFA
GFP-GBF1 A795E
α-GBF1
α-Golgin-160
α-Giantin
B)
GFP-GARG

Figure A-2: GBF1 A795E and GARG can promote the surface delivery of RUSH β1AR to the plasma membrane in the presence of BFA. (A-B) HeLa cells that were either expressing RUSH β1AR alone (A) or co-expressing RUSH β1AR with GBF1 A795E (B) were pretreated with BFA for 45 minutes before biotin was added for the indicated times to release β1AR from the ER. Surface staining was performed to visualize the effects of BFA and GBF1 A795E on the plasma membrane delivery of β1AR. The surface pool was detected using rabbit anti-mCherry followed by Alexa Fluor 488 anti-rabbit IgG, and was compared to total β1AR localization measured by mCherry fluorescence. Mouse anti-GBF1 was used, followed by Cy5 anti-mouse IgG, to detect endogenous and transfected GBF1. (C) Cells were transfected and pretreated with BFA identically to (A-B) and the surface pool of β1AR was quantified using the availability of β1AR to bind the cell-impermeable radiolabeled ligand [3H]CGP-12177. Radioactive counts per minute were normalized to β1AR expression levels. A representative experiment is shown. (D) The same protocol was used as in (C), but cells were transfected with RUSH β1AR alone or RUSH β1AR and GARG.

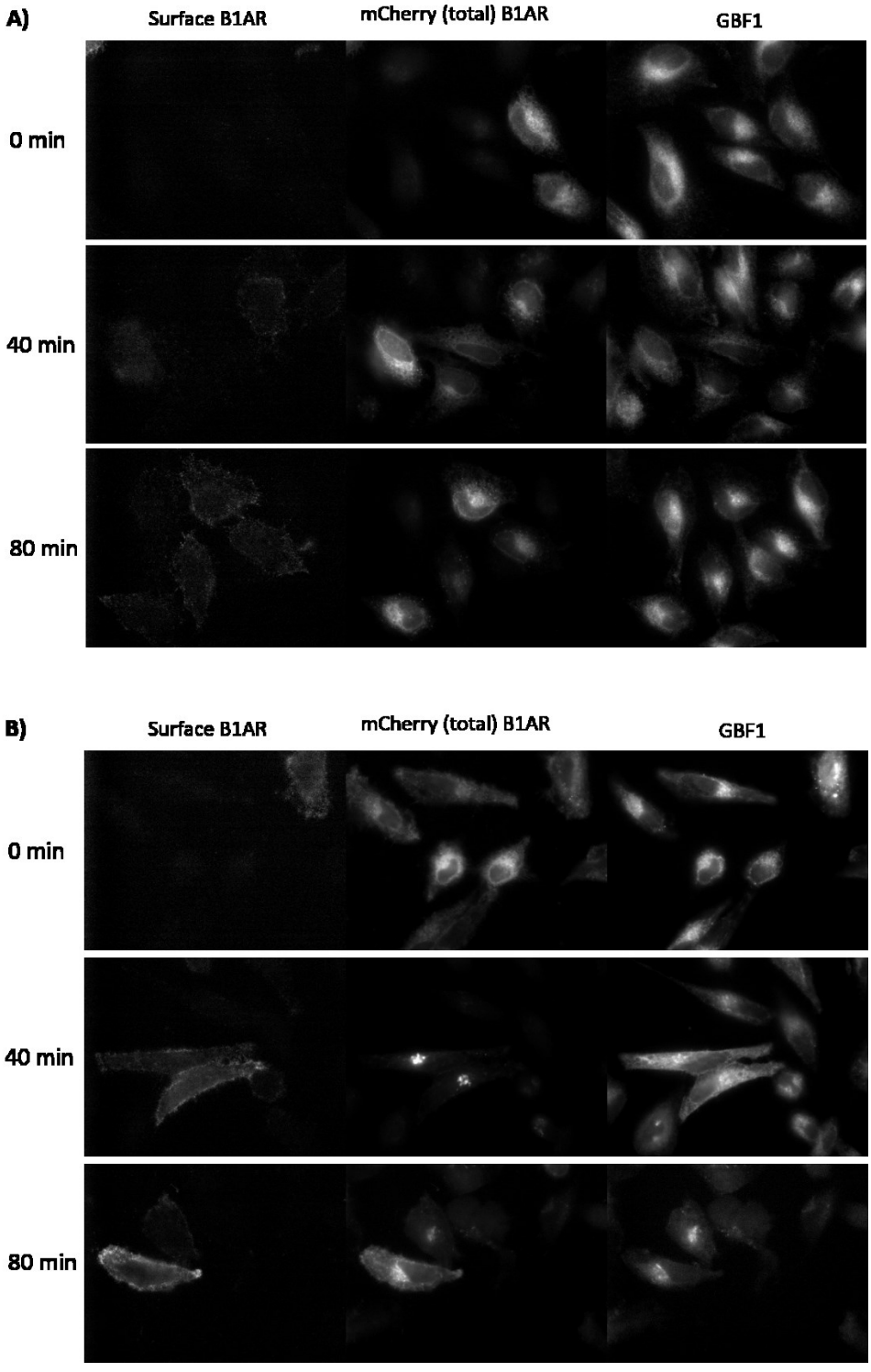
A)
Surface B1AR
mCherry (total) B1AR
GBF1
0 min
40 min
80 min
B)
Surface B1AR
mCherry (total) B1AR
GBF1
0 min
40 min
80 min

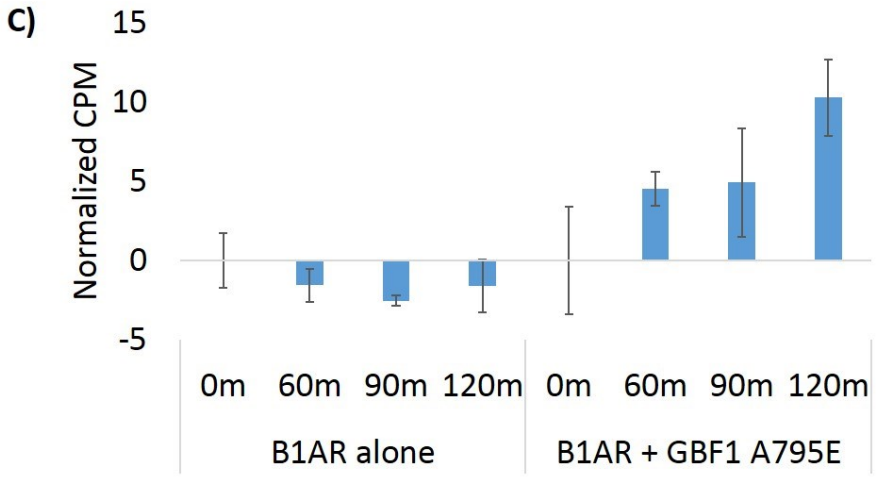
C)
15
10
5
0
-5
Normalized CPM
0m
60m
90m
120m
0m
60m
90m
120m
B1AR alone
B1AR + GBF1 A795E

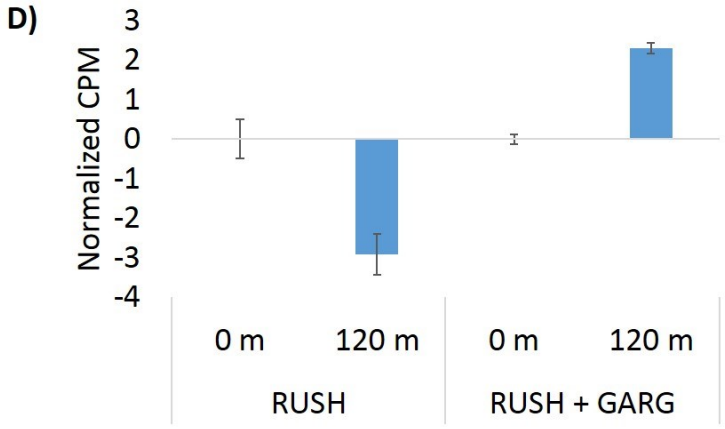
D)
3
2
1
0
-1
-2
-3
-4
Normalized CPM
0 m
120 m
0 m
120 m
RUSH
RUSH + GARG

Figure A-3. GARG does not prevent the β1AR-induced loss of golgin-160 Golgi localization. Representative images of HeLa cells transfected with mCherry-β1AR alone, mCherry-β1AR and HA-GBF1, or mCherry-β1AR and HA-GARG for 18 h. Cells were labeled with rabbit anti-golgin-160 and mouse anti-GM130, followed by Cy5 anti-rabbit IgG and Alexa Fluor 488 anti-mouse IgG. mCherry fluorescence was used to identify transfected and co-transfected cells. Arrows indicate the Golgi regions of β1AR expressing cells. (C) Quantification of golgin-160 dispersal. The GM130 signal was used to outline the Golgi region in each cell, and the amount of golgin-160 fluorescent signal was calculated within the Golgi and divided by the total golgin-160 fluorescence in the cell to obtain the percent of golgin-160 at the Golgi. Each fluorescence intensity value was normalized to nontransfected cells. n=39-43 cells.

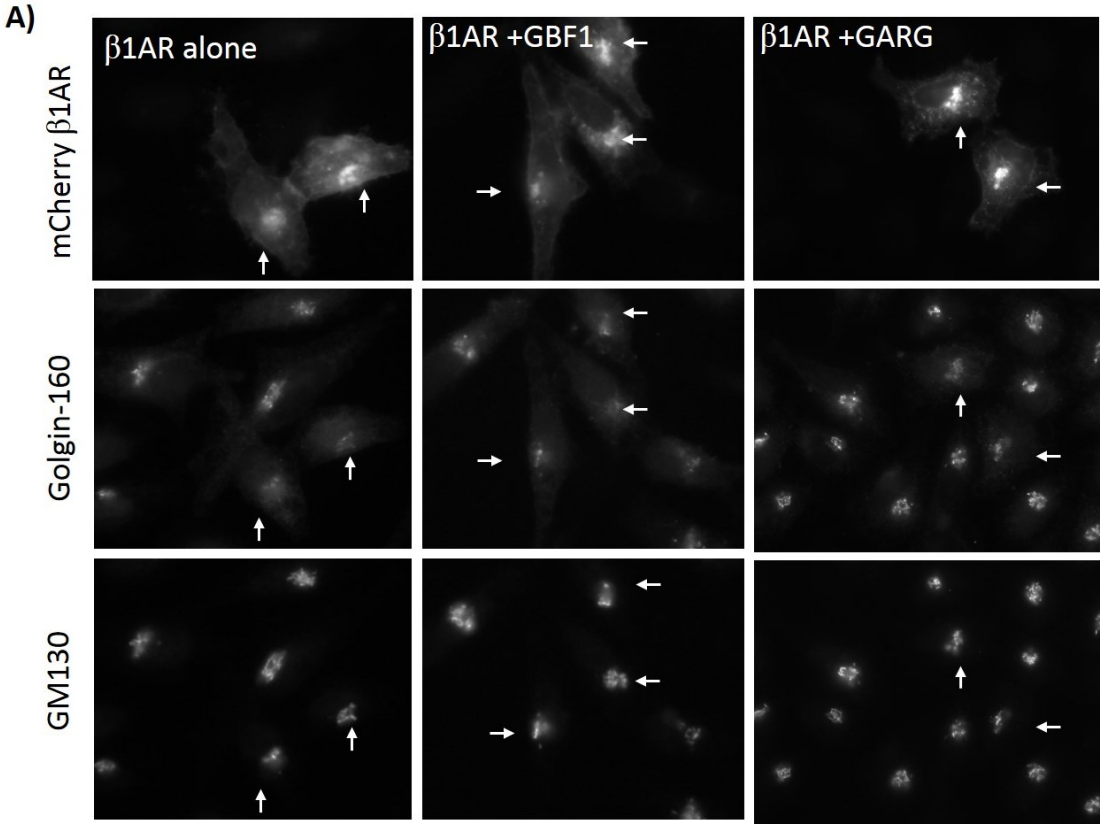
A)
β1AR alone
β1AR +GBF1
β1AR +GARG
mCherry β1AR
Golgin-160
GM130

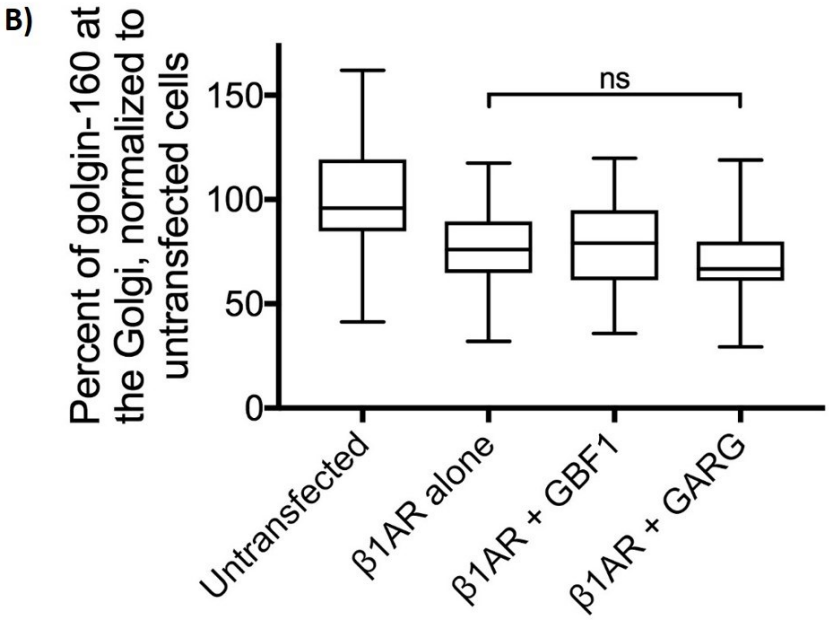
B)
Percent of golgin-160 at the Golgi, normalized to untransfected cells
150
100
50
0
ns
Untransfected
β1AR alone
β1AR + GBF1
β1AR + GARG

Overall, these data show that both GBF1 and the sec7 chimera GARG can promote the localization and function of golgin-160. Experiments in BFA-treated cells demonstrated the sufficiency of GBF1 for this role. This is important as ARF1 also localizes to the *trans*-Golgi where it is activated by two other large GEFs, brefeldin A-inhibited guanine nucleotide exchange proteins 1 and 2 (BIG1/2). Golgin-160 facilitates a late-Golgi trafficking step to promote β1AR surface delivery; therefore an attractive hypothesis is that golgin-160 can be recruited by ARF1 to both the *cis*- and *trans*-Golgi. While these experiments show that overall β1AR trafficking is restored by coexpression of GBF1 or GARG in the presence of BFA, further experiments will be needed to determine if this is the maximal surface delivery, or if BIG1/2-mediated recruitment of golgin-160 to the *trans*-Golgi is needed for golgin-160-enhanced β1AR trafficking.

Materials and Methods

HeLa Cell Culture

HeLa cells were maintained in Dulbecco's Modified Eagle's Medium (DMEM; Life technologies, Grand Island, NY, USA) supplemented with 10% fetal bovine serum (Atlanta Biologicals, Flowery Branch, GA, USA) and 0.1 mg/mL Normocin (InvivoGen, San Diego, CA, USA) at 37^{o}C with 5% CO_2.

Expression Plasmids and Transfection

HA-GBF1 A795E and HA-GARG were provided by Elizabeth Sztul (University of Alabama at Birmingham, Birmingham, AL, USA). They were subcloned into the eGFP C1 backbone (Clontech, Mountain View, CA, USA). Human FLAG- β1AR was provided by Randy Hall (Emory University, Atlanta, GA, USA). The mCherry β1AR and RUSH β1AR plasmids were constructed as described in Chapter 3. All plasmids were confirmed by sequencing.

HeLa cells were plated in 35 mm dishes and transfected at ~70% confluency using X-tremeGENE9 DNA transfection reagent (Roche, Indianapolis, IN, USA) according to manufacturer instructions. For immunofluorescence, 0.5 ug of each plasmid was used. For radiolabeled ligand binding, 1 ug of each construct was used. RUSH β1AR was transfected for 20 h before cells were manipulated as described below. All other constructs were transfected for 16-17 h.

Antibodies

Rabbit anti-golgin-160 N-terminal head domain was previously described (Chandran and Machamer, 2008). Mouse anti-GBF1 and -GM130 were obtained from BD Transduction Laboratories (San Jose, CA, USA). Mouse anti-mCherry was obtained from Sigma-Aldrich (St. Louis, MO, USA). Rabbit anti-giantin was obtained from Covance/BioLegend (San Diego, CA, USA). Rabbit anti-β1AR was obtained from Santa Cruz Biotechnology (Santa Cruz, CA, USA). -Alexa Fluor 568 anti-mouse IgG and Alexa Fluor 488 rabbit IgG were from Life Technologies (Grand Island, NY, USA). Cy5-conjugated AffiniPure donkey anti-rabbit IgG and Cy5 conjugated donkey anti mouse IgG were obtained from Jackson ImmunoResearch Laboratories, Inc. (West Grove, PA, USA. IRDye 680RD donkey anti-rabbit IgG were obtained from LI-COR, Inc. (Lincoln, NE, USA).

Brefeldin A and Biotin Treatments

BFA was obtained from Sigma and diluted in DMSO for a stock concentration of 5 mg/mL. This was diluted to a 0.5 mg/mL working concentration in DMEM prior to being added to cells. Cells were pre-treated for 45 min before being processed for imaging or (for RUSH β1AR experiments) before biotin was added. Biotin (from Sigma) was diluted to 40 uM in serum free DMEM and was filter sterilized with a 0.22 um filter. Biotin was further diluted to 10 uM in DMEM supplemented with 10% FBS prior to being added to cells. Where appropriate, BFA was maintained in the media during biotin treatment.

Immunofluorescence Microscopy

Cells were permeabilized for 10 min with 0.02% saponin (CalBiochem/Sigma) and 10 mM glycine (Sigma) in phosphate buffered saline (PBS; Sap/PBS/gly buffer). Coverslips were incubated 15 min in primary antibody diluted in Sap/PBS/gly buffer with 1% bovine serum albumin (BSA). Cells were washed 2 times with Sap/PBS/gly buffer before being incubated in secondary antibody diluted as above. Cells were washed again before being incubated for 3 min in 0.1 μg/mL Hoechst 33258 diluted in PBS. Coverslips were then mounted in glycerol with 0.1 M N-propyl gallate.

For surface staining, after BFA and biotin treatment for the indicated times, cells were washed with ice cold PBS before intact cells were incubated with primary antibody diluted in PBS on ice for 15 min. Cells were then permeabilized and labeled with internal and secondary antibodies as described above.

Cells were imaged on an Axioskop microscope (Zeiss, Thornwood, NY, USA) equipped with epifluorescence using an ORCA-03G charge-coupled device camera (Hamamatsu, Japan) using iVision software (BioVision Technologies, Exton, PA, USA). For Figure A-3, the Golgi regions of interest (ROI) were created using the GM130 image. The integrated pixel density of the golgin-160 signal in each Golgi ROI as well as in the whole cell was determined using FIJI (National Institutes of Health, Bethesda, MD, USA). To calculate the percent of golgin-160 at the Golgi, the integrated pixel density at the Golgi was divided by that of the whole cell. This percent was then normalized to untransfected cells by dividing each individual percent by the average percent in untransfected cells.

Radiolabeled Surface Ligand Binding Assay

Four 35 mm dishes were split for each condition, three for the radiolabeled surface ligand binding assay, one to lyse to control for β1AR expression level. For the ligand binding assay, cells were pretreated with BFA and incubated for the appropriate amount of time, as indicated. Cells were washed 3 times in ice cold PBS and cold KRH buffer (136 mM NaCl, 4.7 mM KCl, 1.25 mM MgSO4, 1.25 mM CaCl2, 20 mM HEPES pH 7.4, 2 mg/mL BSA) with 5 nM (-)-[3H]CGP-12177 (PerkinElmer, Boston, MA, USA). Dishes were rocked for 3 h at 4^{o}C. Cells were then washed 3 times in ice cold PBS before cells were lysed in the dishes with detergent solution (1% NP-40, 0.4% deoxycholic acid, 50 mM Tris pH 8, 62.5 mM EDTA pH 8 with protease inhibitors) for 10 min on ice. The lysate was then suspended in Bio-Safe II Biodegradable Scintillation Cocktail (Research Products International, Mt. Prospect, IL, USA) and counted on a LS 6500 Multi-Purpose Scintillation Counter (Beckman-Coulter, Brea, CA, USA).

To normalize for β1AR expression level, the fourth dish was lysed on ice for 10 min in detergent solution. The protein was separated on a 10% polyacrylamide gel, and β1AR was detected by immunoblotting after transfer to Immobilon-FL PVDF (EMD Millipore, Billerica, MA, USA), by near-infrared fluorescent imaging on the Odyssey CLx Imaging System (LI-COR, Lincoln, NE, USA). Protein levels were calculated using Image Studio version 4.0 (LI-COR) and normalized to β1AR alone expression levels. The counts per minute from the ligand binding assay were divided by the normalized β1AR expression levels.

Statistical Analysis

Statistical analysis of golgin-160 localization during co-expression of GARG and β1AR was obtained using GraphPad Prism version 7.00 for Mac OS X (GraphPad Software, La Jolla, CA, USA). One-way ANOVA followed by Tukey's multiple comparisons test were performed.

REFERENCES

Abraham, O., Gotliv, K., Parnis, a., Boncompain, G., Perez, F., and Cassel, D. (2016). Control of protein trafficking by reversible masking of transport signals. Mol. Biol. Cell *27*, 1310–1319.

Agarwala, R. *et al.* (2016). Database resources of the National Center for Biotechnology Information. Nucleic Acids Res. *44*, D7–D19.

Akhmanova, A., and Hammer, J. a. (2010). Linking molecular motors to membrane cargo. Curr. Opin. Cell Biol. *22*, 479–487.

Anitei, M., and Hoflack, B. (2011). Exit from the trans-Golgi network: from molecules to mechanisms. Curr. Opin. Cell Biol. *23*, 443–451.

Antonny, B., Beraud-Dufour, S., Chardin, P., and Chabre, M. (1997). N-terminal hydrophobic residues of the G-protein ADP-ribosylation factor-1 insert into membrane phospholipids upon GDP to GTP exchange. Biochemistry *36*, 4675–4684.

Arnspang, E. C., Sundbye, S., Nelson, W. J., and Nejsum, L. N. (2013). Aquaporin-3 and aquaporin-4 are sorted differently and separately in the trans-Golgi network. PLoS One *8*, e73977.

Bachert, C., and Linstedt, A. D. (2010). Dual anchoring of the GRASP membrane tether promotes trans pairing. J. Biol. Chem. *285*, 16294–16301.

Banu, Y., Matsuda, M., Yoshihara, M., Kondo, M., Sutou, S., and Matsukuma, S. (2002). Golgi matrix protein gene, Golga3/Mea2, rearranged and re-expressed in pachytene spermatocytes restores spermatogenesis in the mouse. Mol. Reprod. Dev. *61*, 288–301.

Barinaga-Rementeria Ramirez, I., and Lowe, M. (2009). Golgins and GRASPs: Holding the Golgi together. Semin. Cell Dev. Biol. *20*, 770–779.

Barr, F. A. (2009). Rab GTPase function in Golgi trafficking. Semin. Cell Dev. Biol. *20*, 780–783.

Behnia, R., and Munro, S. (2005). Organelle identity and the signposts for membrane traffic. Nature *438*, 597–604.

Bentson, L. F., Agbor, V. a, Agbor, L. N., Lopez, a C., Nfonsam, L. E., Bornstein, S. S., Handel, M. a, and Linder, C. C. (2013). New point mutation in Golga3 causes multiple defects in spermatogenesis. Andrology *1*, 440–450.

Boncompain, G., Divoux, S., Gareil, N., de Forges, H., Lescure, A., Latreche, L., Mercanti, V., Jollivet, F., Raposo, G., and Perez, F. (2012). Synchronization of secretory protein traffic in populations of cells. Nat. Methods *9*, 493–498.

Boncompain, G., and Perez, F. (2013). Fluorescence-based analysis of trafficking in mammalian cells, Elsevier Inc.

Bonifacino, J. S., and Glick, B. S. (2004). The Mechanisms of Vesicle Budding and Fusion. Cell *116*, 153–166.

Bonifacino, J. S., and Lippincott-Schwartz, J. (2003). Coat proteins: shaping membrane transport. Nat. Rev. Mol. Cell Biol. *4*, 409–414.

Bouschet, T., Martin, S., and Henley, J. (2005). Receptor-activity-modifying proteins are required for forward trafficking of the calcium-sensing receptor to the plasma membrane. J. Cell Sci. *118*, 4709–4720.

Bristow, M. R., Minobe, W. a, Raynolds, M. V, Port, J. D., Rasmussen, R., Ray, P. E., and Feldman, a M. (1993). Reduced beta 1 receptor messenger RNA abundance in the failing human heart. J. Clin. Invest. *92*, 2737–2745.

Bundis, F., Neagoe, I., and Schwappach, B. (2006). Involvement of Golgin-160 in Cell Surface Transport of Renal ROMK Channel : Co-expression of Golgin-160 Increases ROMK Currents. Cell. Physiol. Biochem. Biochem., 1–12.

Caviston, J. P., and Holzbaur, E. L. F. (2009). Huntingtin as an essential integrator of intracellular vesicular trafficking. Trends Cell Biol. *19*, 147–155.

Cha, H., Smith, B. L., Gallo, K., Machamer, C. E., and Shapiro, P. (2004). Phosphorylation of golgin-160 by mixed lineage kinase 3. J. Cell Sci. *117*, 751–760.

Chandran, S., and Machamer, C. E. (2008). Acute perturbations in golgi organization impact de novo sphingomyelin synthesis. Traffic *9*, 1894–1904.

Chavrier, P., and Goud, B. (1999). The role of ARF and Rab GTPases in membrane transport. Curr. Opin. Cell Biol. *11*, 466–475.

Cheung, P. Y. P., Limouse, C., Mabuchi, H., and Pfeffer, S. R. (2015). Protein flexibility is required for vesicle tethering at the Golgi. Elife *4*, 1–17.

Choudhury, R. R., Hyvola, N., and Lowe, M. (2005). Phosphoinositides and membrane traffic at the trans-Golgi network. Biochem Soc Symp *38*, 31–38.

Christensen, G. L., Aplin, M., and Hansen, J. L. (2010). Therapeutic potential of functional selectivity in the treatment of heart failure. Trends Cardiovasc. Med. *20*, 221–227.

Christis, C., and Munro, S. (2012). The small G protein Arl1 directs the trans-Golgi-specific targeting of the Arf1 exchange factors BIG1 and BIG2. J. Cell Biol. *196*, 327–335.

Claude, A., Zhao, B., Kuziemsky, C. E., Dahan, S., Berger, S. J., Yan, J., Armold, A. D., Sullivan, E. M., and Melançon, P. (1999). Exchange Factor That Displays Specificity for ADP-ribosylation Factor 5. J. Cell Biol. *146*, 71–84.

Cotecchia, S., Stanasila, L., and Diviani, D. (2012). Protein-protein interactions at the adrenergic receptors. Curr. Drug Targets *13*, 15–27.

D'Souza-Schorey, C., and Chavrier, P. (2006). ARF proteins: roles in membrane traffic and beyond. Nat. Rev. Mol. Cell Biol. *7*, 347–358.

Dash, R. *et al.* (2001). Interactions Between Phospholamban and -Adrenergic Drive May Lead to Cardiomyopathy and Early Mortality. Circulation *103*, 889–896.

Day, K. J., Staehelin, L. A., and Glick, B. S. (2013). A three-stage model of Golgi structure and function. Histochem. Cell Biol. *140*, 239–249.

Dittié, A. S., Hajibagheri, N., and Tooze, S. a. (1996). The AP-1 adaptor complex binds to immature secretory granules from PC12 cells, and is regulated by ADP-ribosylation factor. J. Cell Biol. *132*, 523–536.

Donaldson, J. G., Cassel, D., Kahn, R. a, and Klausner, R. D. (1992). ADP-ribosylation factor, a small GTP-binding protein, is required for binding of the coatomer protein beta-COP to Golgi membranes. Proc. Natl. Acad. Sci. U. S. A. *89*, 6408–6412.

Donaldson, J. G., and Honda, A. (2005). Localization and function of Arf family GTPases. Biochem. Soc. Trans. *33*, 639–642.

Donaldson, J. G., and Jackson, C. L. (2011). ARF family G proteins and their regulators: roles in membrane transport, development and disease. Nat. Rev. Mol. Cell Biol. *12*, 362–375.

Dong, C., Filipeanu, C. M., Duvernay, M. T., and Wu, G. (2007). Regulation of G protein-coupled receptor export trafficking. Biochim. Biophys. Acta *1768*, 853–870.

Dong, C., Nichols, C., Guo, J., and Huang, W. (2012). A Triple Arg Motif Mediates α2B-Adrenergic Receptor Interaction with Sec24C/D and Export. Traffic *13*, 706–721.

Dong, C., Zhang, X., Zhou, F., Dou, H., Duvernay, M. T., Zhang, P., and Wu, G. (2010). ADP-ribosylation factors modulate the cell surface transport of G protein-coupled receptors. J. Pharmacol. Exp. Ther. *333*, 174–183.

Duvernay, M. T., Dong, C., Zhang, X., Robitaille, M., Hebert, T. E., and Wu, G. (2009). A Single Conserved Leucine Residue on the First Intracellular Loop Regulates ER Export of G Protein-Coupled Receptors. Traffic *10*, 552–566.

Egerer, J. *et al.* (2015). GORAB Missense Mutations Disrupt RAB6 and ARF5 Binding and Golgi Targeting. J. Invest. Dermatol. *135*, 2368–2376.

Farhat, R., Séron, K., Ferlin, J., Fénéant, L., Belouzard, S., Goueslain, L., Jackson, C. L., Dubuisson, J., and Rouillé, Y. (2016). Identification of class II ADP-ribosylation factors as cellular factors required for hepatitis C virus replication. Cell. Microbiol. *18*, 1121–1133.

Farr, G. A., Hull, M., Stoops, E. H., Bateson, R., and Caplan, M. J. (2015). Dual pulse-chase microscopy reveals early divergence in the biosynthetic trafficking of the Na,K-ATPase and E-cadherin. Mol. Biol. Cell *26*, 4401–4411.

Feng, S., and Arnold, D. B. (2016). Techniques for studying protein trafficking and molecular motors in neurons. Cytoskeleton *73*, 508–515.

Fölsch, H., Mattila, P. E., and Weisz, O. a (2009). Taking the scenic route: biosynthetic traffic to the plasma membrane in polarized epithelial cells. Traffic *10*, 972–981.

Fritzler, M. J., Hamel, J. C., Ochs, R. L., and Chan, E. K. L. (1993). Molecular Characterization of Two Human Autoantigens: Unique cDNAs Encoding 95- and 160-kD Proteins of a Putative Family in the Golgi Complex. J. Exp. Med. *178*, 49–62.

Fu, M. M., and Holzbaur, E. L. F. (2014). Integrated regulation of motor-driven organelle transport by scaffolding proteins. Trends Cell Biol. *24*, 564–574.

Gardner, L. a, Delos Santos, N. M., Matta, S. G., Whitt, M. a, and Bahouth, S. W. (2004). Role of the cyclic AMP-dependent protein kinase in homologous resensitization of the beta1-adrenergic receptor. J. Biol. Chem. *279*, 21135–21143.

Gardner, L. a, Naren, A. P., and Bahouth, S. W. (2007). Assembly of an SAP97-AKAP79-cAMP-dependent protein kinase scaffold at the type 1 PSD-95/DLG/ZO1 motif of the human beta(1)-adrenergic receptor generates a receptosome involved in receptor recycling and networking. J. Biol. Chem. *282*, 5085–5099.

Gardner, L. a, Tavalin, S. J., Goehring, A. S., Scott, J. D., and Bahouth, S. W. (2006). AKAP79-mediated targeting of the cyclic AMP-dependent protein kinase to the beta1-

adrenergic receptor promotes recycling and functional resensitization of the receptor. J. Biol. Chem. *281*, 33537–33553.

Ghosh, P., Dahms, N. M., and Kornfeld, S. (2003). Mannose 6-phosphate receptors: new twists in the tale. Nat. Rev. Mol. Cell Biol. *4*, 202–213.

Gilbert, C. E., Zuckerman, D. M., Currier, P. L., and Machamer, C. E. (2014). Three basic residues of intracellular loop 3 of the beta-1 adrenergic receptor are required for golgin-160-dependent trafficking. Int. J. Mol. Sci. *15*, 2929–2945.

Gillingham, A. K., and Munro, S. (2007). The Small G Proteins of the Arf Family and Their Regulators. Annu. Rev. Cell Dev. Biol. *23*, 579–611.

Gillingham, A. K., and Munro, S. (2016). Finding the Golgi: Golgin Coiled-Coil Proteins Show the Way. Trends Cell Biol. *26*, 399–408.

Gleeson, P. a., Lock, J. G., Luke, M. R., and Stow, J. L. (2004). Domains of the TGN: Coats, tethers and G proteins. Traffic *5*, 315–326.

Glick, B. S. (2000). Organization of the Golgi apparatus. Curr. Opin. Cell Biol. *12*, 450–456.

Gosavi, P., and Gleeson, P. a. (2017). The Function of the Golgi Ribbon Structure - An Enduring Mystery Unfolds! BioEssays *1700063*, 1700063.

Govers, R. (2014). Molecular mechanisms of GLUT4 regulation in adipocytes. Diabetes Metab. *40*, 400–410.

Hamelin, E., Thériault, C., Laroche, G., and Parent, J.-L. (2005). The Intracellular Trafficking of the G Protein-coupled Receptor TPβ Depends on a Direct Interaction with Rab11. J. Biol. Chem. *280*, 36195–36205.

Hara-Kuge, S., Kuge, O., Orci, L., Amherdt, M., Ravazzola, M., Wieland, F. T., and Rothman, J. E. (1994). En Bloc incorporation of coatomer subunits during the assembly of COP-coated vesicles. J. Cell Biol. *124*, 883–892.

He, J., Bellini, M., Xu, J., Castleberry, A. M., and Hall, R. a (2004). Interaction with cystic fibrosis transmembrane conductance regulator-associated ligand (CAL) inhibits beta1-adrenergic receptor surface expression. J. Biol. Chem. *279*, 50190–50196.

Hebert, S. C. (1995). An ATP-regulated, inwardly rectifying potassium channel from rat kidney (ROMK). Kidney Int *48*, 1010–1016.

Hicks, S. W., Horn, T. a, McCaffery, J. M., Zuckerman, D. M., and Machamer, C. E. (2006). Golgin-160 promotes cell surface expression of the beta-1 adrenergic receptor. Traffic *7*, 1666–1677.

Hicks, S. W., and Machamer, C. E. (2002). The NH2-terminal domain of Golgin-160 contains both Golgi and nuclear targeting information. J. Biol. Chem. *277*, 35833–35839.

Hicks, S. W., and Machamer, C. E. (2005). Isoform-specific interaction of golgin-160 with the Golgi-associated protein PIST. J. Biol. Chem. *280*, 28944–28951.

Hirst, J., Seaman, M. N. J., Buschow, S. I., and Robinson, M. S. (2007). The role of cargo proteins in GGA recruitment. Traffic *8*, 594–604.

Houndolo, T., Boulay, P.-L., and Claing, A. (2005). G Protein-coupled Receptor Endocytosis in ADP-ribosylation Factor 6-depleted Cells. J. Biol. Chem. *280*, 5598–5604.

Hu, F., Shi, X., Li, B., Huang, X., Morelli, X., and Shi, N. (2015). Structural basis for the interaction between the Golgi reassembly-stacking protein GRASP65 and the Golgi matrix protein GM130. J. Biol. Chem. *290*, 26373–26382.

Hu, L. a, Tang, Y., Miller, W. E., Cong, M., Lau, a G., Lefkowitz, R. J., and Hall, R. a (2000). beta 1-adrenergic receptor association with PSD-95. Inhibition of receptor internalization and facilitation of beta 1-adrenergic receptor interaction with N-methyHu, L. a, Tang, Y., Miller, W. E., Cong, M., Lau, a G., Lefkowitz, R. J., & Hall, R. a. (2000. J. Biol. Chem. *275*, 38659–38666.

Hutagalung, A. H., and Novick, P. J. (2011). Role of Rab GTPases in Membrane Traffic and Cell Physiology. Physiol. Rev. *91*, 119–149.

Huttlin, E. L. *et al.* (2015). The BioPlex Network: A Systematic Exploration of the Human Interactome. Cell *162*, 425–440.

Irannejad, R., Pessino, V., Mika, D., Huang, B., Wedegaertner, P. B., Conti, M., and von Zastrow, M. (2017). Functional selectivity of GPCR-directed drug action through location bias. Nat. Chem. Biol. *13*, 799–806.

Jackson, L. P. (2014). Structure and mechanism of COPI vesicle biogenesis. Curr. Opin. Cell Biol. *29*, 67–73.

Jensen, C. S., Watanabe, S., Rasmussen, H. B., Schmitt, N., Olesen, S.-P., Frost, N. A., Blanpied, T. A., and Misonou, H. (2014). Specific Sorting and Post-Golgi Trafficking of Dendritic Potassium Channels in Living Neurons. J. Biol. Chem. *289*, 10566–10581.

Jost, M., Simpson, F., Kavran, J. M., Lemmon, M. a., and Schmid, S. L. (1998). Phosphatidylinositol-4,5-bisphosphate is required for endocytic coated vesicle formation. Curr. Biol. *8*, 1399–1404.

Klumperman, J., Schweizer, a, Clausen, H., Tang, B. L., Hong, W., Oorschot, V., and Hauri, H. P. (1998). The recycling pathway of protein ERGIC-53 and dynamics of the ER-Golgi intermediate compartment. J. Cell Sci. *111 (Pt 2*, 3411–3425.

Kudelko, M., Brault, J. B., Kwok, K., Li, M. Y., Pardigon, N., Peiris, J. S. M., Bruzzone, R., Despre, P., Nal, B., and Wang, P. G. (2012). Class II ADP-ribosylation factors are required for efficient secretion of dengue viruses. J. Biol. Chem. *287*, 767–777.

Kumari, S., and Mayor, S. (2008). ARF1 is directly involved in dynamin-independent endocytosis. Nat. Cell Biol. *10*, 30–41.

Kupfer, A., Louvard, D., and Singer, S. J. (1982). Polarization of the Golgi apparatus and the microtubule-organizing center in cultured fibroblasts at the edge of an experimental wound. Proc. Natl. Acad. Sci. U. S. A. *79*, 2603–2607.

Lachance, V., Cartier, A., Génier, S., Munger, S., Germain, P., Labrecque, P., and Parent, J.-L. (2011). Regulation of β 2 -Adrenergic Receptor Maturation and Anterograde Trafficking by an Interaction with Rab Geranylgeranyltransferase. J. Biol. Chem. *286*, 40802–40813.

Langemeyer, L., and Barr, F. a (2012). Analysis of rab GTPases. Curr. Protoc. Cell Biol. *Chapter 15*, Unit 15.18.

Lanke, K. H. W., van der Schaar, H. M., Belov, G. a., Feng, Q., Duijsings, D., Jackson, C. L., Ehrenfeld, E., and van Kuppeveld, F. J. M. (2009). GBF1, a Guanine Nucleotide Exchange Factor for Arf, Is Crucial for Coxsackievirus B3 RNA Replication. J. Virol. *83*, 11940–11949.

Lavieu, G., Dunlop, M. H., Lerich, A., Zheng, H., Bottanelli, F., and Rothman, J. E. (2014). The Golgi ribbon structure facilitates anterograde transport of large cargoes. Mol. Biol. Cell *25*, 3028–3036.

Lavieu, G., Zheng, H., and Rothman, J. E. (2013). Stapled Golgi cisternae remain in place as cargo passes through the stack. Elife *2*.

Lee, I., Doray, B., Govero, J., and Kornfeld, S. (2008). Binding of cargo sorting signals to AP-1 enhances its association with ADP ribosylation factor 1 – GTP. *180*, 467–472.

Lee, S. Y., Yang, J. S., Hong, W., Premont, R. T., and Hsu, V. W. (2005). ARFGAP1 plays a central role in coupling COPI cargo sorting with vesicle formation. J. Cell Biol. *168*, 281–290.

Leto, D., and Saltiel, A. R. (2012). Regulation of glucose transport by insulin: traffic control of GLUT4. Nat. Rev. Mol. Cell Biol. *13*, 383–396.

Lieu, Z. Z., Lock, J. G., Hammond, L. a, La Gruta, N. L., Stow, J. L., and Gleeson, P. a (2008). A trans-Golgi network golgin is required for the regulated secretion of TNF in activated macrophages in vivo. Proc. Natl. Acad. Sci. U. S. A. *105*, 3351–3356.

Lippincott-Schwartz, J., Donaldson, J. G., Schweizer, A., Berger, E. G., Hauri, H. P., Yuan, L. C., and Klausner, R. D. (1990). Microtubule-dependent retrograde transport of proteins into the ER in the presence of brefeldin a suggests an ER recycling pathway. Cell *60*, 821–836.

Liu, Y., Kahn, R. a., and Prestegard, J. H. (2009). Structure and Membrane Interaction of Myristoylated ARF1. Structure *17*, 79–87.

Lock, J. G., Hammond, L. a, Houghton, F., Gleeson, P. a, and Stow, J. L. (2005). E-cadherin transport from the trans-Golgi network in tubulovesicular carriers is selectively regulated by golgin-97. Traffic *6*, 1142–1156.

Lowery, J., Szul, T., Styers, M., Holloway, Z., Oorschot, V., Klumperman, J., and Sztul, E. (2013). The Sec7 Guanine Nucleotide Exchange Factor GBF1 Regulates Membrane Recruitment of BIG1 and BIG2 Guanine Nucleotide Exchange Factors to the Trans-Golgi Network (TGN). J. Biol. Chem. *288*, 11532–11545.

Maag, R. S., Mancini, M., Rosen, A., and Machamer, C. E. (2005). Caspase-resistant Golgin-160 disrupts apoptosis induced by secretory pathway stress and ligation of death receptors. Mol. Biol. Cell *16*, 3019–3027.

Magalhaes, A. C., Dunn, H., and Ferguson, S. S. G. (2012). Regulation of GPCR activity, trafficking and localization by GPCR-interacting proteins. Br. J. Pharmacol. *165*, 1717–1736.

Mancini, M., Machamer, C. E., Roy, S., Nicholson, D. W., Thornberry, N. a, Casciola-Rosen, L. a, and Rosen, a (2000). Caspase-2 is localized at the Golgi complex and cleaves golgin-160 during apoptosis. J. Cell Biol. *149*, 603–612.

Manolea, F., Chun, J., Chen, D., Clarke, I., Summerfeldt, N., Dacks, J. B., and Melançon, P. (2010). Arf3 is Activated Uniquely at the trans-Golgi Network by Brefeldin A-inhibited Guanine Nucleotide Exchange Factors. Mol. Biol. Cell *21*, 1836–1849.

Martínez-Alonso, E., Ballesta, J., and Martínez-Menárguez, J. a. (2007a). Low-temperature-induced Golgi tubules are transient membranes enriched in molecules regulating intra-Golgi transport. Traffic *8*, 359–368.

Martínez-Alonso, E., Egea, G., Ballesta, J., and Martínez-Menárguez, J. a. (2005). Structure and dynamics of the Golgi complex at 15 °C: Low temperature induces the formation of Golgi-derived tubules. Traffic *6*, 32–44.

Martínez-Alonso, E., Tomás, M., Ballesta, J., and Martínez-Menárguez, J. a. (2007b). Low temperature (15°C) induces COPII dissociation from membranes and slow exit from the endoplasmic reticulum in HeLa cells. Histochem. Cell Biol. *128*, 379–384.

Matlin, K. S., and Simons, K. (1983). Reduced temperature prevents transfer of a membrane glycoprotein to the cell surface but does not prevent terminal glycosylation. Cell *34*, 233–243.

Matsukuma, S., Kondo, M., Yoshihara, M., Matsuda, M., Utakoji, T., and Sutou, S. (1999). Mea2/Golga3 gene is disrupted in a line of transgenic mice with a reciprocal translocation between chromosomes 5 and 19 and is responsible for a defective spermatogenesis in homozygotes. Mamm. Genome *10*, 1–5.

De Matteis, M. A., and Luini, A. (2008). Exiting the Golgi complex. Nat. Rev. Mol. Cell Biol. *9*, 273–284.

Mattila, P. E., Youker, R. T., Mo, D., Bruns, J. R., Cresawn, K. O., Hughey, R. P., Ihrke, G., and Weisz, O. a (2012). Multiple biosynthetic trafficking routes for apically secreted proteins in MDCK cells. Traffic *13*, 433–442.

Mihov, D., and Spiess, M. (2015). Glycosaminoglycans: Sorting determinants in intracellular protein traffic. Int. J. Biochem. Cell Biol. *68*, 87–91.

Mironov, A. A., Sesorova, I. S., Seliverstova, E. V., and Beznoussenko, G. V. (2017). Different Golgi ultrastructure across species and tissues: Implications under functional and pathological conditions, and an attempt at classification. Tissue Cell *49*, 186–201.

Misumi, Y., Sohda, M., Yano, A., Fujiwara, T., and Ikehara, Y. (1997). Molecular characterization of GCP170, a 170-kDa protein associated with the cytoplasmic face of the Golgi membrane. J. Biol. Chem. *272*, 23851–23858.

Molloy, S. S., Thomas, L., Vanslyke, J. K., Stenberg1, P. E., and Thomas2, G. (1994). Intracellular trafficking and activation of the furin proprotein convertase: localization to the TGN and recycling from the cell surface. EMBO J. *13*, 18–33.

Monetta, P. (Universidad N. de C., Slavin, I. (Universidad N. de C., Romero, N. (Universidad N. de C., and Alvarez, C. (Universidad N. de C. (2007). Rab1b interacts with GBF1 and modulates both ARF1 dynamics and COPI association. Mol. Biol. Cell *18*, 2400–2410.

Munro, S. (2005). The Arf-like GTPase Arl1 and its role in membrane traffic. Biochem. Soc. Trans. *33*, 601–605.

Munro, S. (2011). The golgin coiled-coil proteins of the Golgi apparatus. Cold Spring Harb. Perspect. Biol. *3*, 1–14.

Murchison, C. F., Zhang, X.-Y., Zhang, W.-P., Ouyang, M., Lee, A., and Thomas, S. a (2004). A distinct role for norepinephrine in memory retrieval. Cell *117*, 131–143.

Nakamura, N., Wei, J. H., and Seemann, J. (2012). Modular organization of the mammalian Golgi apparatus. Curr. Opin. Cell Biol. *24*, 467–474.

Nawrotek, A., Zeghouf, M., and Cherfils, J. (2016). Allosteric regulation of Arf GTPases and their GEFs at the membrane interface. Small GTPases *7*, 0.

Nguyen, M. K., Kim, C. Y., Kim, J. M., Park, B. O., Lee, S., Park, H., and Heo, W. Do (2016). Optogenetic oligomerization of Rab GTPases regulates intracellular membrane trafficking. Nat. Chem. Biol. *12*, 431–436.

Nickel, W., Malsam, J., Gorgas, K., Ravazzola, M., Jenne, N., Helms, J. B., and Wieland, F. T. (1998). Uptake by COPI-coated vesicles of both anterograde and retrograde cargo is inhibited by GTPgammaS in vitro. J. Cell Sci. *111 (Pt 2*, 3081–3090.

Niu, T.-K., Pfeifer, A. C., Lippincott-Schwartz, J., and Jackson, C. L. (2005). Dynamics of GBF1, a Brefeldin A-Sensitive Arf1 Exchange Factor at the Golgi. Mol. Biol. Cell *16*, 1213–1222.

O'Keeffe, M. B., Reid, H. M., and Kinsella, B. T. (2008). Agonist-dependent internalization and trafficking of the human prostacyclin receptor: A direct role for Rab5a GTPase. Biochim. Biophys. Acta - Mol. Cell Res. *1783*, 1914–1928.

Opat, A. S., Van Vliet, C., and Gleeson, P. a. (2001). Trafficking and localisation of resident Golgi glycosylation enzymes. Biochimie *83*, 763–773.

Orci, L., Palmer, D. J., Amherdt, M., and Rothman, J. E. (1993). Coated vesicle assembly in the Golgi requires only coatomer and ARF proteins from the cytosol. Nature *364*, 732–734.

Park, J. J., Gondre-Lewis, M. C., Eiden, L. E., and Loh, Y. P. (2011). A distinct trans-Golgi network subcompartment for sorting of synaptic and granule proteins in neurons and neuroendocrine cells. J. Cell Sci. *124*, 735–744.

Pepperkok, R., Whitney, J. a, Gomez, M., and Kreis, T. E. (2000). COPI vesicles accumulating in the presence of a GTP restricted arf1 mutant are depleted of anterograde and retrograde cargo. J. Cell Sci. *113 (Pt 1*, 135–144.

Pfeffer, S. R. (2010). How the Golgi works: A cisternal progenitor model. Proc. Natl. Acad. Sci. *107*, 19614–19618.

Port, J. D., and Bristow, M. R. (2001). Altered beta-adrenergic receptor gene regulation and signaling in chronic heart failure. J. Mol. Cell. Cardiol. *33*, 887–905.

Presley, J. F., Ward, T. H., Pfeifer, A. C., Siggia, E. D., Phair, R. D., and Lippincott-Schwartz, J. (2002). Dissection of COPI and Arf1 dynamics in vivo and role in Golgi membrane transport. Nature *417*, 187–193.

Rapacciuolo, A., Suvarna, S., Barki-Harrington, L., Luttrell, L. M., Cong, M., Lefkowitz, R. J., and Rockman, H. a (2003). Protein kinase A and G protein-coupled receptor kinase phosphorylation mediates beta-1 adrenergic receptor endocytosis through different pathways. J. Biol. Chem. *278*, 35403–35411.

Robinson, M. S. (2004). Adaptable adaptors for coated vesicles. Trends Cell Biol. *14*, 167–174.

Roboti, P., Witkos, T. M., and Lowe, M. (2013). Biochemical analysis of secretory trafficking in mammalian cells, Elsevier Inc.

Rodriguez-Boulan, E., and Müsch, A. (2005). Protein sorting in the Golgi complex: Shifting paradigms. Biochim. Biophys. Acta - Mol. Cell Res. *1744*, 455–464.

Saitoh, A., Shin, H. W., Yamada, A., Waguri, S., and Nakayama, K. (2009). Three homologous ArfGAPs participate in coat protein imediated transport. J. Biol. Chem. *284*, 13948–13957.

Sandnes, D., Gjerde, I., Refsnes, M., and Jacobsen, S. (1987). Down-regulation of surface beta-adrenoceptors on intact human mononuclear leukocytes. Biochem. Pharmacol. *36*, 1303–1311.

Saraste, J., and Kuismanen, E. (1984). Pre- and post-golgi vacuoles operate in the transport of semliki forest virus membrane glycoproteins to the cell surface. Cell *38*, 535–549.

Saraste, J., and Svensson, K. (1991). Distribution of the intermediate elements operating in ER to Golgi transport. J. Cell Sci. *100 (Pt 3*, 415–430.

Shin, H.-W., Morinaga, N., Noda, M., and Nakayama, K. (2004). BIG2, A Guanine Nucleotide Exchange Factor for ADP-Ribosylation Factors: Its Localization to Recycling Endosomes and Implication in the Endosome Integrity. Mol. Biol. Cell *15*, 5283–5294.

Short, B., Haas, A., and Barr, F. a. (2005). Golgins and GTPases, giving identity and structure to the Golgi apparatus. Biochim. Biophys. Acta - Mol. Cell Res. *1744*, 383–395.

Simon, D. B., Karet, F. E., Rodriguez-Soriano, J., Hamdan, J. H., DiPietro, A., Trachtman, H., Sanjad, S. a., and Lifton, R. P. (1996). Genetic heterogeneity of Barter's syndrome revealed by mutations in the K+ channel, ROMK. Nat. Genet. *14*, 152–156.

Sinka, R., Gillingham, A. K., Kondylis, V., and Munro, S. (2008). Golgi coiled-coil proteins contain multiple binding sites for Rab family G proteins. J. Cell Biol. *183*, 607–615.

Soloveva, V., Graves, R. A., Rasenick, M. M., Spiegelman, B. M., and Ross, S. R. (1997). The Beta 1-Adrenergic Receptor in Adipose Tissue Are Resistant to Obesity. Mol. Endocrinol. *11*, 27–38.

Spang, A. (2013). Retrograde traffic from the golgi to the endoplasmic reticulum. Cold Spring Harb. Perspect. Biol. *5*, 1–10.

Spang, A., Shiba, Y., and Randazzo, P. a. (2010). Arf GAPs: Gatekeepers of vesicle generation. FEBS Lett. *584*, 2646–2651.

Stamnes, M. a., and Rothman, J. E. (1993). The binding of AP-1 clathrin adaptor particles to Golgi membranes requires ADP-ribosylation factor, a small GTP-binding protein. Cell *73*, 999–1005.

Stanley, P. (2011). Golgi glycosylation. Cold Spring Harb. Perspect. Biol. *3*, 1–13.

Stenmark, H. (2009). Rab GTPases as coordinators of vesicle traffic. Nat. Publ. Gr. *10*, 513–525.

Surma, M. a., Klose, C., and Simons, K. (2012). Lipid-dependent protein sorting at the trans-Golgi network. Biochim. Biophys. Acta - Mol. Cell Biol. Lipids *1821*, 1059–1067.

Szul, T., Garcia-Mata, R., Brandon, E., Shestopal, S., Alvarez, C., and Sztul, E. (2005). Dissection of membrane dynamics of the ARF-guanine nucleotide exchange factor GBF1. Traffic *6*, 374–385.

Tang, Y., Hu, L. A., Miller, W. E., Ringstad, N., Hall, R. A., Pitcher, J. A., Decamilli, P., and Lefkowitz, R. J. (1999). Identification of the endophilins (SH3p4/p8/p13) as novel binding partners for the beta1-adrenergic receptor. Proc. Natl. Acad. Sci. U.S.A. *96*, 12559–12564.

Teal, S. B., Hsu, V. W., Peters, P. J., Klausner, R. D., and Donaldson, J. G. (1994). An activating mutation in ARF1 stabilizes coatomer binding to Golgi membranes. J. Biol. Chem. *269*, 3135–3138.

Truebestein, L., and Leonard, T. a. (2016). Coiled-coils: The long and short of it. BioEssays *38*, 903–916.

Uhlen, M. *et al.* (2015). Tissue-based map of the human proteome. Science (80-.). *347*, 1260419–1260419.

Volpicelli-Daley, L. A., Li, Y., Zhang, C. J., and Kahn, R. A. (2005). Isoform-selective Effects of the Depletion of ADP-Ribosylation Factors 1-5 on Membrane Traffic. Mol. Biol. Cell *16*, 4495–4508.

Wallukat, G. (2002). The beta-adrenergic receptors. Herz *27*, 683–690.

Wang, G., and Wu, G. (2012). Small GTPase regulation of GPCR anterograde trafficking. Trends Pharmacol. Sci. *33*, 28–34.

Warne, T., Serrano-vega, M. J., Baker, J. G., Moukhametzianov, R., Edwards, C., Henderson, R., Leslie, A. G. W., and Tate, C. G. (2008). Structure of a β1-adrenergic G-protein-coupled receptor. Nature *454*, 486–491.

Williams, D., Hicks, S. W., Machamer, C. E., and Pessin, J. E. (2006). Golgin-160 Is Required for the Golgi Membrane Sorting of the Insulin-responsive Glucose Transporter GLUT4 in Adipocytes. Mol. Biol. Cell *17*, 5346–5355.

Wilson, C., Venditti, R., Rega, L. R., Colanzi, A., D'Angelo, G., and De Matteis, M. A. (2011). The Golgi apparatus: an organelle with multiple complex functions. Biochem. J. *433*, 1–9.

Witkos, T. M., and Lowe, M. (2017). Recognition and tethering of transport vesicles at the Golgi apparatus. Curr. Opin. Cell Biol. *47*, 16–23.

Wong, M., Gillingham, A. K., and Munro, S. (2017). The golgin coiled-coil proteins capture different types of transport carriers via distinct N-terminal motifs. BMC Biol. *15*, 3.

Wong, M., and Munro, S. (2014). The specificity of vesicle traffic to the Golgi is encoded in the golgin coiled-coil proteins. Science (80-.). *346*.

Woo, A. Y. H., and Xiao, R. (2012). β-Adrenergic receptor subtype signaling in heart: from bench to bedside. Acta Pharmacol. Sin. *33*, 335–341.

Xiang, Y. K. (2011). Compartmentalization of beta-adrenergic signals in cardiomyocytes. Circ. Res. *109*, 231–244.

Yadav, S., Puri, S., and Linstedt, A. D. (2009). A Primary Role for Golgi Positioning in Directed Secretion, Cell Polarity, and Wound Healing. Mol. Biol. Cell *20*, 1728–1736.

Yadav, S., Puthenveedu, M. A., and Linstedt, A. D. (2012). Golgin160 Recruits the Dynein Motor to Position the Golgi Apparatus. Dev. Cell *23*, 153–165.

Yao, R., Ito, C., Natsume, Y., Sugitani, Y., Yamanaka, H., Kuretake, S., Yanagida, K., Sato, A., Toshimori, K., and Noda, T. (2002). Lack of acrosome formation in mice lacking a Golgi protein, GOPC. Proc. Natl. Acad. Sci. U. S. A. *99*, 11211–11216.

Zhang, C. J., Rosenwald, A. G., Willingham, M. C., Skuntz, S., Clark, J., and Kahn, R. a. (1994). Expression of a dominant allele of human ARF1 inhibits membrane traffic in vivo. J. Cell Biol. *124*, 289–300.

Zhang, X., and Wang, Y. (2016a). Glycosylation Quality Control by the Golgi Structure. J. Mol. Biol. *428*, 3183–3193.

Zhang, X., and Wang, Y. (2016b). GRASPs in Golgi Structure and Function. Front. Cell Dev. Biol. *3*, 1–8.

Zhao, J., Li, B., Huang, X., Morelli, X., and Shi, N. (2017). Structural Basis for the Interaction between Golgi Reassembly-stacking Protein GRASP55 and Golgin45. J. Biol. Chem. *292*, 2956–2965.

Zhen, Y., and Stenmark, H. (2015). Cellular functions of Rab GTPases at a glance. J. Cell Sci. *128*, 3171–3176.

Zuckerman, D. M., Hicks, S. W., Charron, G., Hang, H. C., and Machamer, C. E. (2011). Differential regulation of two palmitoylation sites in the cytoplasmic tail of the beta1-adrenergic receptor. J. Biol. Chem. *286*, 19014–19023.

CURRICULUM VITAE

The Johns Hopkins University School of Medicine

Catherine E. Gilbert December 20, 2017

Educational History:

Ph.D. expected	2017	Program in Biochemistry, Cellular, and Molecular Biology	Johns Hopkins University School of Medicine
B.A.	2011	Molecular Biology	Scripps College

Other Professional Experience:

Internship	2014	Noble Life Sciences
Research Rotation	2012	Lab of Dr. J. Marie Hardwick, Johns Hopkins University School of Medicine
Research Rotation	2011	Lab of Dr. Susan Michaelis, Johns Hopkins University School of Medicine

Honors:

Lewis Travel Award	2015	Department of Cell Biology, Johns Hopkins School of Medicine
Travel Award	2015	Graduate Student Association, Johns Hopkins School of Medicine
Cum laude	2011	Scripps College

Publications:

Gilbert CE, Sztul E, Machamer CE. Commonly used trafficking blocks disrupt ARF1 activation and the localization and function of specific Golgi proteins. (In review.)

Gilbert CE, Zuckerman DM, Currier, PL, Machamer CE. Three basic residues of intracellular loop 3 of the beta-1 adrenergic receptor are required for golgin-160-dependent trafficking. Int J Mol Sci. 2014 Feb 20; 15(2):2929-45. PubMed PMID: 24566136.

Teng X, Dayhoff-Brannigan M, Cheng WC, **Gilbert CE**, Sing CN, Diny NL, Wheelan SJ, Dunham MJ, Boeke JD, Pineda FJ, Hardwick JM. Genome-wide consequences of deleting any single gene. Mol Cell. 2013 Nov 21; 52(4):485-94. PubMed PMID: 24211263.

Posters:

Gilbert, CE, Sztul, E, Machamer, CE (2016) Localization of golgin-160 at the Golgi is dynamic. American Society for Cell Biology, San Francisco, CA.

Gilbert, CE, Machamer, CE (2015) Golgin-facilitated trafficking of the beta-1 adrenergic receptor. American Society for Cell Biology, San Diego, CA.

Gilbert, CE, Machamer, CE (2014) Golgin-160 facilitated trafficking of the beta-1 adrenergic receptor. Biochemistry, Cellular and Molecular Biology poster session, Baltimore, MD.

Gilbert, CE, Machamer, CE (2013) Golgin-160 facilitated trafficking of the beta-1 adrenergic receptor. Biochemistry, Cellular and Molecular Biology annual retreat, St. Michael's, MD.

Service and Leadership:

2014-2015	Biochemistry, Cellular and Molecular Biology Graduate Program Student Colloquium Coordinator
2012-2013	Genetics Teaching Assistant
2012-2013	Cell Structure and Dynamics Teaching Assistant